NASA CONTRACTOR REPORT

NASA CR-1062

NASA CR-1062

AN ANALYSIS OF THE COUPLED CHEMICALLY REACTING BOUNDARY LAYER AND CHARRING ABLATOR

Part III
Nonsimilar Solution of the Multicomponent Laminar Boundary Layer by an Integral Matrix Method

by Eugene P. Bartlett and Robert M. Kendall

Prepared by
ITEK CORPORATION, VIDYA DIVISION
Palo Alto, Calif.
for Manned Spacecraft Center

NATIONAL AERONAUTICS AND SPACE ADMINISTRATION • WASHINGTON, D. C. • JUNE 1968

NASA CR-1062

AN ANALYSIS OF THE COUPLED CHEMICALLY REACTING BOUNDARY LAYER AND CHARRING ABLATOR

Part III

Nonsimilar Solution of the Multicomponent Laminar Boundary Layer by an Integral Matrix Method

By Eugene P. Bartlett and Robert M. Kendall

Issued by Originator as Aerotherm Report No. 66-7, Part III

Prepared under Contract No. NAS 9-4599 by
ITEK CORPORATION, VIDYA DIVISION
Palo Alto, Calif.

for Manned Spacecraft Center

NATIONAL AERONAUTICS AND SPACE ADMINISTRATION

For sale by the Clearinghouse for Federal Scientific and Technical Information
Springfield, Virginia 22151 – CFSTI price $3.00

FOREWORD

The present report is one of a series of six reports, published simultaneously, which describe analyses and computational procedures for: 1) prediction of the in-depth response of charring ablation materials, based on one-dimensional thermal streamtubes of arbitrary cross-section and considering general surface chemical and energy balances, and 2) nonsimilar solution of chemically reacting laminar boundary layers, with an approximate formulation for unequal diffusion and thermal diffusion coefficients for all species and with a general approach to the thermochemical solution of mixed equilibrium-nonequilibrium, homogeneous or heterogeneous systems. Part I serves as a summary report and describes a procedure for coupling the charring ablator and boundary layer routines. The charring ablator procedure is described in Part II, whereas the fluid-mechanical aspects of the boundary layer and the boundary-layer solution procedure are treated in Part III. The approximations for multicomponent transport properties and the chemical state models are described in Parts IV and V, respectively. Finally, in Part VI an analysis is presented for the in-depth response of charring materials taking into account char-density buildup near the surface due to coking reactions in depth.

The titles in the series are:

Part I Summary Report: An Analysis of the Coupled Chemically Reacting Boundary Layer and Charring Ablator, by R. M. Kendall, E. P. Bartlett, R. A. Rindal, and C. B. Moyer.

Part II Finite Difference Solution for the In-depth Response of Charring Materials Considering Surface Chemical and Energy Balances, by C. B. Moyer and R. A. Rindal.

Part III Nonsimilar Solution of the Multicomponent Laminar Boundary Layer by an Integral Matrix Method, by E. P. Bartlett and R. M. Kendall.

Part IV A Unified Approximation for Mixture Transport Properties for Multicomponent Boundary-Layer Applications, by E. P. Bartlett, R. M. Kendall, and R. A. Rindal.

Part V A General Approach to the Thermochemical Solution of Mixed Equilibrium-Nonequilibrium, Homogeneous or Heterogeneous Systems, by R. M. Kendall.

Part VI An Approach for Characterizing Charring Ablator Response with In-depth Coking Reactions, by R. A. Rindal.

This effort was conducted for the Structures and Mechanics Division of the Manned Spacecraft Center, National Aeronautics and Space Administration under Contract No. NAS9-4599 to Vidya Division of Itek Corporation with Mr. Donald M. Curry and Mr. George Strouhal as the NASA Technical Monitors. The work was initiated by the present authors while at Vidya and was completed by Aerotherm Corporation under subcontract to Vidya (P.O. 8471 V9002) after Aerotherm purchased the physical assets of the Vidya Thermodynamics Department. Dr. Robert M. Kendall of Aerotherm was the Program Manager and Principal Investigator.

ABSTRACT

A laminar nonsimilar boundary-layer procedure is described which yields accurate solutions for a broad range of problems. In its current formulation, solutions can be obtained for any equilibrium chemical environment with specified rate-controlled reactions at the surface. It has been used to treat a variety of ablating and nonablating surface boundary conditions including coupled energy and mass balances. The formulation considers unequal diffusion and thermal diffusion coefficients for all species in a particularly convenient manner through a bifurcation approximation for binary diffusion coefficients. The multicomponent viscosity and thermal conductivity of the mixture are determined by use of Sutherland-Wassiljewa type approximations. The procedure is readily applicable to inclusion of one-dimensional radiation emission and absorption and a general nonequilibrium chemical model.

The procedure combines features of the general integral relations approach with those of matrix solution techniques. Following the former, smooth functions (in particular, cubic spline functions) are chosen to relate the principal dependent variables to their derivatives. This enables the attainment of an accurate solution with relatively few entries into the conservation equations (3 to 4 place accuracy with 7 to 11 spline points). From the latter, the concept of treating the entire solution as a set of simultaneous, nonlinear algebraic equations is adopted. This technique results in linearized coupling between all relations required to characterize the boundary layer, and thus assures a general, rapid, and stable iterative convergence. As a consequence, the damping of corrections has seldom been required. Computational speed appears to be an attractive feature based on the few comparisons with other techniques which have been possible to date.

TABLE OF CONTENTS

LIST OF TABLES

LIST OF FIGURES

LIST OF FIGURES (Concluded)

LIST OF SYMBOLS

c	constant introduced in the α_H constraint (Eqs. (34) and (36))
c_t	constant introduced in the approximation for multicomponent thermal diffusion coefficients embodied in Eq. (26). Tentatively established by correlation of data to be -0.5
C	product of density and viscosity normalized by their reference values (defined by Eq. (45))
$\bar{C}_p$	frozen specific heat of the gas mixture (defined by Eq. (12))
$\tilde{C}_p$	property of the gas mixture which reduces to $\bar{C}_p$ when diffusion coefficients are assumed equal for all species (defined by Eq. (28))
C_{p_i}	specific heat of species i
d_0, d_1, d_2	coefficients defined in finite-difference representation of streamwise derivatives (defined in Eqs. (88) and (89) for two- and three-point difference relations, respectively)
$\bar{D}$	a reference binary diffusion coefficient introduced by the approximation for binary diffusion coefficients embodied in Eq. (19)
D_i^T	multicomponent thermal diffusion coefficient for species i
D_{ij}	multicomponent diffusion coefficient for species i and j
$\mathscr{D}_{ij}$	binary diffusion coefficient for species i and j
ERROR	errors for the various equations during Newton-Raphson iteration (driven toward zero in the iteration)
f	stream function (defined by Eq. (35))
F_i	diffusion factor for species i introduced by the approximation for binary diffusion coefficients embodied in Eq. (19)
h	static enthalpy of the gas (defined by Eq. (10))
h_w	static enthalpy of the gas at the wall
$\tilde{h}$	property of the gas mixture which reduces to the static enthalpy h when diffusion coefficients are assumed equal for all species (defined by Eq. (28))
h_c	enthalpy of surface material (e.g., char) removed by combustion, sublimation, or vaporization
h_g	enthalpy of gas which enters boundary layer without phase change <u>at the surface</u> (e.g., pyrolysis gases)
h_i	enthalpy of species i (defined by Eq. (11))
h_i^o	heat of formation

h_ℓ	enthalpy of ℓ^{th} component surface material (e.g., silica) removed in the condensed phase (e.g., by melting with subsequent liquid runoff or by spallation)
H_T	total enthalpy (defined by Eq. (9))
I	total number of species
j_i	diffusional mass flux of species i per unit area away from the surface
j_k	diffusional mass flux of element k per unit area away from the surface
K	one less than the number of elements (e.g., C, H, O, N) or other set of base gases (see footnote on page 27)
K_i	mass fraction of molecular species i
$\tilde{K}_{c_k}$	total mass fraction of element (or base gas) k contained in surface material (e.g., char) removed by combustion, sublimation, or vaporization
$\tilde{K}_{g_k}$	total mass fraction of element (or base gas) k contained in gas which enters boundary layer without phase change at the surface (e.g., pyrolysis gases)
$\tilde{K}_k$	total mass fraction of element (or base gas) k irrespective of molecular configuration (defined by Eq. (16))
$\tilde{K}_{\ell k}$	total mass fraction of element (or base gas) k contained in ℓ^{th} component of surface material (e.g., silica) which is removed in the condensed phase (e.g., by melting with subsequent liquid runoff or by spallation)
$K_{p_{eq}}(T_w)$	equilibrium constant
$\dot{m}$	mass flow rate per unit area
$\dot{m}_c$	mass removal rate per unit area of surface material (e.g., char) by combustion, sublimation, or vaporization
$\dot{m}_g$	mass flow rate per unit area of gas which enters boundary layer without phase change at the surface (e.g., pyrolysis gases)
$\dot{m}_{r_\ell}$	mass removal rate per unit area of ℓ^{th} component surface material (e.g., silica) in the condensed phase (e.g., by melting with subsequent liquid runoff or by spallation
$\mathcal{M}$	molecular weight of the gas mixture
$\mathcal{M}_i$	molecular weight of species i
N	number of nodal points across the boundary layer selected for the purpose of the numerical solution procedure
p	dummy variable representing f', H_T, or $\tilde{K}_k$
P	pressure
P_i	partial pressure of species i

Pr	frozen Prandtl number of the gas mixture (defined by Eq. (51))
q_a	diffusional heat flux per unit area away from the surface
q_{cond}	heat conduction per unit area into the surface material
q_r	one-dimensional radiant heat flux (toward the surface), that is, the net rate per unit area at which radiant energy is transferred across a plane in the boundary layer parallel to the surface
r_c	radius of curvature of a surface streamline
r_o	local radius of body in a meridian plane for an axisymmetric shape
R	universal gas constant
R_{eff}	effective nose radius for Newtonian flow
s	distance along body from stagnation point or leading edge
$\overline{Sc}$	reference system Schmidt number (defined by Eq. (46))
T	static temperature
u	velocity component parallel to body surface
v	velocity component normal to body surface
x_i	mole fraction of species i
$XP_1, XP_2, \ldots$	truncated series obtained in Taylor series expansion of $\int_{i-1}^{i} f'pd\eta$ (defined by Eqs. (86))
y	distance from surface into the boundary layer, measured normal to the surface
Z_i	a quantity for species i which is introduced as a result of the approximation for binary diffusion coefficients and reduces to K_i when all diffusion coefficients are assumed equal (defined by Eq. (21))
$\tilde{Z}_k$	a quantity for element (or base species) k which is introduced as a result of the approximation for binary diffusion coefficients and reduces to $\tilde{K}_k$ when all diffusion coefficients are assumed equal (defined by Eq. (25))
$ZP_1, ZP_2, \ldots$	truncated series obtained in Taylor series expansion of integrals involving nonsimilar terms (defined by Eq. (94))
α^*	flux normalizing parameter (defined by Eq. (44))
α_H	normalizing parameter used in definition of $\bar{\eta}$ (see Eq. (33) defined implicitly by use of a constraint such as Eq. (34)

LIST OF SYMBOLS (Continued)

α_{ki}	mass fraction of element (or base species) k in species i
β	streamwise pressure-gradient parameter (defined by Eq. (53))
$\ell^{\Delta}\ell-1$	logarithmic distance between two streamwise positions denoted by the subscripts ℓ and $\ell-1$ (defined by Eq. (90))
$\Delta f_i, \Delta f_i', \ldots$	corrections for f_i, f_i',... during Newton-Raphson iteration (defined by Eq. (115))
$\delta\eta$	distance between two boundary layer nodal points (defined by Eq. (74))
ϵ_w	emissivity of wall material
$\eta, \bar{\eta}$	transformed coordinate in a direction normal to the surface (defined by Eqs. (32) and (33)). Note: the bar is dropped from $\bar{\eta}$ throughout most of the report
λ	thermal conductivity
μ	shear viscosity
$\mu_1, \mu_2, \mu_3, \mu_4$	properties of the gas mixture (defined by Eqs. (22) and (28)) which reduce to unity, to m, to $1/m$, and to $\ell n\, m$, respectively, for assumed equal diffusion coefficients
ν	kinematic viscosity
$\xi, \bar{\xi}$	transformed streamwise coordinate (defined by Eqs. (31) and (33)). Note: the bar is dropped from $\bar{\xi}$ throughout most of the report
ρ	density
$\rho_w v_w$	total mass flux per unit area into the boundary layer
$\rho\epsilon_{D_i}$	turbulent eddy diffusivity (defined by Eq. (2))
$\rho\epsilon_H$	turbulent eddy conductivity (defined by Eq. (13))
$\rho\epsilon_M$	turbulent eddy viscosity (defined by Eq. (6))
σ	Stefan-Boltzmann constant
ϕ_k	elemental source term (see discussion following Eq. (25))
Ψ_i	rate of mass generation of species i per unit volume due to chemical reaction

Subscripts

C	pertains to the element carbon
C_3	pertains to the molecular species C_3
e	reference condition, usually taken as zero streamline from inviscid solution (synonymous with boundary-layer edge in the absence of an entropy layer)
edge	pertains to boundary-layer edge
i	pertains to the i^{th} species or to the i^{th} nodal point in the boundary layer, starting with i = 1 at the surface.
j	pertains to j^{th} species
k,kk,kkk	pertains to k^{th}, kk^{th}, and kkk^{th} element (or base species) respectively
ℓ	pertains to ℓ^{th} streamwise position
m	pertains to m^{th} iteration during the Newton-Raphson iteration process
n	pertains to the n^{th} nodal point, corresponding to the outer edge of the boundary layer solution
N	pertains to the element nitrogen
o	pertains to the stagnation point
w	pertains to wall

Superscripts

$\varkappa$	equal to unity for axisymmetric bodies and zero for two-dimensional bodies
*	signifies that quantity is normalized by α^* (e.g., $j_k^* = j_k/\alpha^*$)
'	represents partial differentiation with respect to η or $\bar{\eta}$ (usually η unless otherwise noted). Represents turbulent fluctuation in Section 2.

Matrix Notation

A_{ij}	coefficient of correction for j^{th} primary variable in Newton-Raphson recurrence formula for i^{th} equation prior to any matrix reduction (defined by Eq. (149))
AF_{ij}	coefficient of correction for j^{th} primary "linear" variable in Newton-Raphson recurrence formula for i^{th} FLUX prior to any matrix reduction (defined by Eq. (157))
AL_{ij}	coefficient of correction for j^{th} primary "linear" variable in Newton-Raphson recurrence formula for i^{th} linear equation prior to any matrix reduction (defined by Eq. (150))

$[AL_{FF}]$, $[AL_{HH}]$,...	coefficients of "linear" corrections $[\Delta VL_F]$, $[\Delta VL_H]$,... in Newton-Raphson recurrence formulas corresponding to linear equations L_F, L_H,... with errors $[EL_F]$ $[EL_H]$,... prior to any matrix reduction (defined by Fig. 3)
$[AL_{pp}]$	corresponds to any of the $[AL_{FF}]$, $[AL_{HH}]$,... defined in Fig. 3
ANL_{ij}	coefficient of correction for j^{th} primary "linear" variable in Newton-Raphson recurrence formula for i^{th} nonlinear equation prior to any matrix reduction (defined by Eq. (150))
$[ANL_{FF}]$, $[ANL_{FH}]$,...	coefficients of "linear" corrections $[\Delta VL_F]$, $[\Delta VL_H]$,... in Newton-Raphson recurrence formulas corresponding to nonlinear equations NL_F with errors $[ENL_F]$ prior to any matrix reduction (defined by Fig. 3)
BF_{ij}	coefficient of correction for j^{th} primary "nonlinear" variable in Newton-Raphson recurrence formula for i^{th} FLUX prior to any matrix reduction (defined by Eq. (157))
$\overline{BF}_{ij}$	coefficient of correction for j^{th} primary "nonlinear" variable in Newton-Raphson recurrence formula for i^{th} FLUX after the matrix reduction embodied in Eq. (159)
$[\overline{BF}_a]$	coefficients of the "nonlinear" corrections $[\Delta VNL_a]$ in the Newton-Raphson recurrence formulas corresponding to the FLUX equations after matrix reduction embodied in Eq. (159))
$[\overline{BF}_b]$	coefficients of the reduced set of "nonlinear" corrections $[\Delta VNL_b]$ in the Newton-Raphson recurrence formulas corresponding to the FLUX equations after matrix reduction embodied in Eq. (159)
$[\overline{\overline{BF}}_b]$	coefficients of the reduced set of "nonlinear" corrections $[\Delta VNL_b]$ in the Newton-Raphson recurrence formulas corresponding to the FLUX equations after matrix reduction embodied in Eq. (163)
BL_{ij}	coefficient of correction for j^{th} primary "nonlinear" variable in Newton-Raphson recurrence formula for i^{th} linear equation prior to any matrix reduction (defined by Eq. (150))
$[BL_{FF}]$, $[BL_{HH}]$,...	coefficients of "nonlinear" corrections $[\Delta VNL_F]$, $[\Delta VNL_H]$,... in Newton-Raphson recurrence formulas corresponding to linear equations L_F, L_H,... with errors $[EL_F]$, $[EL_H]$,... prior to any matrix reduction (defined by Fig. 3)
$[BL_{pp}]$	corresponds to any of the $[BL_{FF}]$, $[BL_{HH}]$,... defined in Fig. 3

LIST OF SYMBOLS (Continued)

BNL_{ij}	coefficient of correction for j^{th} primary "nonlinear" variable in Newton-Raphson recurrence formula for i^{th} nonlinear equation prior to any matrix reduction (defined by Eq. (150))
$\overline{BNL}_{ij}$	coefficient of correction for j^{th} primary "nonlinear" variable in Newton-Raphson recurrence formula for i^{th} nonlinear equation after the matrix reduction embodied in Eq. (153)
$[\overline{BNL}_a]$	coefficients of the "nonlinear" corrections $[\Delta VNL_a]$ in Newton-Raphson recurrence formulas corresponding to nonlinear equations after matrix reduction embodied in Eq. (153)
$[\overline{BNL}_b]$	coefficients of the reduced set of "nonlinear" corrections $[\Delta VNL_b]$ in the Newton-Raphson recurrence formulas corresponding to nonlinear equations after matrix reduction embodied in Eq. (153))
$[BNL_{FF}]$, $[BNL_{FH}]$,...	coefficients of "nonlinear" corrections $[\Delta VNL_F]$, $[\Delta VNL_H]$,... in Newton-Raphson recurrence formulas corresponding to nonlinear equations NL_F with errors $[ENL_F]$ prior to any matrix reduction (defined by Fig. 3). Similarly, the $[BNL_{HF}]$, $[BNL_{HH}]$,... correspond to equations NL_H, and so on.
$[C]$	coefficients of the reduced set of "nonlinear" corrections $[\Delta VNL_b]$ in Newton-Raphson recurrence formulas corresponding to the nonlinear wall boundary conditions after matrix reduction of the FLUX equations embodied in Eq. (163)
$[D]$	constants in nonlinear wall boundary conditions arising from matrix reduction of FLUX equations embodied in Eq. (164)
E_i	error for i^{th} equation during m^{th} iteration prior to any matrix reduction (defined by Eq. (149))
$\overline{EF}_i$	error for i^{th} FLUX during m^{th} iteration after the matrix reduction embodied in Eq. (160)
$\overline{\overline{EF}}_i$	error for i^{th} FLUX during m^{th} iteration after the matrix reduction embodied in Eq. (164)
EL_i	error for i^{th} linear equation during m^{th} iteration prior to any matrix reduction (defined by Eq. (150))
$[EL_F]$, $[EL_H]$,...	errors corresponding to linear equations L_F, L_H,... during m^{th} iteration prior to any matrix reduction (defined by Fig. 3)
$[EL_p]$	corresponds to any of the $[EL_F]$, $[EL_H]$,... defined in Fig. 3

ENL_i	error for i^{th} nonlinear equation during m^{th} iteration prior to any matrix reduction (defined by Eq. (150))
$\overline{ENL}_i$	error for i^{th} nonlinear equation during m^{th} iteration after the matrix reduction embodied in Eq. (154)
$[ENL_F]$, $[ENL_H]$,...	errors corresponding to nonlinear equations NL_F, NL_H,... during m^{th} iteration prior to any matrix reduction (defined by Fig. 3)
FLUX	refers to $-j^*_{k_w}$ and/or $-q^*_{a_w}$ in the event they are needed for nonlinear wall boundary conditions
L_F	linear boundary conditions and Taylor series expansions for f and its first and second derivatives prior to any matrix reduction
L_H	linear boundary conditions and Taylor series expansions for H_T and H'_T prior to any matrix reduction
L_K	linear boundary conditions and Taylor series expansions for k^{th} $\tilde{K}_k$ and $\tilde{K}'_k$ prior to any matrix reduction
NL_F	momentum equation evaluated between each neighboring pair of nodal stations, nonlinear edge boundary conditions for f' and f", and α_H constraint
NL_H	energy equation evaluated between each neighboring pair of nodal stations prior to any matrix reduction
NL_K	k^{th} elemental species equation evaluated between each neighboring pair of nodal stations prior to any matrix reduction
$[\Delta FLUX]$	corresponds to corrections in $-j^*_{k_w}$ and/or $-q^*_{a_w}$ (see FLUX)
ΔV_j	correction for j^{th} primary variable in Newton-Raphson recurrence formulas (defined by Eq. (149))
ΔVL_j	correction for j^{th} "linear" primary variable in Newton-Raphson recurrence formulas (defined by Eq. (150))
$[\Delta VL_F]$	corrections for the "linear" primary variables f_2, f_3,..., f_n, f'_w, f'_2,..., f'_n, f''_w, f''_2,..., f''_{n-1} in Newton-Raphson recurrence formulas (defined by Fig. 3)
$[\Delta VL_H]$	corrections for the "linear" primary variables H''_{T_n}, H_{T_2}, H_{T_3},..., H_{T_n}, H'_{T_w}, H'_{T_2},... H'_{T_n} in Newton-Raphson recurrence formulas (defined by Fig. 3)
$[\Delta VL_K]$	corrections for the "linear" primary variables $\tilde{K}''_{k_n}$ $\tilde{K}_{k_2}$, $\tilde{K}_{k_3}$,..., $\tilde{K}_{k_n}$, $\tilde{K}'_{k_w}$, $\tilde{K}'_{k_2}$,..., $\tilde{K}'_{k_n}$ for k^{th} elemental species in Newton-Raphson recurrence formulas (defined by Fig. 3)

LIST OF SYMBOLS (Concluded)

$[\Delta VL_p]$	corresponds to any of the $[\Delta VL_F]$, $[\Delta VL_H]$,... defined in Fig. 3
ΔVNL_j	correction for j^{th} "nonlinear" primary variable in Newton-Raphson recurrence formulas (defined by Eq. (150))
$[\Delta VNL_a]$	corrections for the "nonlinear" primary variables α_H, f_n'', f_w''', f_2''',..., f_n''', H_{T_w}'', H_{T_2}'',..., $H_{T_{n-1}}''$ and the $\tilde{K}_{k_w}''$, $\tilde{K}_{k_2}''$,..., $\tilde{K}_{k_{n-1}}''$ in the Newton-Raphson recurrence formulas
$[\Delta VNL_b]$	corrections to the reduced set of "nonlinear" primary variables f_w, H_{T_w}, and the $\tilde{K}_{k_w}$ in Newton-Raphson recurrence formulas
$[\Delta VNL_F]$	corrections for the "nonlinear" primary variables α_H, f_w, f_n'', f_w''', f_2''',..., f_n''' in the Newton-Raphson recurrence formulas (defined by Fig. 3)
$[\Delta VNL_H]$	corrections for the "nonlinear" primary variables H_{T_w}, H_{T_w}'', H_{T_2}'',..., $H_{T_{n-1}}''$ in Newton-Raphson recurrence formulas (defined by Fig. 3)
$[\Delta VNL_K]$	corrections for the "nonlinear" primary variables $\tilde{K}_{k_w}$, $\tilde{K}_{k_w}''$, $\tilde{K}_{k_2}''$,..., $\tilde{K}_{k_{n-1}}''$ for k^{th} elemental species in Newton-Raphson recurrence formulas (defined by Fig. 3)
$[\Delta VNL_p]$	corresponds to any of the $[\Delta VNL_F]$, $[\Delta VNL_H]$,... defined in Fig. 3

AN INTEGRAL-MATRIX METHOD FOR NONSIMILAR SOLUTION OF THE MULTICOMPONENT LAMINAR BOUNDARY LAYER

SECTION 1
INTRODUCTION

A computational procedure is described which is suitable for obtaining accurate numerical solutions of the nonsimilar multicomponent laminar boundary layer with arbitrary equilibrium or nonequilibrium chemical systems, unequal diffusion and thermal diffusion coefficients for all species, radiation absorption and emission, and a variety of surface boundary conditions including intimate coupling with transient charring-ablation energy and mass balances. A Fortran IV computer program has been developed in accordance with this analysis with the exceptions that 1) the chemical system is presently limited to equilibrium, with or without selected rate-controlled surface reactions or surface catalyzed reactions, and 2) radiation absorption and emission is not currently permitted. This computer program, designated BLIMP, for Boundary Layer Integral Matrix Procedure, is described in Ref. 1.

The computational procedure has been developed while attempting to take advantage of the most attractive features of other boundary-layer procedures. In light of the application of the procedure to be adopted, certain specific requirements seemed appropriate. In particular, minimization of the number of "nodal points" required to obtain a solution was judged to be of prime importance as a consequence of the relatively large times associated with state calculations for a general chemical environment and, in the streamwise direction, because of the desire to couple the boundary layer procedure to a transient internal conduction or ablation solution.

For a given accuracy, the number of necessary "nodal points" in the surface normal direction is controlled primarily by the nature of the functions which relate the dependent variables (and their derivatives) to the independent variable. Thus the continuous functions typically used in integral relations approaches require fewer "nodal points"* than the discontinuous functions implied by most finite difference approximations. In order to permit relatively flexible profiles, sets of connected cubics were selected to represent enthalpy, velocity, and elemental concentrations. The first and second derivatives of these cubics were made continuous at the connecting points. The advantages of such a "spline fit" are considered, for example, in Ref. 2.

*The term "nodal point" is meant to encompass the integral strips of Pallone[3] and the matching points used by Dorodnitsyn.[4]

If the general integral relations approach is followed, weighting functions must be selected. In the present study this selection was based primarily on the complexity of the resultant algebra. Studies were made using Dirac delta weighting functions (i.e., a differential approach*) and step weighting functions similar to those used by Pallone[3] which indicated,** when other aspects of the procedure were unchanged, no definite superiority in terms of accuracy or stability. Because all of the complexities introduced by the generalization of the thermodynamic and transport properties of the system occur within a divergence term, step weighting functions produce markedly simpler algebra and, consequently, were adopted for the present procedure.

In the past when relatively large spacing in the streamwise direction has been desired, iterative procedures have generally been used to assure accuracy and stability. In many instances[5,6] these procedures have treated the solution in a manner resembling those used for similar solutions but with the addition of finite difference representations for the nonsimilar terms, a procedure which eliminates the necessity of special starting techniques. Using this basic approach, the specific treatment adopted in the current study follows most closely the matrix procedure used by Leigh[6] wherein the iteration is a consequence of the solution of a set of linear and nonlinear algebraic relations. Whereas a special successive approximation procedure was used by Leigh, the general Newton-Raphson technique was used in the present procedure. This technique results in linearized coupling between all relations required to characterize the boundary layer, and thus assures a more general, rapid and stable iterative convergence.

The present document concentrates on the fluid mechanical aspects of the problem and describes the basic numerical solution procedure. The procedures employed for calculating the equilibrium state of the gas and suggested for including rate-controlled reactions are described elsewhere[7] since they are conveniently treated as subroutines to the basic boundary layer computational procedure. However, the terms which are directly involved in the boundary layer equations such as the "elemental source term" which arises from kinetic considerations are included in the present development. Similarly, radiation absorption and emission enters directly into the conservation equations only as a net radiation flux term in the energy equation. The calculation of this term could also be conveniently accomplished by a subroutine. A one-dimensional model for net radiation flux which represents an extension of the work of Cess[8] to allow an angular-dependent incident radiation flux at the boundary-layer edge is presented in Appendix E.

*This correspondence is pointed out by Dorodnitsyn.[4]

**The results of these studies are discussed in an appendix to this report.

Multicomponent transport properties are based on a newly developed approximation described in Ref. 9. Modification of the conservation equations as a consequence of this approximation is described herein. Finally, the procedures employed for coupling to a transient charring ablation program are described in Ref. 10.

The governing differential equations for laminar or turbulent flow are presented in Section 2. The laminar form of the equations are normalized by a modified Levy-Lees transformation in Section 3. The modification consists of a coordinate stretching parameter which permits the establishment of an efficient universal boundary layer nodal network. In Section 4, the transformed conservation equations are integrated and the connected-cubic functional relationships are introduced through truncated Taylor series expansions. The procedure utilized to solve these equations is described in Section 5. First, the Newton-Raphson linear recurrence formulas are developed. A matrix reduction procedure is then described which takes full advantage of the linear Taylor series expansions and simplifies the generalization of surface boundary conditions.

In Section 6, comparisons to other numerical solutions are shown for several uncoupled nonreacting boundary layer problems. Generally, 3- to 4-place accuracy is obtained for 7-point boundary-layer solutions, and the solution usually converges in 3 or 4 iterations. Solutions for chemically reacting boundary layers are presented in Section 7.

SECTION 2
BOUNDARY LAYER CONSERVATION EQUATIONS

In this section are presented the differential equations which govern laminar or turbulent flow in a planar or axisymmetric compressible boundary layer with mass addition, equilibrium or nonequilibrium chemical reactions, multicomponent diffusion, thermal diffusion, and radiation. Unequal diffusion and thermal diffusion coefficients for all diffusing pairs are in accordance with the unified approximation presented in Ref. 9. The equations derived are essentially an extension of those derived in Ref. 11 to include radiation, thermal diffusion, and unequal binary-diffusion coefficients. The diffusion introduced by pressure gradients and body forces are neglected.

The standard definitions of time-averaged turbulent quantities and relative order of magnitude are employed (Refs. 11 and 12). The turbulent transport terms are expressed in the Boussinesq form, that is, eddy viscosity, eddy diffusion, and eddy conductivity. Hence, all the terms in the equations

are time-averaged quantities and no need exists for using a superscript bar.* In the order-of-magnitude arguments, terms of the following types have been eliminated: 1) triple correlations, 2) derivatives of turbulent correlations parallel to the wall, and 3) correlations involving turbulent components of molecular transport mechanisms.

A mass balance of an individual species in a unit volume results in the relationship

$$\frac{1}{r_o^{\varkappa}} \frac{\partial}{\partial s} \left(\rho u K_i r_o^{\varkappa} \right) + \frac{\partial}{\partial y} \left(\rho v K_i \right) = \frac{\partial}{\partial y} \left(\rho \epsilon_{D_i} \frac{\partial K_i}{\partial y} - j_i \right) + \psi_i \tag{1}$$

where s and y are the streamwise and normal coordinates, respectively, u and v are the velocity components in the s and y directions, respectively, K_i is the mass fraction of species i, r_o is the radius of the body in a meridian plane for an axisymmetric shape, $\varkappa$ is zero for a flat plate and unity for a body of revolution, ρ is the density, ψ_i represents the rate of mass generation of species i per unit volume due to chemical reaction, $\rho\epsilon_{D_i}$ is defined in terms of the correlation of the fluctuating components of concentration and normal velocity, that is,

$$\rho\epsilon_{D_i} = - \frac{\overline{(\rho v)' K_i'}}{\partial K_i / \partial y} \tag{2}$$

and j_i is the mass-diffusion rate of species i due to molecular processes.

When Eq. (1) is summed over all the species in the system, utilizing

$$\sum_i \rho\epsilon_{D_i} \frac{\partial K_i}{\partial y} = \sum_i j_i = 0$$

which results from the definition of mass diffusion, and utilizing

$$\sum_i \psi_i = 0$$

*Accordingly, ρv represents $\overline{\rho v}$, not $\overline{\rho}\,\overline{v}$.

which results from conservation of mass, there results

$$\frac{1}{r_o^{\varkappa}} \frac{\partial \rho u r_o^{\varkappa}}{\partial s} + \frac{\partial \rho v}{\partial y} = 0 \tag{3}$$

which is the familiar global continuity equation.

When Eq. (3) is considered together with Eq. (1), the more conventional species conservation equation is obtained:

$$\rho u \frac{\partial K_i}{\partial s} + \rho v \frac{\partial K_i}{\partial y} = \frac{\partial}{\partial y} \left(\rho \epsilon_{D_i} \frac{\partial K_i}{\partial y} - j_i \right) + \psi_i \tag{4}$$

The streamwise momentum equation can be written as

$$\rho u \frac{\partial u}{\partial s} + \rho v \frac{\partial u}{\partial y} = \frac{\partial}{\partial y} \left[\rho (\nu + \epsilon_M) \frac{\partial u}{\partial y} \right] - \frac{\partial P}{\partial s} \tag{5}$$

where P is the pressure and the eddy viscosity is defined in terms of the Reynolds stresses of turbulent flow by

$$\rho \epsilon_M = - \frac{\overline{(\rho v)' u'}}{\partial u / \partial y} \tag{6}$$

The momentum equation for forces and fluxes normal to the surface is given by

$$\left(\frac{\partial P}{\partial y} \right)_s = \frac{\rho u^2}{r_c} \tag{7}$$

where r_c is the radius of curvature of a surface streamline.

The energy equation for this general system is

$$\rho u \frac{\partial H_T}{\partial s} + \rho v \frac{\partial H_T}{\partial y} = \frac{\partial}{\partial y} \left[\rho \left(\epsilon_M + \nu \right) \frac{\partial (u^2/2)}{\partial y} + \left(\lambda + \rho \epsilon_H \overline{C}_P \right) \frac{\partial T}{\partial y} \right.$$

(equation continued on next page)

(equation continued from previous page)

$$+\sum_i \left(\rho\epsilon_{D_i}\frac{\partial K_i}{\partial y} - j_i\right) h_i - \frac{RT}{\rho}\sum_i\sum_j \frac{x_i D_i^T}{\mathcal{M}_i \mathcal{D}_{ij}}\left(\frac{j_i}{K_i} - \frac{j_j}{K_j}\right) + q_r\Bigg] \quad (8)$$

where H_T is the total enthalpy (static plus kinetic)

$$H_T = h + \frac{u^2}{2} \quad (9)$$

h is the static enthalpy including chemical as well as sensible contributions

$$h = \sum_i K_i h_i \quad (10)$$

h_i is the static enthalpy of species i

$$h_i = \int_0^T C_{p_i}\, dT + h_i^o \quad (11)$$

T is the temperature, h_i^o is the heat of formation of species i, C_{p_i} is the specific heat of species i, $\overline{C}_p$ is the frozen specific heat of the gaseous mixture

$$\overline{C}_p = \sum_i K_i C_{p_i} \quad (12)$$

λ is the thermal conductivity, R is the gas constant, x_j is the mole fraction of species j, $\mathcal{M}_i$ is the molecular weight of species i, $\mathcal{D}_{ij}$ is the binary diffusion coefficient of species i into j, D_i^T is the multicomponent thermal diffusion coefficient of species i, the turbulent enthalpy-transport coefficient is defined by

$$\rho\epsilon_H = -\frac{\sum_i K_i \overline{(\rho v)' h_i'}}{\sum_i K_i (\partial h_i/\partial y)} \quad (13)$$

and q_r is the net one-dimensional energy flux towards the surface due to radiation absorption and emission.* In Eq. (8) the turbulent contribution to the DuFour effect (the double summation term) has been neglected since significant diffusion thermo occurs only in the laminar region where temperature gradients are severe.

When the assumption of equal diffusion coefficients is made, a substantial simplification of the problem results if the species conservation Equations (4) are multiplied by α_{ki}, defined as the mass fraction of element k in species i, and the resulting terms are summed over all species (known as the Shvab-Zeldovich transformation). When this is done, there is a reduction in the number of conservational equations from the number of species (typically 20 to 50) to the number of elements (usually 2 to 6). In addition, the resulting equations are simplified since the source terms are eliminated. Furthermore, elements vary more smoothly across the boundary layer than do the molecular species, and hence are better represented numerically. To illustrate, when all binary-diffusion coefficients are assumed equal and in the absence of thermal diffusion, the j_i can be expressed by Fick's law

$$j_i = -\rho \mathcal{D}_{12} \frac{\partial K_i}{\partial y} \tag{14}$$

Substituting this into Eq. (4) and performing the Shvab-Zeldovich transformation results in the following elemental conservation equations for the laminar or turbulent boundary layer:

$$\rho u \frac{\partial \tilde{K}_k}{\partial s} + \rho v \frac{\partial \tilde{K}_k}{\partial y} = \frac{\partial}{\partial y}\left[\rho(\epsilon_D + \mathcal{D}_{12}) \frac{\partial \tilde{K}_k}{\partial y}\right] \tag{15}$$

where $\tilde{K}_k$ is the mass fraction of element k in the system defined by

$$\tilde{K}_k \equiv \sum_i \alpha_{ki} K_i \tag{16}$$

It has also been assumed that all $\epsilon_{D_i} = \epsilon_D$.

When diffusion coefficients are not equal, Fick's law does not apply. The diffusional fluxes, j_i, must then be expressed in terms of multicomponent diffusion coefficients, $\mathcal{D}_{ij}$

*A model for q_r which allows an angular-dependent incident radiation flux at the boundary-layer edge is developed in Appendix E.

$$j_i = \frac{\rho}{m^2} \sum_{j \neq i} m_i m_j D_{ij} \frac{\partial x_j}{\partial y} - D_i^T \frac{\partial \ell n\, T}{\partial y} \tag{17}$$

or via the Stefan-Maxwell relations[13]

$$\frac{\partial x_i}{\partial y} = \sum_j \frac{x_i x_j}{\rho \mathcal{D}_{ij}} \left[\frac{j_j + D_j^T \frac{\partial \ell n\, T}{\partial y}}{K_j} - \frac{j_i + D_i^T \frac{\partial \ell n\, T}{\partial y}}{K_i} \right] \tag{18}$$

Utilization of the Stefan-Maxwell equations in conjunction with the species conservation equations is awkward even in the absence of thermal diffusion effects, since the diffusional flux, j_i, is expressed implicitly in terms of mole fractions and their gradients. Hence, use is often made of Eq. (17) together with the multicomponent diffusion coefficients, for example, in Refs. 14 through 16. However, each of the (I^2-I) multicomponent diffusion coefficients depends upon local concentrations and upon $(I^2-I)/2$ symmetric binary diffusion coefficients, $\mathcal{D}_{ij}$, where I is the total number of species being considered.

A bifurcation approximation to binary diffusion coefficients introduced by Bird[17] and utilized herein permits explicit solution of the Stefan-Maxwell relations for j_i in terms of gradients and properties of species i and of the system as a whole. The approximation can be expressed in the form:

$$\mathcal{D}_{ij} \approx \overline{D}/F_i F_j \tag{19}$$

with $\overline{D}(T,P)$ a property of the given multicomponent mixture and $F_i(T)$ a property of the i^{th} species in the mixture.* It is apparent when considering more than 3 species** that Eq. (19) is indeed approximate, since $(I^2-I)/2$ diffusion coefficients, $\mathcal{D}_{ij}$, are replaced by I diffusion factors, F_i. Equation (19) should thus be viewed as a correlation equation for actual binary diffusion coefficient data. The F_i are determined for a given chemical system by a least-squares fit of actual diffusion data.

*The effect of pressure can be absorbed entirely into the $\overline{D}$ since $\mathcal{D}_{ij}$ is inversely proportional to pressure. It will be shown that the dominant temperature effect can also be absorbed into the $\overline{D}$ so that the F_i are nearly constants for a given molecular set.

**Eq. (19) is exact for a ternary system.

The accuracy of the correlation was investigated by Bird[17] for a five component mixture containing hydrogen and shown to be surprisingly good, the maximum error in any $\mathscr{D}_{ij}$ being 4 percent. In order to establish more generally the adequacy of the approximation, correlations were performed for several chemical systems including a 16-component (120 $\mathscr{D}_{ij}$) C-H-O-N system.[9] These studies have demonstrated that Eq. (10) has general applicability, and represents the $\mathscr{D}_{ij}$ for nearly all diffusing pairs within 5 percent. The largest single error in $\mathscr{D}_{ij}$ obtained in these correlations has never exceeded 15 percent or so.

Introducing this approximation into the Stefan-Maxwell relations, it is shown in Ref. 9 that the j_i can be expressed explicitly as

$$j_i = -\left\{ \frac{\rho \bar{D} \mu_2}{\mu_1 \mathscr{M}} \left[\frac{\partial z_i}{\partial y} + (z_i - K_i) \frac{\partial \ell n\, \mu_2}{\partial y} + \frac{K_i \mathscr{M}}{\mu_2} \left(\frac{1}{F_i} \frac{d\, \ell n\, F_i}{d\, \ell n\, T} - \sum_j \frac{K_j}{F_j} \frac{d\, \ell n\, F_j}{d\, \ell n\, T} \right) \frac{\partial\, \ell n\, T}{\partial y} \right] + D_i^T \frac{\partial\, \ell n\, T}{\partial y} \right\} \tag{20}$$

where z_i is a quantity which for unequal diffusion lies between a mass and a mole fraction and is defined by

$$z_i \equiv \frac{\mathscr{M}_i x_i}{F_i \mu_2} \tag{21}$$

and μ_1 and μ_2 are system quantities defined by

$$\mu_1 \equiv \sum_j x_j F_j \qquad \mu_2 \equiv \sum_j \frac{\mathscr{M}_j x_j}{F_j} \tag{22}$$

It can be seen from Eqs. (21) and (22) that $\sum z_i = 1$. When diffusion coefficients are assumed equal, setting $F_i = 1$ yields $z_i = K_i$, $\mu_1 = 1$, and $\mu_2 = \mathscr{M}$.

In Ref. 9 it was observed that the F_i are weak functions of temperature. Thus Eq. (20) can often be simplified to

$$j_i = -\left\{\frac{\rho\bar{D}\mu_2}{\mu_1 \mathcal{M}}\left[\frac{\partial Z_i}{\partial y} + (Z_i - K_i)\frac{\partial \ell n\, \mu_2}{\partial y}\right] + D_i^T \frac{\partial \ell n\, T}{\partial y}\right\} \tag{23}$$

Substituting Eq. (23) into the boundary-layer species conservation equation (Eq. (4)) and performing the Shvab-Zeldovich transformation yields[9] the following conservation equations for chemical elements in a multicomponent, laminar or turbulent boundary layer with unequal diffusion coefficients:

$$\rho u \frac{\partial \tilde{K}_k}{\partial s} + \rho v \frac{\partial \tilde{K}_k}{\partial y} = \frac{\partial}{\partial y}\left\{\rho \epsilon_D \frac{\partial \tilde{K}_k}{\partial y} + \frac{\rho\bar{D}\mu_2}{\mu_1 \mathcal{M}}\left[\frac{\partial \tilde{Z}_k}{\partial y} + (\tilde{Z}_k - \tilde{K}_k)\frac{\partial \ell n\, \mu_2}{\partial y}\right] + \sum_i \alpha_{ki} D_i^T \frac{\partial \ell n\, T}{\partial y}\right\} + \phi_k \tag{24}$$

where $\tilde{K}_k$ is defined by Eq. (16) and

$$\tilde{Z}_k \equiv \sum_i \alpha_{ki} Z_i \tag{25a}$$

$$\phi_k \equiv \sum_i \alpha_{ki} \psi_i \tag{25b}$$

The term ϕ_k requires some discussion. Introduction of the Shvab-Zeldovich transformation eliminates the chemical production terms ψ_i when the boundary layer is everywhere in local equilibrium since ψ_k is then equal to zero. With the introduction of nonequilibrium, the approach of Ref. 7 generalizes the term "element" and results in an expanded (in terms of "elements", k) α_{ki} array, taking advantage of all equilibrium aspects of the system. As a consequence, the ϕ_k may no longer equal zero and thus cannot, in general, be omitted from Eq. (24). This general mixed equilibrium, nonequilibrium approach results in more equations of the form of Eq. (24) than in the purely equilibrium system. Except in the limit of all reactions being kinetically controlled, the number of equations of the form of Eq. (24) is, however, less than the number of molecular

conservation equations (Eq. (4)). The local state of the gas for this nonequilibrium system is defined in terms of the expanded set of "elements". The production or destruction rates, ϕ_k, of these "elements" becomes a state property and can be evaluated along with other local system properties.

It should be noted that the Shvab-Zeldovich transformation is still possible without the approximation for $\mathcal{D}_{ij}$ embodied in Eq. (19), but solution then depends upon (I^2-I) multicomponent diffusion coefficients, each of which depends upon $(I^2-I)/2$ symmetric binary diffusion coefficients and upon concentrations of all species. Therefore, use of the approximation for $\mathcal{D}_{ij}$ embodied in Eq. (19) should be looked upon as a computational convenience.

At this point the multicomponent thermal diffusion coefficients, D_i^T, still appear in the conservation relations. Theoretical equations for D_i^T are quite complicated[13] and these have to be solved at every boundary-layer point since they are strongly concentration dependent. Therefore, a correlation of binary thermal diffusion data was conducted[9] which yielded, upon generalization to multicomponent systems, the following simple relation:

$$D_i^T \approx \frac{c_t \rho \bar{D} \mu_2}{\mu_1 \mathcal{M}} (Z_i - K_i) \tag{26}$$

with the empirical constant c_t about -0.5. This approximation for D_i^T satisfies the requirement that they sum to zero,[13] the observation that they are independent of fluxes, and the assumption that thermal diffusion of species i should behave nearly as though it were in a system of species i and a species representative of the mixture as a whole. The approximation represents binary thermal diffusion data reasonably well (within 10 percent or so, considering a wide range of molecular weights and variation of mass fractions from zero to 100 percent). An accuracy study of multicomponent D_i^T has not yet been accomplished. However, the generalizations which were employed appear to be in basic accord with the approximate model for multicomponent thermal diffusion coefficients developed by Laranjeira.[18]

Inserting this approximation into Eqs. (24) and (8) and performing all summations yields the following relations for diffusive mass flux of species i, j_i, diffusive mass flux of element k, j_k, and diffusive heat flux, q_a, respectively

$$j_i = -\frac{\rho \bar{D} \mu_2}{\mu_1 \mathcal{M}} \left[\frac{\partial Z_i}{\partial y} + (Z_i - K_i) \frac{\partial \mu_4}{\partial y} \right] \tag{27a}$$

$$j_k = -\frac{\rho \bar{D} \mu_2}{\mu_1 \mathcal{M}} \left[\frac{\partial \tilde{Z}_k}{\partial y} + (\tilde{Z}_k - \tilde{K}_k) \frac{\partial \mu_4}{\partial y} \right] \tag{27b}$$

$$q_a = -\left\{ \rho(\varepsilon_M + \nu) \frac{\partial (u^2/2)}{\partial y} + (\lambda + \rho \varepsilon_H \bar{C}_p) \frac{\partial T}{\partial y} + \rho \varepsilon_D \left(\frac{\partial h}{\partial y} - \bar{C}_p \frac{\partial T}{\partial y} \right) \right.$$
$$\left. + \frac{\rho \bar{D} \mu_2}{\mu_1 \mathcal{M}} \left[\frac{\partial \tilde{h}}{\partial y} - \left(\tilde{C}_p + \frac{c_t^2 R}{\mu_1 \mu_2} \right) \frac{\partial T}{\partial y} + c_t R T \frac{\partial \mu_3}{\partial y} + (\tilde{h} - h + c_t R T \mu_3) \frac{\partial \mu_4}{\partial y} \right] \right\} \tag{27c}$$

where

$$\left.\begin{aligned} \tilde{C}_p &\equiv \sum_i Z_i C_{p_i} \qquad & \tilde{h} &\equiv \sum_i Z_i h_i \\ \mu_3 &\equiv \sum_i \frac{Z_i}{\mathcal{M}_i} \qquad & \mu_4 &\equiv \ell n (\mu_2 T^{c_t}) \end{aligned}\right\} \tag{28}$$

The elemental species conservation equation thus becomes

$$\rho u \frac{\partial \tilde{K}_k}{\partial s} + \rho v \frac{\partial \tilde{K}_k}{\partial y} = \frac{\partial}{\partial y} \left\{ \rho \varepsilon_D \frac{\partial \tilde{K}_k}{\partial y} - j_k \right\} + \phi_k \tag{29}$$

while the energy equation can be expressed as

$$\rho u \frac{\partial H_T}{\partial s} + \rho v \frac{\partial H_T}{\partial y} = \frac{\partial}{\partial y} \left\{ - q_a + q_r \right\} \tag{30}$$

Equations (27a) through (27c) are derived in Appendix A. For assumed equal diffusion coefficients, $\mu_3 = 1/\mathcal{M}$, $\tilde{C}_p = \bar{C}_p$, and $\tilde{h} = h$. When thermal diffusion is to be neglected $c_t = 0$ and $\mu_4 = \ell n\, \mu_2$.

Equations (3), (5), (7), (29), and (30) comprise the boundary-layer conservation equations incorporating the approximations for unequal thermal and multicomponent diffusion coefficients embodied in Eqs. (19) and (26). It

should be emphasized that the numerical solution procedure described in a later section is not dependent upon the use of these convenient approximations.

Any consistent set of boundary conditions can be applied which yield, in effect, u/u_e, H_T, and the $\tilde{K}_k$ and their first derivatives at the edge of the boundary layer, and wall values of u/u_e, mass flux, H_T (or its gradient), and the $\tilde{K}_k$ (or their gradients). Specific boundary conditions will be introduced in Section 3.

The mathematical specification of the boundary-layer problem is completed by introduction of the remaining multicomponent transport properties, the equation of state for a gaseous mixture, the equilibrium relations, and the kinetic relations. These are described in Refs. 7 and 9.

SECTION 3

THE TRANSFORMED NONSIMILAR LAMINAR BOUNDARY-LAYER EQUATIONS

From the original formulations of Blasius, a continuing effort has been expended in the search for more general means of reducing the partial-differential equations of the boundary layer to total-differential equations. Basically, this involves the search for a new coordinate system (η,ξ) related to the original system (y,s) and certain of the dependent variables, in which the ξ-wise variations of functions of the dependent variable either vanish or become of second order. A successful similarity transformation, as this is called, results in ξ-derivatives vanishing, but this occurs only under certain conditions which are generally quite restrictive. Currently, the most popular transformation represents a combination of the Levy and Mangler and the Howarth-Dorodnitsyn transformations. This particular form was suggested by Lees (Ref. 19) among others, and is known by a variety of names including Lees-Dorodnitsyn, Levy-Lees, Mangler-Dorodnitsyn, and Dorodnitsyn-Stepanov. This transformation is as follows:

$$\xi = \int_0^s u_e \rho_e \mu_e r_o^{2\kappa}\, ds \tag{31}$$

$$\eta = \frac{r_o^{\kappa} u_e}{\sqrt{2\xi}} \int_0^y \rho\, dy \tag{32}$$

where, in this and subsequent equations, the subscripts w and e refer, respectively, to the wall and to a reference condition which can be taken as the boundary-layer edge in the absence of an entropy layer (to be discussed).

In this section, a slightly modified form of this transformation is applied to the laminar form of the boundary-layer conservational equations presented in Section 2. Although the boundary-layer equations remain partial-differential equations when the nonsimilar terms are retained, the Levy-Lees transformation is still quite advantageous, since it aids in the specification of the boundary conditions, it eliminates the global conservation equation from the set of relations to be solved, and it normalizes the boundary-layer thickness. In addition, the nonsimilar terms are often small; hence, they can be investigated individually and eliminated for certain classes of problems.

If the conventional Levy-Lees transformation embodied in Eqs. (31) and (32) is utilized, the transformed boundary-layer thickness is uniform for a similar boundary layer. However, when the boundary layer is highly nonsimilar (e.g., as a result of large blowing or suction, severe pressure gradients, or surface discontinuities) the transformed boundary-layer thickness can vary by a factor of two or more. Therefore, it is useful to normalize the boundary layer further by stretching the η coordinate:

$$\bar{\xi} = \xi \qquad \bar{\eta} = \frac{\eta}{\alpha_H} \tag{33}$$

where α_H is a function of $\bar{\xi}$ only and is determined implicitly during the numerical solution. This makes possible the efficient use of a universally applicable nodal network which can be chosen a priori once and for all. The use of such a universal nodal network is highly desirable as the linearity of a large body of equations (Taylor series expansions of primary variables) during the numerical solution procedure is retained. In addition, it reduces the variation of boundary-layer parameters along a grid line from one streamwise station to the next.

Since a new variable $\alpha_H(\bar{\xi})$ is introduced, an additional relation is required. This is conveniently supplied by constraining an internal nodal point near the boundary-layer edge, $\bar{\eta}_c$, to have a specified streamwise velocity, c, near (but something less than) the edge value:

$$f'\Big|_{\bar{\eta}_c} = cf'\Big|_{\bar{\eta}_e} \tag{34}$$

where f is the stream function defined as

$$f - f_w = \int_0^{\eta} \frac{u}{u_e} d\eta = \alpha_H \int_0^{\bar{\eta}} \frac{u}{u_e} d\bar{\eta} \tag{35}$$

and the prime denotes partial differentiation with respect to $\bar{\eta}$, so that

$$f' = \alpha_H \frac{u}{u_e} \tag{36}$$

To illustrate, selection of $\bar{\eta}_e = 4.0$, $\bar{\eta}_c = 2.4$, and $c = 0.90$ yields $\alpha_H \approx 1.0$ for the Blasius problem (incompressible flow along a flat plate at zero incidence with no mass addition). The $f'|_{\eta e}$ is utilized in Eq. (34) in anticipation that the u/u_e may not be unity at the edge of the boundary layer for superorbital reentry problems involving an entropy layer or nonadiabatic flow field.

In order to illustrate further the procedure, two extreme velocity distributions are compared in Figure 1 to the Blasius solution. The profiles shown are those for a boundary layer near separation and one near blowoff. These were calculated using the integral matrix method for numerical solution of the boundary layer (described later). It can be seen that by the use of the transformation (Eq. (33)) together with the arbitrarily chosen constraint (Eq. (34)) that the boundary-layer edge occurs at about the same value of $\bar{\eta}$ for the three problems. It should be noted that this is accomplished with little mathematical complexity; only two terms involving derivatives of α_H appear (both in the momentum equation).

Variation of α_H with Reynolds number (proportional to ξ) is shown in Figure 2 for a nonsimilar boundary layer with constant blowing and one with constant suction. These results were also obtained using the integral matrix technique. The behavior of α_H is indicative of the increase (and decrease) of the η at the edge of the boundary layer. The desirability of the stretching transformation is made apparent by this example. Without the use of the transformation to $\bar{\eta}$, the choice of an η_{max} sufficiently large to characterize accurately the boundary layer at large distances from the leading edge would be inefficient near the leading edge. Furthermore, it would be required to make an estimate for η_{max} as it is not known a priori.

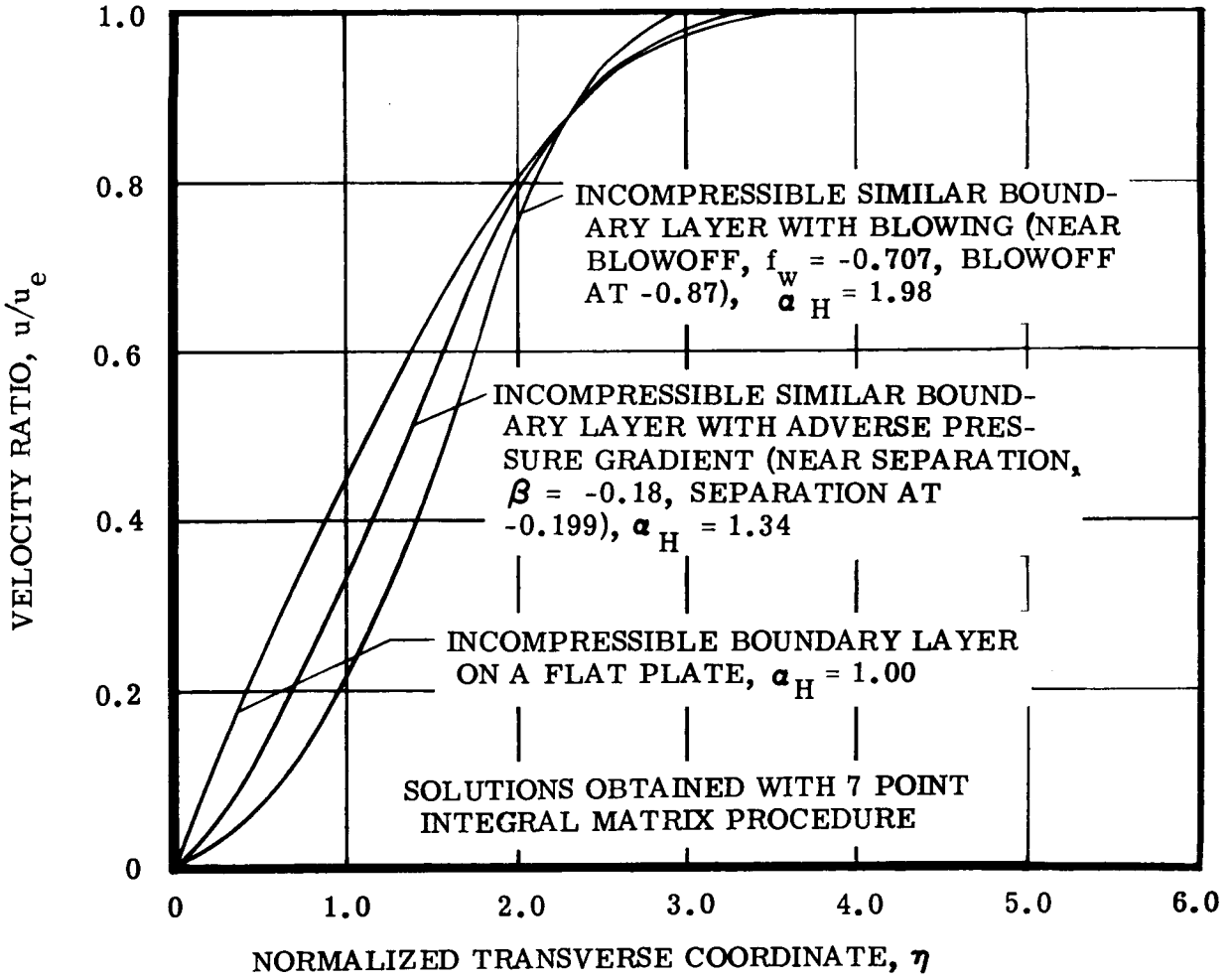

Figure 1. Several Velocity Profiles in Terms of $\bar{\eta}$ with the Velocity Ratio Constrained to be 0.90 at $\bar{\eta}$ = 2.4

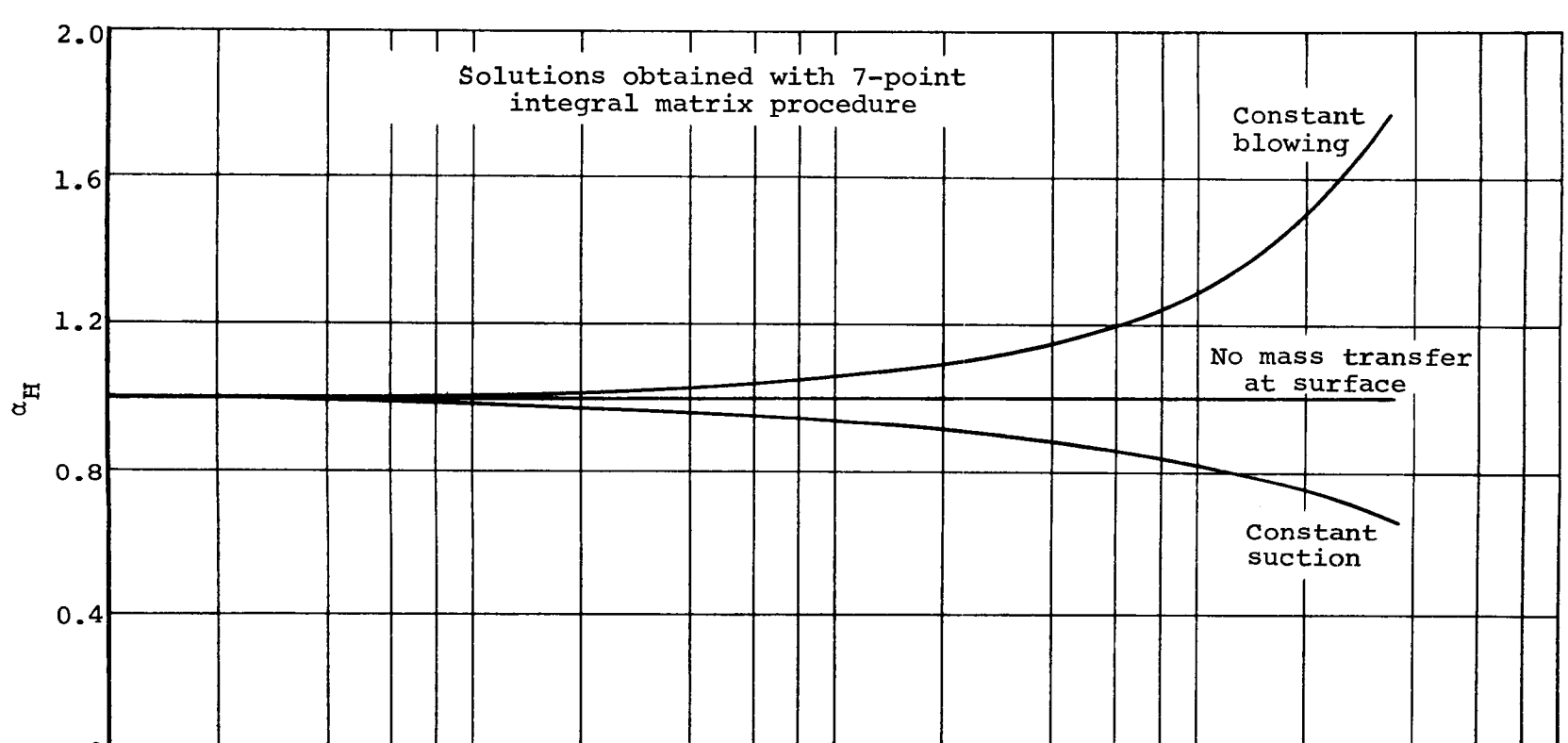

Figure 2. Variation of α_H with Reynolds number for Incompressible Boundary Layers with Constant Blowing and Suction, $\rho_w v_w / \rho_e u_e = 1 \times 10^{-3}$

Transformation of the independent variables s and y into the Levy-Lees variables ξ and η is conveniently accomplished through the use of the operator

$$\rho u \frac{\partial}{\partial s} + \rho v \frac{\partial}{\partial y} = \rho\rho_e u_e^{\,a} \mu_e r_o^{\,a\kappa} \left[f' \frac{\partial}{\partial \xi} - \left(\frac{f}{2\xi} + \frac{\partial f}{\partial \xi} \right) \frac{\partial}{\partial \eta} \right] \tag{37}$$

In addition, the partial derivatives are given by

$$\left(\frac{\partial}{\partial s} \right)_y = \rho_e u_e \mu_e r_o^{\,a\kappa} \left(\frac{\partial}{\partial \xi} \right)_\eta + \left(\frac{\partial \eta}{\partial s} \right)_y \left(\frac{\partial}{\partial \eta} \right)_\xi \tag{38}$$

$$\left(\frac{\partial}{\partial y} \right)_s = \frac{u_e r_o^{\,\kappa} \rho}{(2\xi)^{1/a}} \left(\frac{\partial}{\partial \eta} \right)_\xi \tag{39}$$

where

$$\left(\frac{\partial}{\partial \xi} \right)_\eta = \left(\frac{\partial}{\partial \bar{\xi}} \right)_{\bar{\eta}} - \frac{\bar{\eta}}{\alpha_H} \frac{d\alpha_H}{d\bar{\xi}} \left(\frac{\partial}{\partial \bar{\eta}} \right)_{\bar{\xi}} \tag{40}$$

$$\left(\frac{\partial}{\partial \eta} \right)_\xi = \frac{1}{\alpha_H} \left(\frac{\partial}{\partial \bar{\eta}} \right)_{\bar{\xi}} \tag{41}$$

Equations (37) through (41) are derived in Appendix B.

Utilization of Eqs. (37) through (41) results in the following transformed equations for diffusive fluxes and conservation of momentum, elemental species, and energy in a laminar compressible nonsimilar boundary layer with mass addition, chemical reactions, and unequal diffusion and thermal diffusion coefficients (using the approximations embodied in Eqs. (19) and (26)). These equations are derived in Appendix B. Throughout the remainder of this document the bar is dropped from $\bar{\xi}$, $\bar{\eta}$ and the prime refers to partial differentiation with respect to $\bar{\eta}$ except when noted otherwise:

Diffusive flux of i^{th} species

$$j_i = \alpha^* j_i^* \tag{42}$$

where j_i^* is a normalized diffusive flux of species i

$$j_i^* = - \frac{C}{\alpha_H \overline{Sc}} \left[Z_i' + (Z_i - K_i)\mu_4' \right] \tag{43}$$

α^* is the normalizing parameter defined by

$$\alpha^* \equiv \frac{\rho_e u_e \mu_e r_o^{\kappa}}{(2\xi)^{1/2}} \tag{44}$$

C is defined by

$$C \equiv \frac{\rho\mu}{\rho_e \mu_e} \tag{45}$$

and $\overline{Sc}$ is a system property defined by

$$\overline{Sc} \equiv \frac{\mu_1 \mu \mathcal{M}}{\rho \bar{D} \mu_2} \tag{46}$$

The $\overline{Sc}$ is a Schmidt number based on the self diffusion coefficient for a ficticious species representative of the system as a whole.

Diffusive flux of k^{th} elemental species

$$j_k = \alpha^* j_k^* \tag{47}$$

where j_k^* is a normalized diffusive flux of element k

$$j_k^* = -\frac{C}{\alpha_H \overline{Sc}} \left[\tilde{Z}_k' + (\tilde{Z}_k - \tilde{K}_k)\mu_4' \right] \tag{48}$$

Diffusive heat flux

$$q_a = \alpha^* q_a^* \tag{49}$$

where q_a^* is a normalized diffusive heat flux

$$q_a^* = -\frac{C}{\alpha_H} \left(\frac{f'f'' u_e^2}{\alpha_H^2} + \frac{\bar{C}_p T'}{Pr} \right) - \sum_j j_j^* \left(h_j + \frac{c_t RT}{\mathcal{M}_j} \left(1 - \frac{F_j}{\mu_1} \right) \right)$$

$$= -\frac{C}{\alpha_H} \left[\frac{f'f''}{\alpha_H^2} u_e^2 + \frac{\bar{C}_p}{Pr} T' + \frac{1}{\overline{Sc}} \left(\tilde{h}' - \left(\tilde{C}_p + \frac{c_t^2 R}{\mu_1 \mu_2} \right) T' \right. \right.$$

$$\left. \left. + c_t RT\mu_3' + (\tilde{h} - h + c_t RT\mu_3)\mu_4' \right) \right] \tag{50}$$

and Pr is the Prandtl number based on the frozen specific heat

$$Pr \equiv \frac{\bar{c}_p \mu}{\lambda} \tag{51}$$

Streamwise momentum equation

$$ff'' + \left[\frac{Cf''}{\alpha_H}\right]' - \frac{2\xi\alpha_H^2}{\rho u_e^2}\left\{\frac{\partial P}{\partial \xi} - P'\frac{\eta}{\alpha_H}\frac{d\alpha_H}{d\xi} + P'\alpha_H\left[\frac{\partial}{\partial \xi}\left(\frac{r_o^{\kappa} u_e}{\alpha_H (2\xi)^{1/2}}\int_o^y \rho\, dy\right)\right]_y\right\} - \beta f'^2$$

$$= 2\left(f'\frac{\partial f'}{\partial \ell n\, \xi} - f''\frac{\partial f}{\partial \ell n\, \xi} - f'^2\frac{d \ell n\, \alpha_H}{d \ell n\, \xi}\right) \tag{52}$$

where β is the streamwise pressure-gradient parameter

$$\beta \equiv 2\frac{d \ell n\, u_e}{d \ell n\, \xi} \tag{53}$$

Normal momentum equation

$$P' - \frac{u_e (2\xi)^{1/2} (f')^2}{\alpha_H r_c r_o^{\kappa}} = 0 \tag{54}$$

In the present study it will be assumed that the pressure is constant across the boundary layer. Equation (54) is therefore replaced by that statement, and the partial derivatives of pressure in Eq. (52) can be changed to a total derivative. Also, from the compressible Bernoulli equation, Eq. (52) becomes

Streamwise momentum equation (P = P(ξ) only)

$$ff'' + \left[\frac{Cf''}{\alpha_H}\right]' + \beta\left(\alpha_H^2\frac{\rho_e}{\rho} - f'^2\right)$$

$$= 2\left(f'\frac{\partial f'}{\partial \ell n\, \xi} - f''\frac{\partial f}{\partial \ell n\, \xi} - f'^2\frac{d \ell n\, \alpha_H}{d \ell n\, \xi}\right) \tag{55}$$

Energy equation

$$fH_T' + \left[-q_a^* + q_r^*\right]' = 2\left(f' \frac{\partial H_T}{\partial \ell n\, \xi} - H_T' \frac{\partial f}{\partial \ell n\, \xi}\right) \tag{56}$$

where q_a^* is the normalized diffusive heat flux away from the surface given by Eq. (50) and q_r^* is the normalized radiant heat flux toward the surface

$$q_r^* = q_r/\alpha^* \tag{57}$$

where α^* is given by Eq. (44).

Elemental species equations

$$f\tilde{K}_k' + \left[-j_k^*\right]' + \alpha_H \phi_k = 2\left(f' \frac{\partial \tilde{K}_k}{\partial \ell n\, \xi} - \tilde{K}_k' \frac{\partial f}{\partial \ell n\, \xi}\right) \tag{58}$$

where j_k^* is given by Eq. (48). The transformation also yields the following relations between f_w and $\rho_w v_w$ (see Appendix B):

$$\rho_w v_w = -\alpha^* \left(f_w + 2\xi \frac{df_w}{d\xi}\right) \tag{59}$$

where α^* is the normalizing parameter defined by Eq. (44) or, equivalently

$$f_w = -(2\xi)^{-\frac{1}{2}} \int_o^{\xi} \frac{\rho_w v_w d\xi}{\rho_e u_e \mu_e r_o^{\varkappa}} \tag{60}$$

When certain groupings of parameters are constant so that the similarity assumption is valid, the terms on the right-hand side of the conservation equations (Eqs. (52) or (55), (56) and (58)) vanish, in which case the conservation equations become ordinary differential equations. It should be emphasized that the equations as presented herein are equivalent to the corresponding boundary-layer equations presented in Section 2. That is, no similarity assumptions have been made in their development.

Equations (44), (53), and (60) for α^*, β, and f_w, respectively, are indeterminant at the stagnation point of a blunt body. Special forms for these equations valid at the stagnation point are shown in Appendix C to be given by

$$\alpha_o^* = \left(\rho_e \mu_e \frac{du_e}{ds} \Big/ \beta\right)_o^{\frac{1}{2}} \tag{44a}$$

$$f_{w_o} = -(\rho_w v_w/\alpha^*)_o \tag{60a}$$

where for Newtonian flow

$$\beta_o = 1/(\varkappa + 1) \tag{53a}$$

and

$$\left.\frac{du_e}{ds}\right|_o = (2p/\rho)_o^{\frac{1}{2}} \Big/ R_{eff}$$

with R_{eff} an effective nose radius taking into account the shock shape. Alternatively, β_o and $(du_e/ds)_o$ can be computed from curve fits of the inviscid pressure distribution.

In addition, in order to improve the accuracy of numerical integration procedures in the nose region, ξ and f_w can be computed by the following relations

$$\xi = \frac{1}{2(\varkappa + 1)} \int_o^{s^{2\varkappa+2}} \left[\rho_e \mu_e \left(\frac{u_e}{s}\right)\left(\frac{r_o}{s}\right)^{2\varkappa}\right] d(s^{2\varkappa+2}) \tag{31a}$$

$$f_w = -\frac{(2\xi)^{-\frac{1}{2}}}{(\varkappa + 1)} \int_o^{s^{\varkappa+1}} \left[\rho_w v_w \left(\frac{r_o}{s}\right)^{\varkappa}\right] d(s^{\varkappa+1}) \tag{60b}$$

which take advantage of the fact that u_e/s and r_o/s vary more nearly linearly in the stagnation region than do u_e and r_o. Equations (31a) and (60b) are also derived in Appendix C. Of course, the original Equations (31) and (60) are more applicable on the afterbody.

The surface boundary conditions can assume numerous forms. The simplest of these are the requirement of zero slip at the surface which yields

$$f_w' = 0 \tag{61}$$

and assignment* of numerical values for $\rho_w v_w$ (or f_w), h_w (or T_w), and $\tilde{\kappa}_{k_w}$. In the event that $\rho_w v_w$ is assigned, the f_w can be calculated by use of Eq. (60). Alternatively, Eq. (61) can be utilized together with the assignment of wall mass diffusive fluxes, j_{k_w}, and h_w (or T_w) or with the assignment

*It is physically unrealistic in most cases to assign $\tilde{\kappa}_{k_w}$ when diffusion coefficients are unequal since the contribution to $\tilde{\kappa}_{k_w}$ by preferential diffusion of the various elements to the surface is not known a priori.

of wall mass diffusive fluxes and the requirement that the surface material either be in equilibrium with the gas adjacent to the surface or satisfy surface reaction kinetic relations. (Surface chemistry considerations are discussed in Ref. 7.)

Additional wall boundary conditions of interest admit the addition of chemically active species arising from the pyrolysis of an internally decomposing material, surface combustion or phase change, and liquid-layer removal. In this case $\rho_w v_w$ (and thus f_w by means of Eq. (60)), f'_w, H_{T_w} and $\tilde{K}_{k_w}$ are supplied through surface chemistry considerations, the zero slip condition (Eq. (61)), an energy balance, and elemental mass balances.

The surface energy and elemental mass balances are supplied by transient internal conduction solutions such as those described in Ref. 20. The procedure for accomplishing this is discussed in Ref. 10. The resultant equation for the surface energy balance is given by

$$\dot{m}^*_g h_g + \dot{m}^*_c h_c - \sum_\ell \dot{m}^*_{r_\ell} h_\ell - (\rho_w v_w)^* h_w - q^*_{a_w} + q^*_{r_w} - q^*_{cond} = 0 \qquad (62)$$

where $\dot{m}_g$ is the mass flow rate per unit area and h_g the enthalpy of gas which enters the boundary layer without phase change <u>at the surface</u> (e.g., pyrolysis gases), $\dot{m}_g{}^*$ is a normalized $\dot{m}_g$ given by $\dot{m}_g{}^* = \dot{m}_g/\alpha^*$ (typical), $\dot{m}_c$ is the mass removal rate per unit area and h_c the enthalpy of surface material (e.g., char) removed by chemical reactions or phase change. $\dot{m}_{r_\ell}$ is the mass removal rate per unit area and h_ℓ the enthalpy of that material which is removed in the condensed phase (e.g., by melting with subsequent liquid run-off or by mechanical spallation). h_w is the enthalpy of the gas phase at the wall, $q^*_{a_w}$ is the normalized diffusive heat flux away from the wall (Eq. (50) evaluated at the wall), q_{r_w} is the net radiative flux to the wall (including reradiation from the surface), and $q_{cond} = \lambda_w(\partial T/\partial y)_w$ is conduction into the surface material (with λ_w the thermal conductivity of the surface material). The elemental mass balances are given by

$$\dot{m}^*_g \tilde{K}_{g_k} + \dot{m}^*_c \tilde{K}_{c_k} - \sum_\ell \dot{m}^*_{r_\ell} \tilde{K}_{\ell k} - (\rho_w v_w)^* \tilde{K}_{k_w} - j^*_{k_w} = 0 \qquad (63)$$

where the subscripts g, c, r and w and the asterisk have the same meaning and $j^*_{k_w}$ is the normalized diffusive net mass flux of elemental species k away from the wall, given by Eq. (48) evaluated at the wall.

To illustrate a simplified special case for this surface boundary condition, consider the case of steady-state ablation of a homogeneous material

such as carbon, neglecting mechanical spallation and radiation absorption and emission with the exception of reradiation from the surface. In this case $\dot{m}_g = 0$, $\dot{m}_{r_\ell} = 0$, $\dot{m}_c = \rho_w v_w$, $q_{r_w} = -\sigma \epsilon_w T_w^4$, $\tilde{K}_{k_C}$ is unity for carbon and zero for nitrogen, and $q_{cond} = \dot{m}_c(h_c - h_\infty)$ where $h_\infty = 0$ if the carbon is initially at the base state of 298°K. Therefore Eqs. (62) and (63) become

$$(\rho_w v_w)^* h_w + q^*_{a_w} + \sigma \epsilon_w T_w^4 / \alpha^* = 0 \tag{64}$$

for the energy balance and

$$\left.\begin{aligned} (\rho_w v_w)^* (\tilde{K}_{C_w} - 1) + j^*_{C_w} &= 0 \\ (\rho_w v_w)^* \tilde{K}_{N_w} + j^*_{N_w} &= 0 \end{aligned}\right\} \tag{65}$$

for elemental species balances for carbon and nitrogen, respectively.* In the absence of mechanical removal, equilibrium of the gas phase at the surface can be satisfied by considering any one of the equilibrium relations, for example

$$(1/3) \ell n \, P_{C_{3_w}} - K_{P_{eq}}(T_w) = 0 \tag{66}$$

where $P_{C_{3_w}}$ is the partial pressure of C_3 at the wall and $K_{p_{eq}}(T_w)$ is the equilibrium constant for the reaction

$$C(s) \rightarrow (1/3) C_3 \tag{67}$$

Eqs. (64) through (66) together with Eq. (61) comprise the complete set of surface boundary conditions for this specific example of steady-state carbon ablation.

*It is necessary to consider individual elemental species balances for only one less than the number of elements (see footnote at bottom of page 27).

Returning to the general problem, edge conditions of interest admit the possibility of an entropy layer:

$$\left.\begin{aligned} f'_{edge} &= \alpha_H \left[\frac{u}{u_e}(f,\xi)\right]_{edge} \\ f''_{edge} &= \alpha_H \left\{ f' \frac{d\left[\frac{u}{u_e}(f,\xi)\right]}{df} \right\}_{edge} \end{aligned}\right\} \quad (68)$$

$$\left.\begin{aligned} H_{T_{edge}} &= H_{T_{edge}}\Big|_{actual} \\ H'_{T_{edge}} &= 0 \end{aligned}\right\} \quad (69)$$

$$\left.\begin{aligned} \tilde{K}_{k_{edge}} &= \tilde{K}_{k_{edge}}\Big|_{actual} \\ \tilde{K}'_{k_{edge}} &= 0 \end{aligned}\right\} \quad (70)$$

where the subscript "e" refers to a reference condition, conveniently taken as the $f = 0$ streamline (see Appendix D) and the subscript "edge" refers to η_{edge} chosen to be outside of the boundary layer but possibly in the entropy layer. When there is no entropy layer, the reference condition e can be considered as the edge condition, e = edge. In this case, Eqs. (68) simplify to:

$$\left.\begin{aligned} f'_{edge} &= f'_e = \alpha_H \\ f''_{edge} &= f''_e = 0 \end{aligned}\right\} \quad (71)$$

In the next section, the boundary-layer equations and boundary conditions presented in this section are cast into a form suitable for numerical solution by an integral matrix method.

SECTION 4

THE LAMINAR BOUNDARY LAYER EQUATIONS IN INTEGRAL MATRIX FORM

The solution of the transformed boundary layer equations presented in Section 3 utilizes an integral matrix method which has been developed specifically for the solution of chemically reacting, nonsimilar, coupled boundary layers. In this procedure, the primary dependent variables f, H_T, and $\tilde{K}_k$ and their derivatives with respect to η are related by Taylor series expansions such that f', H_T, and $\tilde{K}_k$ are represented by connected cubics with continuous first and second derivatives at the junction points (commonly called a spline fit). Primarily for convenience, the conservation equations are integrated using a weighting function which is unity between adjacent nodal points and zero elsewhere. The linear Taylor series expansions together with linear boundary conditions form a very sparse matrix which has to be inverted only once for a given problem. The nonlinear boundary-layer equations and the nonlinear boundary conditions are then linearized, the errors being driven to zero using Newton-Raphson iteration.

In this section, the Taylor series expansions are presented. The boundary-layer equations are integrated, and the integrals which appear are also expanded in Taylor series. The resulting equations are precisely those which have been programmed for solution on high-speed digital computers to represent a coupled chemically reacting boundary layer such as surrounds an ablating heat shield during superorbital reentry. Special cases corresponding to a nonreacting (homogeneous) boundary layer and to an incompressible boundary layer are also discussed. The procedure utilized for solving the sets of linear and nonlinear algebraic equations developed in this section are presented in Section 5.

Consider the boundary layer in the region of a given station s as being divided into $N-1$ strips connected by N nodal points. These nodal points are designated by η_i where $i = 1$ at the wall and $i = N$ at the edge of the boundary layer.

Consider a function $p(x)$ which with all its derivatives is continuous in the neighborhood of the point $x = a$. Then, for any value of x in this neighborhood, $p(x)$ may be expressed in a Taylor series expansion as

$$p(x) = p(a) + \frac{p'(a)}{1!}(x - a) + \frac{p''(a)}{2!}(x - a)^2 + \frac{p'''(a)}{3!}(x - a)^3 + \frac{p''''(a)}{4!}(x - a)^4 + \ldots \quad (72)$$

Considering the point a as η_i and the x as η_{i+1}

$$p_{i+1} = p_i + p_i'\delta\eta + p_i''\frac{\delta\eta^2}{2} + p_i'''\frac{\delta\eta^3}{6} + p_i''''\frac{\delta\eta^4}{24} + \ldots \tag{73}$$

where

$$\delta\eta = \eta_{i+1} - \eta_i \tag{74}$$

The p_i can be considered to be any of f_i, f_i', f_i'', f_i''', H_{T_i}, H_{T_i}', H_{T_i}'', $\tilde{K}_{k_i}$, $\tilde{K}_{k_i}'$, or $\tilde{K}_{k_i}''$. To illustrate:

$$f_{i+1}' = f_i' + f_i''\,\delta\eta + f_i'''\frac{\delta\eta^2}{2} + f_i''''\frac{\delta\eta^3}{6} + \ldots \tag{75}$$

Since the highest derivatives of the dependent variables which appear in the boundary-layer equations are f_i''', H_{T_i}'' and $\tilde{K}_{k_i}''$, it is reasonable to truncate the series at the next highest derivative and to consider that derivative as being constant between η_i and η_{i+1}, that is:

$$\left.\begin{aligned} {}_i f_{i+1}'''' &= \frac{f_{i+1}''' - f_i'''}{\delta\eta} \\ {}_i H_{T_{i+1}}''' &= \frac{H_{T_{i+1}}'' - H_{T_i}''}{\delta\eta} \\ {}_i \tilde{K}_{k_{i+1}}''' &= \frac{\tilde{K}_{k_{i+1}}'' - \tilde{K}_{k_i}''}{\delta\eta} \end{aligned}\right\} \tag{76}$$

The following set of $[3 + 2(1 + K)](N - 1)$ linear equations are thus obtained where K is the number of elemental species minus one* and N is the number of nodal points across the boundary layer:

$$-f_{i+1} + f_i + f_i'\delta\eta + f_i''\frac{\delta\eta^2}{2} + f_i'''\frac{\delta\eta^3}{8} + f_{i+1}'''\frac{\delta\eta^3}{24} = 0 \tag{77}$$

*For example, if 4 elements C, H, O, N are under consideration, K = 3. Conservation of the remaining element is supplied through overall mass balance.

$$- p_{i+1} + p_i + p_i' \delta\eta + p_i'' \frac{\delta\eta^2}{3} + p_{i+1}'' \frac{\delta\eta^2}{6} = 0 \tag{78}$$

$$- p_{i+1}' + p_i' + p_i'' \frac{\delta\eta}{2} + p_{i+1}'' \frac{\delta\eta}{2} = 0 \tag{79}$$

where in Eqs. (78) and (79) the p_i represents f_i', represents H_{T_i}, and represents each of the K $\tilde{K}_{k_i}$.

Thus, between each i and i+1 the f is represented as a quartic; the f', H_T and $\tilde{K}_k$ are represented as cubics; and the f'', H_T' and $\tilde{K}_k'$ are represented as quadratics; whereas the f''', H_T'' and $\tilde{K}_k''$ are considered to vary linearly and the f'''', H_T''' and $\tilde{K}_k'''$ are considered to be constants between each pair of η-stations. Of course, all of these functions with the exception of f'''', H_T''' and $\tilde{K}_k'''$ join continuously at the nodal points. Herein lies one of the major distinguishing features of integral methods in general and of the integral matrix method in particular. Conventional finite difference methods are generally based on a representation which is not too unlike the first term in a Taylor series expansion and thus yield discontinuous functions. Integral methods generally use smoother functions and hence can be made to yield comparable accuracy with far fewer nodal points. This is extremely important for a chemically reacting boundary layer since the state of the gas (the computation of which is not trivial) must be determined at each nodal point during each iteration. In the past (e.g., Ref. 3) integral methods have employed high-order polynomials from the wall to the boundary-layer edge to obtain smooth profiles for f', H_T and $\tilde{K}_k$. The cubic spline functions employed herein are believed preferable as they are usually better behaved.

The momentum, energy, and elemental species equations are integrated at constant ξ between η_{i-1} and η_i to yield:

Momentum equation:

$$\int_{i-1}^{i} ff''\, d\eta + \left[\frac{Cf''}{\alpha_H}\right]_{i-1}^{i} + \beta\alpha_H^2 \int_{i-1}^{i} \frac{\rho_e}{\rho}\, d\eta - \beta \int_{i-1}^{i} f'^2\, d\eta$$

$$= 2 \int_{i-1}^{i} \left(f' \frac{\partial f'}{\partial\, \ell n\, \xi} - f'' \frac{\partial f}{\partial\, \ell n\, \xi} \right) d\eta - 2 \int_{i-1}^{i} f'^2 \frac{d\, \ell n\, \alpha_H}{d\, \ell n\, \xi}\, d\eta \tag{80}$$

Energy equation:

$$\int_{i-1}^{i} f H_T' \, d\eta + \left[-q_a^* + q_r^* \right]_{i-1}^{i} = 2 \int_{i-1}^{i} \left(f' \frac{\partial H_T}{\partial \ell n \, \xi} - H_T' \frac{\partial f}{\partial \ell n \, \xi} \right) d\eta \qquad (81)$$

Elemental species equations:

$$\int_{i-1}^{i} f \tilde{K}_k' \, d\eta - \left[j_k^* \right]_{i-1}^{i} + \alpha_H \int_{i-1}^{i} \phi_k d\eta = 2 \int_{i-1}^{i} \left(f' \frac{\partial \tilde{K}_k}{\partial \ell n \, \xi} - \tilde{K}_k' \frac{\partial f}{\partial \ell n \, \xi} \right) d\eta \qquad (82)$$

This, in effect, is a square-wave weighting factor of unity between i-1 and i and zero elsewhere. This is equivalent to the step-function weighting factor used by Pallone.[3] As discussed in Appendix F, the primary advantage of this type of integration is algebraic simplicity, the complex terms in the energy and elemental species equations (the q_a^*, q_r^*, and j_k^*) being divergence terms. The use of smoother weighting functions, such as those utilized by Dorodnitsyn,[4] would add considerable algebraic complexity and do not appear warranted on the basis of studies described in Appendix F which indicated that square-wave weighting functions and Dirac delta functions (i.e., a differential approach) yield comparable results as long as equivalent smooth functions are used to relate the primary variables to their derivatives.

The integral of fp', where p is f', H_T or $\tilde{K}_k$, can be expressed as

$$\int_{i-1}^{i} f p' \, d\eta = \left[f \, p \right]_{i-1}^{i} - \int_{i-1}^{i} f' p \, d\eta \qquad (83)$$

The integral of $f'p$ can then be expressed by expanding in a Taylor series about i

$$\int_{i-1}^{i} f' p \, d\eta = f'_i p_i \frac{\delta\eta}{1!} - (f'_i p'_i + f''_i p_i) \frac{\delta\eta^2}{2!}$$

$$+ (f'_i p''_i + 2f''_i p'_i + f'''_i p_i) \frac{\delta\eta^3}{3!}$$

$$- (f'_i p'''_i + 3f''_i p''_i + 3f'''_i p'_i + f''''_i p_i) \frac{\delta\eta^4}{4!}$$

$$+ (4f''_i p'''_i + 6f'''_i p''_i + 4f''''_i p'_i) \frac{\delta\eta^5}{5!}$$

$$- (10f'''_i p''_i + 10f''''_i p''_i) \frac{\delta\eta^6}{6!} + 20f''''_i p'''_i \frac{\delta\eta^7}{7!} + \ldots \qquad (84)$$

where, consistent with the truncation of the Taylor series employed earlier, all derivatives greater than f''''_i and p'''_i have been dropped. Utilizing again Eqs. (76) to eliminate p'''_i, Eq. (84) becomes

$$\int_{i-1}^{i} f' \, p \, d\eta = f'_i \, XP_1 + f''_i \, XP_2 + f'''_i \, XP_3 + f'''_{i-1} \, XP_4 \qquad (85)$$

where

$$\left.\begin{aligned}
XP_1 &= \delta\eta \left(p_i - p'_i \frac{\delta\eta}{2} + p''_i \frac{\delta\eta^2}{8} + p''_{i-1} \frac{\delta\eta^2}{24} \right) \\
XP_2 &= -\delta\eta^2 \left(\frac{p_i}{2} - p'_i \frac{\delta\eta}{3} + p''_i \frac{11\delta\eta^2}{120} + p''_{i-1} \frac{\delta\eta^2}{30} \right) \\
XP_3 &= \delta\eta^3 \left(\frac{p_i}{8} - p'_i \frac{11\delta\eta}{120} + p''_i \frac{11\delta\eta^2}{420} + p''_{i-1} \frac{5\delta\eta^2}{504} \right) \\
XP_4 &= \delta\eta^3 \left(\frac{p_i}{24} - p'_i \frac{\delta\eta}{30} + p''_i \frac{5\delta\eta^2}{504} + p''_{i-1} \frac{\delta\eta^2}{252} \right)
\end{aligned}\right\} \qquad (86)$$

For the axial derivatives, logarithmic two- and three-point difference relations are utilized, namely

$$2\left[\frac{d(\ )}{d\ \ell n\ \xi}\right]_{\ell} = d_o(\ )_{\ell} + d_1(\ )_{\ell-1} + d_2(\ )_{\ell-2} \tag{87}$$

where $(\ )_{\ell-1}$ refers to the previous streamwise station, and

$$d_0 = \frac{2}{\ell\Delta_{\ell-1}} \qquad d_1 = -\frac{2}{\ell\Delta_{\ell-1}} \qquad d_2 = 0 \tag{88}$$

for two-point difference and

$$\left.\begin{aligned} d_0 &= 2\,\frac{\ell\Delta_{\ell-1} + \ell\Delta_{\ell-2}}{\ell\Delta_{\ell-1}\ \ell\Delta_{\ell-2}} \qquad d_1 = -2\,\frac{\ell\Delta_{\ell-2}}{\ell\Delta_{\ell-1}\ \ell-1\Delta_{\ell-2}} \\ d_2 &= 2\,\frac{\ell\Delta_{\ell-1}}{\ell\Delta_{\ell-2}\ \ell-1\Delta_{\ell-2}} \end{aligned}\right\} \tag{89}$$

for three-point difference where typically

$$\ell\Delta_{\ell-1} = \ell n\ \xi_{\ell} - \ell n\ \xi_{\ell-1} = \ell n\ (\xi_{\ell}/\xi_{\ell-1}) \tag{90}$$

The three-point difference relation is utilized unless a similar solution is desired (in which case $d_0 = d_1 = d_2 = 0$) or unless the point in question is the first point after either (1) a similar solution or 2) a discontinuity (e.g., where the body changes shape abruptly, or where mass injection is suddenly terminated).

Similar approaches have been utilized previously in finite difference procedures, for example, by Smith et al[5] and by Leigh.[6] Integral methods, on the other hand, have generally integrated the boundary-layer equations in the streamwise direction (e.g., Pallone[3]). The present approach is considered preferable since the streamwise derivative terms are generally small, and hence are conveniently treated as forcing functions. This avoids the difficulty sometimes experienced during integration when the streamwise step size is too small (see Ref. 6).

Applying Eq. (87) to the streamwise derivative terms

$$2\int_{i-1}^{i}\left(f'\frac{\partial p}{\partial \ell n\,\xi}-p'\frac{\partial f}{\partial \ell n\,\xi}\right)d\eta$$

$$=\int_{i-1}^{i} f'\,(d_0\,p+d_1\,p_{\ell-1}+d_2\,p_{\ell-2})\,d\eta$$

$$-\int_{i-1}^{i} p'\,(d_0\,f+d_1\,f_{\ell-1}+d_2\,f_{\ell-2})\,d\eta \qquad (91)$$

where again this relation applies for the three cases where p is equal to f', H_T and $\tilde{K}_k$. Utilizing Eq. (83) yields

$$2\int_{i-1}^{i}\left(f'\frac{\partial p}{\partial \ell n\,\xi}-p'\frac{\partial f}{\partial \ell n\,\xi}\right)d\eta = 2d_0\int_{i-1}^{i} f'\,p\,d\eta$$

$$+d_1\int_{i-1}^{i} f'\,p_{\ell-1}\,d\eta+d_1\int_{i-1}^{i} f'_{\ell-1}\,p\,d\eta$$

$$+d_2\int_{i-1}^{i} f'\,p_{\ell-2}\,d\eta+d_2\int_{i-1}^{i} f'_{\ell-2}\,p\,d\eta$$

$$-\left[d_0\,f\,p+d_1\,f_{\ell-1}\,p+d_2\,f_{\ell-2}\,p\right]_{i-1}^{i} \qquad (92)$$

Noting that each of the five integrals in Eq. (92) is of the same form as the integral expanded in Eq. (84) by means of Taylor series

$$2\int_{i-1}^{i}\left(f'\frac{\partial p}{\partial \ell n\,\xi}-p'\frac{\partial f}{\partial \ell n\,\xi}\right)d\eta = -\left[d_0\,f\,p+d_1\,f_{\ell-1}\,p+d_2\,f_{\ell-2}\,p\right]_{i-1}^{i}$$

(equation continued on next page)

(equation continued from previous page)

$$+ 2d_0 \left(f_i' \, XP_1 + f_i'' \, XP_2 + f_i''' \, XP_3 + f_{i-1}''' \, XP_4\right)$$

$$+ \left(f_i' \, ZP_1 + f_i'' \, ZP_2 + f_i''' \, ZP_3 + f_{i-1}''' \, ZP_4\right)$$

$$+ \left(p_i \, ZM_1 + p_i' \, ZM_2 + p_i'' \, ZM_3 + p_{i-1}'' \, ZM_4\right) \tag{93}$$

where

$$\left.\begin{aligned}
ZP_1 &= \delta\eta \left(YP_1 - YP_2 \frac{\delta\eta}{2} + YP_3 \frac{\delta\eta^2}{8} + YP_4 \frac{\delta\eta^2}{24} \right) \\
ZP_2 &= -\delta\eta^2 \left(\frac{YP_1}{2} - YP_2 \frac{\delta\eta}{3} + YP_3 \frac{11\delta\eta^2}{120} + YP_4 \frac{\delta\eta^2}{30} \right) \\
ZP_3 &= \delta\eta^3 \left(\frac{YP_1}{8} - YP_2 \frac{11\delta\eta}{120} + YP_3 \frac{11\delta\eta^2}{420} + YP_4 \frac{5\delta\eta^2}{504} \right) \\
ZP_4 &= \delta\eta^3 \left(\frac{YP_1}{24} - YP_2 \frac{\delta\eta}{30} + YP_3 \frac{5\delta\eta^2}{504} + YP_4 \frac{\delta\eta^2}{252} \right)
\end{aligned}\right\} \tag{94}$$

with

$$\left.\begin{aligned}
YP_1 &= d_1 \, p_{\ell-1,i} + d_2 \, p_{\ell-2,i} \\
YP_2 &= d_1 \, p'_{\ell-1,i} + d_2 \, p'_{\ell-2,i} \\
YP_3 &= d_1 \, p''_{\ell-1,i} + d_2 \, p''_{\ell-2,i} \\
YP_4 &= d_1 \, p''_{\ell-1,i-1} + d_2 \, p''_{\ell-2,i-1}
\end{aligned}\right\} \tag{95}$$

and ZM_1, ZM_2, ZM_3, and ZM_4 are equal to ZP_1, ZP_2, ZP_3, and ZP_4, respectively, for the special case that $p = f'$.

Following the same procedure

$$2\int_{i-1}^{i} f'^2 \frac{d\ \ell n\ \alpha_H}{d\ \ell n\ \xi} = \left(d_0 + \frac{d_1\alpha_{H_{\ell-1}} + d_2\alpha_{H_{\ell-2}}}{\alpha_H}\right)\left[f_i' XP_1 + f_i'' XP_2 + f_i''' XP_3 + f_{i-1}''' XP_4\right]_{p_i = f_i'} \tag{96}$$

where use has been made of the fact that the coordinate stretching parameter α_H is a function of ξ only.

Finally, it is necessary to evaluate the integral of the density ratio which appears in the momentum equation and the integral of the elemental source term which appears in the elemental conservation equation. Approximating ρ_e/ρ as a cubic between i and i-1, an exact integration of the resulting approximate integral yields

$$\int_{i-1}^{i} \frac{\rho_e}{\rho}\, d\eta = \left(\frac{\rho_e}{\rho_i} + \frac{\rho_e}{\rho_{i-1}}\right)\frac{\delta\eta}{2} + \left(\frac{\rho_e\rho_i'}{\rho_i^2} - \frac{\rho_e\rho_{i-1}'}{\rho_{i-1}^2}\right)\frac{\delta\eta^2}{12} \tag{97}$$

Similarly for the integral of ϕ_k

$$\int_{i-1}^{i} \phi_k\, d\eta = \left(\phi_{k_i} + \phi_{k_{i-1}}\right)\frac{\delta\eta}{2} - \left(\phi_{k_i}' - \phi_{k_{i-1}}'\right)\frac{\delta\eta^2}{12} \tag{98}$$

These approximations are not quite as good as the approximations for f', H_T and $\tilde{K}_k$ since continuity of derivatives is not guaranteed at the nodal points.

Utilizing Eqs. (83) through (98) the boundary-layer equations (Eqs. (80) through (82)) become

Momentum:

$$\left[\frac{C\ f''}{\alpha_H} + f'\left((1 + d_0)\ f + d_1\ f_{\ell-1} + d_2\ f_{\ell-2}\right)\right]_{i-1}^{i}$$

(equation continued on next page)

(equation continued from previous page)

$$+ \beta \alpha_H^2 \left[\left(\frac{\rho_e}{\rho_i} + \frac{\rho_e}{\rho_{i-1}} \right) \frac{\delta\eta}{2} + \left(\frac{\rho_e \rho'_i}{\rho_i^2} - \frac{\rho_e \rho'_{i-1}}{\rho_{i-1}^2} \right) \frac{\delta\eta^2}{12} \right]$$

$$- \left(1 + \beta + d_0 - \frac{d_1 \alpha_{H_{\ell-1}} + d_2 \alpha_{H_{\ell-2}}}{\alpha_H} \right) \left[f'_i \, XP_1 + f''_i \, XP_2 + f'''_i \, XP_3 \right.$$

$$\left. + f'''_{i-1} \, XP_4 \right]_{p_i = f'_i} - 2 \left[f'_i \, ZP_1 + f''_i \, ZP_2 + f'''_i \, ZP_3 \right.$$

$$\left. + f'''_{i-1} \, ZP_4 \right]_{p_i = f'_i} = 0 \qquad (99)$$

Energy:

$$\left[- q_a^* + q_r^* + H_t \left((1 + d_0) \, f + d_1 \, f_{\ell-1} + d_2 \, f_{\ell-2} \right) \right]_{i-1}^{i}$$

$$- (1 + 2d_0) \left[f'_i \, XP_1 + f''_i \, XP_2 + f'''_i \, XP_3 + f'''_{i-1} \, XP_4 \right]_{p_i = H_{T_i}}$$

$$- \left[f'_i \, ZP_1 + f''_i \, ZP_2 + f'''_i \, ZP_3 + f'''_{i-1} \, ZP_4 \right]_{p_i = H_{T_i}}$$

$$- \left[H_{T_i} \, ZP_1 + H'_{T_i} \, ZP_2 + H''_{T_i} \, ZP_3 + H''_{T_{i-1}} \, ZP_4 \right]_{p_i = f'_i} = 0 \qquad (100)$$

where q_a^* and q_r^* are given by Eqs. (50) and (57), respectively.

Elemental species:

$$\left[- j_k^* + \tilde{K}_k \left| (1 + d_0)\ f + d_1\ f_{\ell-1} + d_2\ f_{\ell-2} \right| \right]_{i-1}^{i}$$

$$+ \alpha_H \left[\left(\phi_{k_i} + \phi_{k_{i-1}} \right) \frac{\delta\eta}{2} - \left(\phi'_{k_i} - \phi'_{k_{i-1}} \right) \frac{\delta\eta^2}{12} \right]$$

$$- (1 + 2d_0) \left[f'_i\ XP_1 + f''_i\ XP_2 + f'''_i\ XP_3 + f'''_{i-1}\ XP_4 \right]_{p_i = \tilde{K}_{k_i}}$$

$$- \left[f'_i\ ZP_1 + f''_i\ ZP_2 + f'''_i\ ZP_3 + f'''_{i-1}\ ZP_4 \right]_{p_i = \tilde{K}_{k_i}}$$

$$- \left[\tilde{K}_{k_i}\ ZP_1 + \tilde{K}'_{k_i}\ ZP_2 + \tilde{K}''_{k_i}\ ZP_3 + \tilde{K}''_{k_{i-1}}\ ZP_4 \right]_{p_i = f'_i} = 0 \qquad (101)$$

where j_k^* is given by Eq. (48).

The boundary-layer equations (Eqs. (99) through (101)) are applicable to the problem of the nonsimilar chemically-reacting boundary layer with unequal diffusion coefficients, thermal diffusion, entropy layer, radiation absorption and emission, and rate-controlled reactions, coupled point by point with a charring ablator solution. In the absence of thermal diffusion c_t is set equal to zero. When the diffusion coefficients are equal, $\tilde{Z}_k = \tilde{K}_k$, $\mu_1 = 1$, $\mu_2 = 1/\mu_3 = \mathcal{M}$, $\tilde{h} = h$, and $\tilde{C}_p = \bar{C}_p$. When the boundary layer does not react chemically, the elemental species equation is inconsequential. Finally, if the boundary layer is incompressible or if Crocco relations are utilized only the momentum equation is needed.

Before discussing the procedure for solving the equations developed in this section, it is appropriate to discuss briefly the thermodynamic and transport properties employed in the solution procedure. These subjects are treated in considerably more detail in Refs. 7 and 9, respectively.

The state at each node is determined with a general purpose chemical equilibrium subprogram of much the same form as those described in Refs. 21 and 22. State derivatives are determined by the same routine. Enthalpy and specific heat values are obtained through accurate curve fits of JANAF or other reliable thermochemical data.

In the present formulation, transport properties are determined as follows. The $\mathcal{D}_{ij}$ and D_i^T are calculated using the approximate Eqs. (19) and (26), respectively. The $\bar{D}$ is given by

$$\bar{D} = 2.628 \times 10^{-3} \frac{T(T/m_{ref})^{1/2}}{P\sigma_{ref}^2 \Omega^{(1,1)*}_{ref}} \quad (cm^2/sec) \tag{102}$$

with T in $^\circ K$, P in atmospheres, and σ in $\mathring{A}$. The subscript "ref" refers to a reference species (often O_2, but conceivably fictional). $\bar{D}$ is thus the self-diffusion coefficient of that species. The F_i are determined by a least-squares correlation of $\mathcal{D}_{ij}$.

The viscosity of the mixture is obtained from an approximate relation of the Sutherland-Wassiljewa type[13]

$$\mu = \sum_i \mu_i \tilde{\chi}_i \tag{103}$$

where μ_i is the viscosity of species i given by

$$\mu_i = \frac{5}{6A_{ii}^*} \rho \mathcal{D}_{ii} \tag{104}$$

and

$$\tilde{\chi}_i^{-1} = 1 + 1.385 \frac{RT\mu_i}{Px_i m_i} \sum_{j \neq i} \frac{x_j}{\mathcal{D}_{ij}} \tag{105}$$

with the 1.385 an empirical constant suggested by Buddenberg and Wilke.[23]

The mixture thermal conductivity, λ, is obtained as the sum of a monatomic thermal conductivity and a contribution from internal degrees of freedom:

$$\lambda = \lambda^{mono} + \lambda^{int} \tag{106}$$

The λ^{mono} is determined by a relation similar to that for μ

$$\lambda^{mono} = \sum_i \lambda_i^{mono} \rho_i \tag{107}$$

where λ_i^{mono} is the monatomic thermal conductivity of species i

$$\lambda_i^{mono} = \frac{15}{4} \frac{R}{m_i} \mu_i \tag{108}$$

and

$$\varphi_i^{-1} = 1 + 1.065 \times 1.385 \frac{RT\mu_i}{Px_i m_i} \sum_{j \neq i} \frac{x_j}{\mathcal{D}_{ij}} \tag{109}$$

with the 1.065 being suggested by Mason and Saxena.[24] The λ^{int} is computed using[25]

$$\lambda^{int} = \sum_i \frac{x_i(\lambda_i - \lambda_i^{mono})}{\mathcal{D}_{ii} \sum_j \frac{x_j}{\mathcal{D}_{ij}}} \tag{110}$$

where

$$\lambda_i - \lambda_i^{mono} = \rho \mathcal{D}_{ii} \frac{m_i}{m} \left(C_{p_i} - \frac{5}{2} \frac{R}{m_i} \right) \tag{111}$$

SECTION 5

SOLUTION OF THE BOUNDARY-LAYER EQUATIONS IN INTEGRAL MATRIX FORM

The solution of the boundary-layer equations presented in Section 4 together with the boundary conditions such as those presented in Section 3 is accomplished by Newton-Raphson iteration. In this section these equations are put into a form suitable for solution by this procedure. The resulting equations are then written in matrix form, and a method is presented for their solution suitable for coupling with an internal conduction solution. The procedure attempts to minimize computational time and computer storage requirements.

In order to illustrate the Newton-Raphson method consider two simultaneous nonlinear algebraic equations

$$F(x,y) = 0 \qquad G(x,y) = 0 \tag{112}$$

the solution for which is given by $x = \bar{x}$, $y = \bar{y}$. Define x_m and y_m as the values of x and y for the m^{th} iteration. The desired solution $f(\bar{x},\bar{y})$ can be expressed in a Taylor series expansion

$$
\left.
\begin{aligned}
0 = F(\bar{x},\bar{y}) &= F(x_m,y_m) + (\bar{x} - x_m)\frac{\partial F(x_m,y_m)}{\partial x} \\
&\quad + (\bar{y} - y_m)\frac{\partial F(x_m,y_m)}{\partial y} + \ldots \\
0 = G(\bar{x},\bar{y}) &= G(x_m,y_m) + (\bar{x} - x_m)\frac{\partial G(x_m,y_m)}{\partial x} \\
&\quad + (\bar{y} - y_m)\frac{\partial G(x_m,y_m)}{\partial y} + \ldots
\end{aligned}
\right\} \qquad (113)
$$

The Newton-Raphson method consists of replacing $(\bar{x}, \bar{y})$ by (x_{m+1}, y_{m+1}) on the right-hand-side of these expressions, neglecting nonlinear terms in $x_{m+1} - x_m$ and $y_{m+1} - y_m$. This yields the set of recurrence formulas

$$
\left.
\begin{aligned}
\Delta x_m \frac{\partial F(x_m,y_m)}{\partial x} + \Delta y_m \frac{\partial F(x_m,y_m)}{\partial y} &= - F(x_m,y_m) \\
\Delta x_m \frac{\partial G(x_m,y_m)}{\partial x} + \Delta y_m \frac{\partial G(x_m,y_m)}{\partial y} &= - G(x_m,y_m)
\end{aligned}
\right\} \qquad (114)
$$

where

$$
\Delta x_m \equiv x_{m+1} - x_m \qquad \Delta y_m \equiv y_{m+1} - y_m \qquad (115)
$$

The Δx_m and Δy_m are the corrections to be added to x_m and y_m, respectively, to yield the values of the dependent variables for the $m+1^{th}$ iteration. Here $F(x_m,y_m)$ and $G(x_m,y_m)$ are the values of the original functions $F(x, y)$ and $G(x, y)$ evaluated for $x = x_m$ and $y = y_m$. As the corrections approach zero, the $F(x_m,y_m)$ and $G(x_m,y_m)$ thus approach zero. Hence, it is appropriate to look upon these as errors associated with the original Equations (112). It is apparent that this procedure can be extended to an arbitrary number of functions and a corresponding number of primary variables.

For the purpose of the present problem, it has been found to be most convenient to consider the primary variables as the f_i, f_i', f_i'', f_i''', H_{T_i}, H_{T_i}', H_{T_i}'', $\tilde{K}_{k_i}$, $\tilde{K}_{k_i}'$, $\tilde{K}_{k_i}''$ at each nodal station i, plus the α_H. This amounts to a total of $(7 + 3K)N + 1$ unknowns where N is the number of nodal points across the boundary layer and K is one less than the number of elements present in the boundary layer. The corresponding number of equations is provided as follows

	Equation numbers	Number of equations
Taylor series expansions	(77)-(79)	(5 + 2K)(N - 1)
Boundary layer equations	(99)-(101)	(2 + K)(N - 1)
Boundary conditions	(61)-(63) and (68)-(70) or equiv.	(7 + 3K)
The α_H constraint	(34)	1
Total		(7 + 3K) N + 1

It is thus necessary to specify the corrections of the other variables (such as density, temperature, etc.) in terms of corrections of the primary variables. The procedure for accomplishing this will be described later.

The Taylor series expansions are linear with respect to the primary variables as are several of the boundary conditions. The boundary layer equations and the remainder of the boundary conditions are nonlinear. The α_H constraint is linear but it must be considered together with the nonlinear equations in order to avoid a singular matrix. The recurrence formulas representing the linear equations will be presented first, after which recurrence formulas appropriate to the nonlinear equations will be developed.

Partial differentiation of the Taylor series expansions with respect to the primary dependent variables in accordance with Equations (114) yields for the m^{th} iteration

$$(-1)\Delta f_{i+1} + (1)\Delta f_i + (\delta\eta)\Delta f'_i + (\frac{\delta\eta^2}{2})\Delta f''_i$$

$$+ (\frac{\delta\eta^3}{8})\Delta f'''_i + (\frac{\delta\eta^3}{24})\Delta f'''_{i+1} = - \text{ERROR} \qquad (116)$$

$$(-1)\Delta p_{i+1} + (1)\Delta p_i + (\delta\eta)\Delta p'_i + (\frac{\delta\eta^2}{3})\Delta p''_i + (\frac{\delta\eta^2}{6})\Delta p''_{i+1} = - \text{ERROR} \qquad (117)$$

$$(-1)\Delta p'_{i+1} + (1)\Delta p'_i + (\frac{\delta\eta}{2})\Delta p''_i + (\frac{\delta\eta}{2})\Delta p''_{i+1} = - \text{ERROR} \qquad (118)$$

where as before p_i represents f'_i, H_{T_i} and $\tilde{K}_{k_i}$. Here Δf_{i+1}, Δf_i, $\Delta f'_i$, and so on represent the respective corrections for f_{i+1}, f_i, f'_i, and so on, the numbers in parentheses represent the partial derivatives of the Taylor series expressions (Equations (77) through (79)) with respect to the primary variables; and the ERRORS are obtained by evaluating the left-hand-sides of the appropriate Equations (77) through (79) for the values of the variables obtained during the m^{th} iteration.

Similarly, the recurrence formulas for the linear boundary conditions (Eqs. (61), (69), and (70)) are given by

$$\Delta f'_w = - \text{ERROR} = - (f'_w)_m \tag{119}$$

$$\Delta H_{T_{edge}} = - \text{ERROR} = - \left[H_{T_{edge}} - H_{T_{edge}} \Big|_{actual} \right]_m \tag{120}$$

$$\Delta H'_{T_{edge}} = - \text{ERROR} = - (H'_{T_{edge}})_m \tag{121}$$

$$\Delta \tilde{K}_{k_{edge}} = - \text{ERROR} = - \left[\tilde{K}_{k_{edge}} - \tilde{K}_{k_{edge}} \Big|_{actual} \right]_m \tag{122}$$

$$\Delta \tilde{K}'_{k_{edge}} = - \text{ERROR} = - (\tilde{K}'_{k_{edge}})_m \tag{123}$$

The recurrence formulas for the nonlinear boundary-layer equations are given by:

Momentum:

$$\left[\frac{C\, f''}{\alpha_H} \left(\frac{\Delta f''}{f''} + \frac{\Delta C}{C} - \frac{\Delta \alpha_H}{\alpha_H} \right) + \left[(1 + d_0) f + d_1 f_{\ell-1} + d_2 f_{\ell-2} \right] \Delta f' \right.$$

$$\left. + f' (1 + d_0) \Delta f \right]_{i-1}^{i} - \beta \alpha_H^2 \frac{\rho_e}{\rho_i^2} \frac{\delta\eta}{2} \left\{ \left(1 + \frac{\delta\eta}{3} \frac{\rho'_i}{\rho_i} \right) \Delta\rho_i - \frac{\delta\eta}{6} \Delta\rho'_i \right.$$

$$\left. + \left(\frac{\rho_i}{\rho_{i-1}} \right)^2 \left[\left(1 - \frac{\delta\eta}{3} \frac{\rho'_{i-1}}{\rho_{i-1}} \right) \Delta\rho_{i-1} + \frac{\delta\eta}{6} \Delta\rho'_{i-1} \right] \right\} + \beta \alpha_H \delta\eta \frac{\rho_e}{\rho_i} \left[1 + \frac{\rho_i}{\rho_{i-1}} \right.$$

$$\left. + \frac{\delta\eta}{6} \left(\frac{\rho'_i}{\rho_i} - \frac{\rho_i}{\rho_{i-1}} \frac{\rho'_{i-1}}{\rho_{i-1}} \right) \right] \Delta\alpha_H - \left[1 + \beta + d_0 - \left(\frac{d_1 \alpha_{H_{\ell-1}} + d_2 \alpha_{H_{\ell-2}}}{\alpha_H} \right) \right] \times$$

$$\times \left[f'_i\, \Delta XP_1 + f''_i\, \Delta XP_2 + f'''_i\, \Delta XP_3 + f'''_{i-1} \Delta XP_4 + XP_1 \Delta f'_i + XP_2 \Delta f''_i \right.$$

$$\left. + XP_3 \Delta f_i''' + XP_4 \Delta f'''_{i-1} \right]_{P_i = f'_i} - \left(\frac{d_1 \alpha_{H_{\ell-1}} + d_2 \alpha_{H_{\ell-2}}}{\alpha_H^2} \right) \left[f'_i XP_1 \right.$$

(equation continued on next page)

(equation continued from previous page)

$$+ f_i'' XP_2 + f_i''' XP_3 + f_{i-1}''' XP_4 \Big] \Delta\alpha_H \Big|_{p_i = f_i'} - 2 \Big[ZP_1 \Delta f_i' + ZP_2 \Delta f_i''$$

$$+ ZP_3 \Delta f_i''' + ZP_4 \Delta f_{i-1}''' \Big]_{p_i = f_i'} = - \text{ERROR} \qquad (124)$$

where the ERROR is given by the left-hand-side of Eq. (99) evaluated for the m^{th} iteration.

Energy:

$$\Big[- \Delta q_a^* + \frac{1}{\alpha^*} \Delta q_r + \Big((1 + d_0) f + d_1 f_{\ell-1} + d_2 f_{\ell-2} \Big) \Delta H_T + H_T (1 + d_0) \Delta f \Big]_{i-1}^{i}$$

$$- (1 + 2d_0) \Big[f_i' \Delta XP_1 + f_i'' \Delta XP_2 + f_i''' \Delta XP_3 + f_{i-1}''' \Delta XP_4 + XP_1 \Delta f_i'$$

$$+ XP_2 \Delta f_i'' + XP_3 \Delta f_i''' + XP_4 \Delta f_{i-1}''' \Big]_{p_i = H_{T_i}} - \Big[ZP_1 \Delta f_i' + ZP_2 \Delta f_i'' + ZP_3 \Delta f_i'''$$

$$+ ZP_4 \Delta f_{i-1}''' \Big]_{p_i = H_{T_i}} - \Big[ZP_1 \Delta H_{T_i} + ZP_2 \Delta H_{T_i}' + ZP_3 \Delta H_{T_i}'' + ZP_4 \Delta H_{T_{i-1}}'' \Big]_{p_i = f_i'}$$

$$= - \text{ERROR} \qquad (125)$$

where the ERROR is given by the left-hand-side of Eq. (100) evaluated for the m^{th} iteration and Δq_a^* is given by

$$\Delta q_a^* = - \Bigg\{ \frac{C\, f' f'' u_e^2}{\alpha_H^3} \Big(\frac{\Delta C}{C} + \frac{\Delta f'}{f'} + \frac{\Delta f''}{f''} - 3 \frac{\Delta \alpha_H}{\alpha_H} \Big) + \frac{C \bar{C}_p T'}{\alpha_H Pr} \Big(\frac{\Delta C}{C} + \frac{\Delta \bar{C}_p}{\bar{C}_p} + \frac{\Delta T'}{T'}$$

$$- \frac{\Delta \alpha_H}{\alpha_H} - \frac{\Delta Pr}{Pr} \Big) + \frac{C}{\alpha_H \bar{Sc}} \Big[\tilde{h}' - \Big(\tilde{C}_p + \frac{c_t^2 R}{\mu_1 \mu_2} \Big) T' + c_t R T \mu_3' + (\tilde{h} - h$$

(equation continued on next page)

(equation continued from previous page)

$$+ c_t RT\mu_3)\mu_4'\Bigg]\left[\frac{\Delta C}{C} - \frac{\Delta\alpha_H}{\alpha_H} - \frac{\Delta\overline{Sc}}{\overline{Sc}}\right] + \frac{C}{\alpha_H \overline{Sc}}\left[\Delta\tilde{h}' - \left(\tilde{C}_p + \frac{c_t^2 R}{\mu_1\mu_2}\right)\Delta T'\right.$$

$$-T'\Delta\tilde{C}_p + \frac{c_t^2 RT'}{(\mu_1\mu_2)^2}\Delta(\mu_1\mu_2) + c_t RT\mu_3'\left(\frac{\Delta T}{T} + \frac{\Delta\mu_3'}{\mu_3'}\right) + (\tilde{h} - h + c_t RT\mu_3)\Delta\mu_4'$$

$$\left.\left. + \mu_4'\left(\Delta\tilde{h} - \Delta h + c_t RT\mu_3\left(\frac{\Delta\mu_3}{\mu_3} + \frac{\Delta T}{T}\right)\right)\right]\right\} \qquad (126)$$

Elemental species:

$$\left[-\Delta j_k^* + \left((1 + d_0)\ f + d_1 f_{\ell-1} + d_2 f_{\ell-2}\right)\Delta\tilde{K}_k + \tilde{K}_k(1 + d_0)\ \Delta f\right]_{i-1}^{i}$$

$$+ \alpha_H \frac{\delta\eta}{2}\left[\Delta\phi_{k_i} + \Delta\phi_{k_{i-1}} - \frac{\delta\eta}{6}\left(\Delta\phi'_{k_i} - \Delta\phi'_{k_{i-1}}\right)\right] + \frac{\delta\eta}{2}\left[\phi_{k_i} + \phi_{k_{i-1}}\right.$$

$$\left. - \left(\phi'_{k_i} - \phi'_{k_{i-1}}\right)\frac{\delta\eta}{6}\right]\Delta\alpha_H - (1 + 2d_0)\left[f_i'\Delta XP_1 + f_i''\Delta XP_2 + f_i'''\Delta XP_3\right.$$

$$\left. + f_{i-1}'''\Delta XP_4 + XP_1\Delta f_i' + XP_2\Delta f_i'' + XP_3\Delta f_i''' + XP_4\Delta f_{i-1}'''\right]_{p_i = \tilde{K}_{k_i}}$$

$$- \left[ZP_1\Delta f_i' + ZP_2\Delta f_i'' + ZP_3\Delta f_i''' + ZP_4\Delta f_{i-1}'''\right]_{p_i = \tilde{K}_{k_i}} - \left[ZP_1\Delta\tilde{K}_{k_i}\right.$$

$$\left. + ZP_2\Delta\tilde{K}'_{k_i} + ZP_3\Delta\tilde{K}''_{k_i} + ZP_4\Delta\tilde{K}''_{k_{i-1}}\right]_{p_i = f_i'} = -\ \text{ERROR} \qquad (127)$$

where the ERROR is given by the left-hand-side of Eq. (101) evaluated for the m^{th} iteration and Δj_k^* is given by

$$\Delta j_k^* = -\frac{C}{\alpha_H \overline{Sc}}\left[\left(\tilde{Z}_k' + (\tilde{Z}_k - \tilde{K}_k)\mu_4'\right)\left(\frac{\Delta C}{C} - \frac{\Delta\alpha_H}{\alpha_H} - \frac{\Delta\overline{Sc}}{\overline{Sc}}\right)\right.$$

$$\left. + \Delta\tilde{Z}_k' + (\tilde{Z}_k - \tilde{K}_k)\Delta\mu_4' + \mu_4'(\Delta\tilde{Z}_k - \Delta\tilde{K}_k)\right] \tag{128}$$

Equations (124), (125), and (127) are reduced to linear equations in terms of the corrections on the primary variables (Δf_i, $\Delta f_i'$, and so on) by noting that the variables C, ρ, $\overline{C}_p$, T, Pr, $\overline{Sc}$, $\tilde{h}$, $\tilde{C}_p$, $\mu_1\mu_2$, μ_3, μ_4, q_r, $\tilde{Z}_k$, and ϕ_k evaluated at any point in the boundary layer can be considered as functions of static enthalpy, static pressure, and elemental composition. With the pressure assumed constant across the boundary layer, it follows that all of the corrections on unprimed variables with the exception of Δq_r can be expressed as

$$\Delta(\ )_i = \sum_{kk} \frac{\partial(\ )_i}{\partial\tilde{K}_{kk_i}} \Delta\tilde{K}_{kk_i} + \frac{\partial(\ )_i}{\partial h_i} \Delta h_i \tag{129}$$

where from Eqs. (9) and (36)

$$h_i = H_{T_i} - \frac{u_e^2}{2}\frac{f_i'^2}{\alpha_H^2} \tag{130}$$

so that

$$\Delta h_i = \Delta H_{T_i} - \frac{u_e^2 f_i'^2}{\alpha_H^2}\left(\frac{\Delta f_i'}{f_i'} - \frac{\Delta\alpha_H}{\alpha_H}\right) \tag{131}$$

The Δq_{r_i} is more complicated in that it depends upon the $\Delta\tilde{K}_{kk_j}$ and Δh_j at all nodal points j.

The η-derivatives of these variables (i.e., the primed quantities) can likewise be expressed in terms of corrections on the primary variables as follows

$$\Delta(\ )_i' = \sum_{kk} \tilde{K}_{kk_i}'\left(\sum_{kkk} \frac{\partial^2(\ )_i}{\partial\tilde{K}_{kk_i}\partial\tilde{K}_{kkk_i}} \Delta\tilde{K}_{kkk_i} + \frac{\partial^2(\ )_i}{\partial\tilde{K}_{kk_i}\partial h_i} \Delta h_i\right)$$

$$+ h_i'\left(\sum_{kk} \frac{\partial^2(\ )_i}{\partial h_i\,\partial\tilde{K}_{kk_i}} \Delta\tilde{K}_{kk_i} + \frac{\partial^2(\ )_i}{\partial h_i^2} \Delta h_i\right)$$

$$+ \sum_{kk} \frac{\partial(\ )_i}{\partial\tilde{K}_{kk_i}} \Delta\tilde{K}_{kk_i}' + \frac{\partial(\ )}{\partial h_i} \Delta h_i' \tag{132}$$

where

$$h'_i = H'_{T_i} - \frac{u_e^2 f'_i f''_i}{\alpha_H^2} \tag{133}$$

so that

$$\Delta h'_i = \Delta H'_{T_i} - \frac{u_e^2 f'_i f''_i}{\alpha_H^2} \left(\frac{\Delta f'_i}{f'_i} + \frac{\Delta f''_i}{f''_i} - 2 \frac{\Delta \alpha_H}{\alpha_H} \right) \tag{134}$$

Use is also made of the following which are obtained by differentiating Equations (86):

$$\left.\begin{aligned}
\Delta XP_1 &= \delta\eta \left(\Delta p_i - \frac{\delta\eta}{2} \Delta p'_i + \frac{\delta\eta^2}{8} \Delta p''_i + \frac{\delta\eta^2}{24} \Delta p''_{i-1} \right) \\
\Delta XP_2 &= -\delta\eta^2 \left(\frac{\Delta p_i}{2} - \frac{\delta\eta}{3} \Delta p'_i + \frac{11\,\delta\eta^2}{120} \Delta p''_i + \frac{\delta\eta^2}{30} \Delta p''_{i-1} \right) \\
\Delta XP_3 &= \delta\eta^3 \left(\frac{\Delta p_i}{8} - \frac{11\,\delta\eta}{120} \Delta p'_i + \frac{11\,\delta\eta^2}{420} \Delta p''_i + \frac{5\,\delta\eta^2}{504} \Delta p''_{i-1} \right) \\
\Delta XP_4 &= \delta\eta^3 \left(\frac{\Delta p_i}{24} - \frac{\delta\eta}{30} \Delta p'_i + \frac{5\delta\eta^2}{504} \Delta p''_i + \frac{\delta\eta^2}{252} \Delta p''_{i-1} \right)
\end{aligned}\right\} \tag{135}$$

The $\Delta ZP_1 = \Delta ZP_2 = \Delta ZP_3 = \Delta ZP_4 = 0$ since ZP_1, ZP_2, ZP_3, and ZP_4 can be computed before the iteration commences.

Substituting Eqs. (126), (128), (129), (131), (132), (134), and (135) into Eqs. (124), (125), and (127), and collecting terms yields, neglecting the off-diagonal terms* arising from the Δq_r, the following recurrence formulas for the momentum, energy, and K^{th} elemental species equations between nodal points i and i-1:

$$c_1 \Delta f_i + c_2 \Delta f_{i-1} + c_3 \Delta f'_i + c_4 \Delta f'_{i-1}$$

$$+ c_5 \Delta f''_i + c_6 \Delta f''_{i-1} + c_7 \Delta f'''_i + c_8 \Delta f'''_{i-1}$$

$$+ c_9 \Delta H_{T_i} + c_{10} \Delta H_{T_{i-1}} + c_{11} \Delta H'_{T_i} + c_{12} \Delta H'_{T_{i-1}}$$

(equation continued on following page)

*As mentioned previously, Δq_{r_i} and $\Delta q_{r_{i-1}}$ produce corrections $\Delta \tilde{K}_{k_j}$, ΔH_{T_j}, $\Delta f'_j$ and $\Delta \alpha_{H_j}$ at all boundary-layer nodal points j.

$$+ c_{13}\Delta H''_{T_i} + c_{14}\Delta H''_{T_{i-1}} + c_{15}\Delta\alpha_{H_i} + c_{16}\Delta\alpha_{H_{i-1}}$$

$$+ \sum_{kk} \Big(c_{kk1}\Delta\tilde{K}_{kk_i} + c_{kk2}\Delta\tilde{K}_{kk_{i-1}} + c_{kk3}\Delta\tilde{K}'_{kk_i}$$

$$+ c_{kk4}\Delta\tilde{K}'_{kk_{i-1}} + c_{kk5}\Delta\tilde{K}''_{kk_i} + c_{kk6}\Delta\tilde{K}''_{kk_{i-1}} \Big) = - \text{ERROR} \qquad (136)$$

where the coefficients for the corrections c_1, c_2, ... differ in form for the momentum, the energy, and the K^{th} elemental species equations and in general yield different numerical results for each elemental species kk and for each nodal position in the boundary layer i. The coefficients for the corrections are listed in Tables I through III for the momentum equation, the energy equation, and the K^{th} elemental species equation, respectively.

In order to complete the set of equations, it is necessary to develop the recurrence formulas for the α_H constraint and for the nonlinear boundary conditions. The α_H constraint (Eq. (34)) yields

$$\Delta f'_{\eta_c} - c\Delta f'_{\eta_e} = - \text{ERROR} = - \left(f'_{\eta_c} - cf'_{\eta_e}\right)_m \qquad (137)$$

The boundary conditions at the boundary-layer edge are nonlinear when an entropy layer is taken into account. In this case, Eqs. (68) are applicable, resulting in the following recurrence formulas:

$$-\Delta f'_{edge} + \left[\frac{u}{u_e}(f,\xi)\right]_{edge} \Delta\alpha_H$$

$$+ \alpha_H \left[\frac{d\left[\frac{u}{u_e}(f,\xi)\right]}{df}\right]_{edge} \Delta f_{edge} = - \text{ERROR}$$

$$= - \left[- f'_{edge} + \alpha_H \left[\frac{u}{u_e}(f,\xi)\right]_{edge}\right]_m \qquad (138)$$

TABLE I

CORRECTION COEFFICIENTS FOR MOMENTUM EQUATION

$$\Delta f_i : \left[(1 + d_0) f'\right]_i \qquad \Delta f_{i-1} : -\left[(1 + d_0) f'\right]_{i-1}$$

$$\Delta f'_i : \left[A_1\right]_i + B_1 \qquad \Delta f'_{i-1} : -\left[A_1\right]_{i-1} + C_1$$

$$\Delta f''_i : \left[\frac{C}{\alpha_H}\right]_i + B_2 \qquad \Delta f''_{i-1} : -\left[\frac{C}{\alpha_H}\right]_{i-1} + C_2$$

$$\Delta f'''_i : B_3 \qquad \Delta f'''_{i-1} : C_3$$

$$\Delta H_{T_i} : \left[\frac{f''}{\alpha_H}\frac{\partial C}{\partial h}\right]_i + (D_2)\frac{\partial}{\partial p} = \frac{\partial}{\partial h} \qquad \Delta H_{T_{i-1}} : -\left[\frac{f''}{\alpha_H}\frac{\partial C}{\partial h}\right]_{i-1} + (D_4)\frac{\partial}{\partial p} = \frac{\partial}{\partial h}$$

$$\Delta H'_{T_i} : D_3\left(\frac{\partial \rho}{\partial h}\right)_i \qquad \Delta H'_{T_{i-1}} : D_5\left(\frac{\partial \rho}{\partial h}\right)_{i-1}$$

$$\Delta H''_{T_i} : 0 \qquad \Delta H''_{T_{i-1}} : 0$$

$$\Delta \tilde{K}_{kk_i} : \left[\frac{f''}{\alpha_H}\frac{\partial C}{\partial \tilde{K}_{kk}}\right]_i + (D_2)\frac{\partial}{\partial p} = \frac{\partial}{\partial \tilde{K}_{kk}} \qquad \Delta \tilde{K}_{kk_{i-1}} : -\left[\frac{f''}{\alpha_H}\frac{\partial C}{\partial \tilde{K}_{kk}}\right]_{i-1} + (D_4)\frac{\partial}{\partial p} = \frac{\partial}{\partial \tilde{K}_{kk}}$$

$$\Delta \tilde{K}'_{kk_i} : D_3\left(\frac{\partial \rho}{\partial \tilde{K}_{kk}}\right)_i \qquad \Delta \tilde{K}'_{kk_{i-1}} : D_5\left(\frac{\partial \rho}{\partial \tilde{K}_{kk}}\right)_{i-1}$$

$$\Delta \tilde{K}''_{kk_i} : 0 \qquad \Delta \tilde{K}''_{kk_{i-1}} : 0$$

$$\Delta \alpha_{H_i} : \left[A_4\right]_i + B_4 \qquad \Delta \alpha_{H_{i-1}} : -\left[A_4\right]_{i-1} + C_4$$

$$A_1 = -\frac{u_e^2}{\alpha_H^3} f' f'' \frac{\partial C}{\partial h} + (1 + d_0) f + d_1 f_{\ell-1} + d_2 f_{\ell-2}$$

$$A_4 = \frac{f''}{\alpha_H^2}\left(\frac{u_e^2}{\alpha_H^2} f'^2 \frac{\partial C}{\partial h} - C\right)$$

$$B_1 = -2\left[D_1 XP_1 + ZP_1\right]_{p_i} = f'_i - \frac{u_e^2}{\alpha_H^2}\left[f''_i D_3\left(\frac{\partial \rho}{\partial h}\right)_i + f'_i (D_2)\frac{\partial}{\partial p} = \frac{\partial}{\partial h}\right]$$

TABLE I (continued)

$$B_2 = -2\left[D_1 XP_2 + ZP_2\right]_{p_i = f_i'} - \frac{u_e^2}{\alpha_H^2} f_i' D_3 \left(\frac{\partial \rho}{\partial h}\right)_i$$

$$B_3 = -2\left[D_1 XP_3 + ZP_3\right]_{p_i = f_i'}$$

$$B_4 = -\left(\frac{d_1 \alpha_{H_{\ell-1}} + d_2 \alpha_{H_{\ell-2}}}{\alpha_H^2}\right)\left[f_i' XP_1 + f_i'' XP_2 + f_i''' XP_3 + f_{i-1}''' XP_4\right]_{p_i = f_i'}$$

$$+ \frac{u_e^2}{\alpha_H^3} f_i' \left[2f_i'' D_3 \left(\frac{\partial \rho}{\partial h}\right)_i + f_i' (D_2)_{\frac{\partial}{\partial p} = \frac{\partial}{\partial h}}\right]$$

$$+ \beta \alpha_H \delta\eta \frac{\rho_e}{\rho_i}\left[1 + \frac{\rho_i}{\rho_{i-1}} + \frac{\delta\eta}{6}\left(\frac{\rho_i'}{\rho_i} - \frac{\rho_i}{\rho_{i-1}}\frac{\rho_{i-1}'}{\rho_{i-1}}\right)\right]$$

$$C_1 = -\frac{u_e^2}{\alpha_H^2}\left[f_{i-1}'' D_5 \left(\frac{\partial \rho}{\partial h}\right)_{i-1} + f_{i-1}' (D_4)_{\frac{\partial}{\partial p} = \frac{\partial}{\partial h}}\right]$$

$$C_2 = -\frac{u_e^2}{\alpha_H^2} f_{i-1}' D_5 \left(\frac{\partial \rho}{\partial h}\right)_{i-1}$$

$$C_3 = -2\left[D_1 XP_4 + ZP_4\right]_{p_i = f_i'}$$

$$C_4 = \frac{u_e^2}{\alpha_H^3} f_{i-1}'\left[2f_{i-1}'' D_5 \left(\frac{\partial \rho}{\partial h}\right)_{i-1} + f_{i-1}' (D_4)_{\frac{\partial}{\partial p} = \frac{\partial}{\partial h}}\right]$$

$$D_1 = 1 + \beta + d_0 - \frac{d_1 \alpha_{H_{\ell-1}} + d_2 \alpha_{H_{\ell-2}}}{\alpha_H}$$

TABLE I (concluded)

$$D_2 = -\beta\,\alpha_H^2\,\frac{\delta\eta}{2}\,\frac{\rho_e}{\rho_i^2}\left\{\left(1+\frac{\delta\eta}{3}\,\frac{\rho_i'}{\rho_i}\right)\left(\frac{\partial\rho}{\partial p}\right)_i - \frac{\delta\eta}{6}\left[\sum_{kkk}\tilde{K}'_{kkk}\left(\frac{\partial^2\rho}{\partial p\partial\tilde{K}_{kkk}}\right)+ h'\left(\frac{\partial^2\rho}{\partial p\partial h}\right)\right]_i\right\}$$

$$D_3 = \beta\,\alpha_H^2\,\frac{\delta\eta^2}{12}\,\frac{\rho_e}{\rho_i^2}$$

$$D_4 = -\beta\,\alpha_H^2\,\frac{\delta\eta}{2}\,\frac{\rho_e}{\rho_{i-1}^2}\left\{\left(1-\frac{\delta\eta}{3}\,\frac{\rho_{i-1}'}{\rho_{i-1}}\right)\left(\frac{\partial\rho}{\partial p}\right)_{i-1} + \frac{\delta\eta}{6}\left[\sum_{kkk}\tilde{K}'_{kkk}\left(\frac{\partial^2\rho}{\partial p\partial\tilde{K}_{kkk}}\right) + h'\left(\frac{\partial^2\rho}{\partial p\partial h}\right)\right]_{i-1}\right\}$$

$$D_5 = -\beta\,\alpha_H^2\,\frac{\delta\eta^2}{12}\,\frac{\rho_e}{\rho_{i-1}^2}$$

TABLE II

CORRECTION COEFFICIENTS FOR ENERGY EQUATION

$\Delta f_i : \left[(1 + d_0)H_T\right]_i$	$\Delta f_{i-1} : -\left[(1 + d_0)H_T\right]_{i-1}$
$\Delta f'_i : \left[A_{15}\right]_i + B_{15}$	$\Delta f'_{i-1} : -\left[A_{15}\right]_{i-1}$
$\Delta f''_i : \left[A_{16}\right]_i + B_{16}$	$\Delta f''_{i-1} : -\left[A_{16}\right]_{i-1}$
$\Delta f'''_i : B_{17}$	$\Delta f'''_{i-1} : C_{17}$
$\Delta H_{T_i} : \left[A_{18}\right]_i + B_{18}$	$\Delta H_{T_{i-1}} : -\left[A_{18}\right]_{i-1}$
$\Delta H'_{T_i} : \left[(D_{14})\frac{\partial}{\partial p} = \frac{\partial}{\partial h}\right]_i + B_{19}$	$\Delta H'_{T_{i-1}} : -\left[(D_{14})\frac{\partial}{\partial p} = \frac{\partial}{\partial h}\right]_{i-1}$
$\Delta H''_{T_i} : B_{20}$	$\Delta H''_{T_{i-1}} : C_{20}$
$\Delta \tilde{K}_{kk_i} : \left[(D_{13})\frac{\partial}{\partial p} = \frac{\partial}{\partial \tilde{K}_{kk}}\right]_i$	$\Delta \tilde{K}_{kk_{i-1}} : -\left[(D_{13})\frac{\partial}{\partial p} = \frac{\partial}{\partial \tilde{K}_{kk}}\right]_{i-1}$
$\Delta \tilde{K}'_{kk_i} : \left[(D_{14})\frac{\partial}{\partial p} = \frac{\partial}{\partial \tilde{K}_{kk}}\right]_i$	$\Delta \tilde{K}'_{kk_{i-1}} : -\left[(D_{14})\frac{\partial}{\partial p} = \frac{\partial}{\partial \tilde{K}_{kk}}\right]_{i-1}$
$\Delta \tilde{K}''_{kk_i} : 0$	$\Delta \tilde{K}''_{kk_{i-1}} : 0$
$\Delta \alpha_{H_i} : \left[A_{21}\right]_i$	$\Delta \alpha_{H_{i-1}} : -\left[A_{21}\right]_{i-1}$

TABLE II (continued)

$$A_{15} = -\frac{u_e^2}{\alpha_H^2}\left[f'\left[D_{13}\right]_{\frac{\partial}{\partial p}=\frac{\partial}{\partial h}} + f''\left(\left[D_{14}\right]_{\frac{\partial}{\partial p}=\frac{\partial}{\partial h}} - \frac{C}{\alpha_H}\right)\right]$$

$$A_{16} = -\frac{u_e^2}{\alpha_H^2} f'\left(\left[D_{14}\right]_{\frac{\partial}{\partial p}=\frac{\partial}{\partial h}} - \frac{C}{\alpha_H}\right)$$

$$A_{18} = \left[D_{13}\right]_{\frac{\partial}{\partial p}=\frac{\partial}{\partial h}} + (1 + d_0)f + d_1 f_{\ell-1} + d_2 f_{\ell-2}$$

$$A_{21} = \frac{u_e^2}{\alpha_H^3} f'\left[f'\left[D_{13}\right]_{\frac{\partial}{\partial p}=\frac{\partial}{\partial h}} + 2f''\left(\left[D_{14}\right]_{\frac{\partial}{\partial p}=\frac{\partial}{\partial h}} - \frac{C}{\alpha_H}\right)\right] - \frac{1}{\alpha_H}\left(D_{12} - q_r^*\right)$$

$$B_{15} = -\left[(1 + 2d_0)\left[XP_1\right]_{p_i = H_{T_i}} + \left[ZP_1\right]_{p_i = H_{T_i}}\right]$$

$$B_{16} = -\left[(1 + 2d_0)\left[XP_2\right]_{p_i = H_{T_i}} + \left[ZP_2\right]_{p_i = H_{T_i}}\right]$$

$$B_{17} = -\left[(1 + 2d_0)\left[XP_3\right]_{p_i = H_{T_i}} + \left[ZP_3\right]_{p_i = H_{T_i}}\right]$$

$$B_{18} = -\left[(1 + 2d_0)\left[XP_1\right]_{p_i = f_i'} + \left[ZP_1\right]_{p_i = f_i'}\right]$$

$$B_{19} = -\left[(1 + 2d_0)\left[XP_2\right]_{p_i = f_i'} + \left[ZP_2\right]_{p_i = f_i'}\right]$$

$$B_{20} = -\left[(1 + 2d_0)\left[XP_3\right]_{p_i = f_i'} + \left[ZP_3\right]_{p_i = f_i'}\right]$$

TABLE II (continued)

$$C_{17} = -\left[(1 + 2d_0)\left[XP_4\right]_{p_i = H_{T_i}} + \left[ZP_4\right]_{p_i = H_{T_i}}\right]$$

$$C_{20} = -\left[(1 + 2d_0)\left[XP_4\right]_{p_i = f_i'} + \left[ZP_4\right]_{p_i = f_i'}\right]$$

$$D_{11} = \tilde{h}' - \left(\tilde{C}_p + \frac{c_t^2 R}{\mu_1 \mu_2}\right) T' + c_t R\, T\, \mu_3' + (\tilde{h} - h + c_t R\, T\, \mu_3)\mu_4'$$

$$D_{12} = \frac{C}{\alpha_H}\left[f' f''\, \frac{u_e^2}{\alpha_H^2} + \frac{\overline{C}_p T'}{Pr} + \frac{D_{11}}{\overline{Sc}}\right] + q_r^*$$

$$D_{13} = (D_{12} - q_r^*)\, \frac{1}{C}\frac{\partial C}{\partial p} + \frac{1}{\alpha^*}\frac{\partial q_r}{\partial p} + \frac{C}{\alpha_H Pr}\left(T' \frac{\partial \overline{C}_p}{\partial p} - \frac{\overline{C}_p T'}{Pr}\frac{\partial Pr}{\partial p}\right)$$

$$+ \frac{C}{\alpha_H \overline{Sc}}\left[(\mu_4'\mu_3 + \mu_3')\, c_t R\, \frac{\partial T}{\partial p} + \mu_4' \frac{\partial \tilde{h}}{\partial p} + \mu_4' c_t R\, T\, \frac{\partial \mu_3}{\partial p} - T' \frac{\partial \tilde{C}_p}{\partial p}\right.$$

$$\left. - \frac{D_{11}}{\overline{Sc}}\frac{\partial \overline{Sc}}{\partial p} + \frac{c_t^2 R\, T'}{(\mu_1 \mu_2)^2}\frac{\partial (\mu_1 \mu_2)}{\partial p}\right] - \left[\frac{C}{\alpha_H \overline{Sc}}\, \mu_4'\right]_{\frac{\partial}{\partial p} = \frac{\partial}{\partial h} \text{ only}}$$

$$+ \left[\frac{C\, \overline{C}_p}{\alpha_H Pr} - \frac{C}{\alpha_H \overline{Sc}}\left(\tilde{C}_p + \frac{c_t^2 R}{\mu_1 \mu_2}\right)\right]\left[\sum_{kkk} \tilde{K}_{kkk}' \left(\frac{\partial^2 T}{\partial p \partial \tilde{K}_{kkk}}\right) + h' \left(\frac{\partial^2 T}{\partial p \partial h}\right)\right]$$

$$+ \frac{C}{\alpha_H \overline{Sc}}\, (c_t R\, T)\left[\sum_{kkk} \tilde{K}_{kkk}' \left(\frac{\partial^2 \mu_3}{\partial p \partial \tilde{K}_{kkk}}\right) + h' \left(\frac{\partial^2 \mu_3}{\partial p \partial h}\right)\right]$$

$$+ \frac{C}{\alpha_H \overline{Sc}}\, (\tilde{h} - h + c_t R\, T\, \mu_3)\left[\sum_{kkk} \tilde{K}_{kkk}' \left(\frac{\partial^2 \mu_4}{\partial p \partial \tilde{K}_{kkk}}\right) + h' \left(\frac{\partial^2 \mu_4}{\partial p \partial h}\right)\right]$$

TABLE II (Concluded)

$$D_{14} = \frac{C}{\alpha_H Pr}\,\overline{C}_p\,\frac{\partial T}{\partial p} + \frac{C}{\alpha_H \overline{Sc}}\left[c_t R\,T\,\frac{\partial \mu_3}{\partial p} + (\tilde{h} - h + c_t R\,T\,\mu_3)\,\frac{\partial \mu_4}{\partial p}\right.$$

$$\left. - \left(\tilde{C}_p + \frac{c_t^2 R}{\mu_1 \mu_2}\right)\frac{\partial T}{\partial p}\right] + \left[\frac{C}{\alpha_H \overline{Sc}}\right]\frac{\partial}{\partial p} = \frac{\partial}{\partial h} \text{ only}$$

TABLE III

CORRECTION COEFFICIENTS FOR K^{th} ELEMENTAL SPECIES EQUATION

$\Delta f_i : \left[(1 + d_0)\tilde{K}_k\right]_i$	$\Delta f_{i-1} : -\left[(1 + d_0)\tilde{K}_k\right]_{i-1}$
$\Delta f'_i : \left[A_7\right]_i + B_7$	$\Delta f'_{i-1} : -\left[A_7\right]_{i-1} + C_7$
$\Delta f''_i : \left[-\frac{u_e^2}{\alpha_H^2} f'(D_6)\frac{\partial}{\partial p} = \frac{\partial}{\partial h}\right]_i + B_8$	$\Delta f''_{i-1} : -\left[-\frac{u_e^2}{\alpha_H^2} f'(D_6)\frac{\partial}{\partial p} = \frac{\partial}{\partial h}\right]_{i-1} + C_8$
$\Delta f'''_i : B_9$	$\Delta f'''_{i-1} : C_9$
$\Delta H_{T_i} : \left[D_7\right]_{i,\ \frac{\partial}{\partial p} = \frac{\partial}{\partial h}} + B_{10}$	$\Delta H_{T_{i-1}} : -\left[D_7\right]_{i-1,\ \frac{\partial}{\partial p} = \frac{\partial}{\partial h}} + C_{10}$
$\Delta H'_{T_i} : \left[D_6\right]_{i,\ \frac{\partial}{\partial p} = \frac{\partial}{\partial h}} - \alpha_H \frac{\delta\eta^2}{12}\left(\frac{\partial \phi_k}{\partial h}\right)_i$	$\Delta H'_{T_{i-1}} : -\left[D_6\right]_{i-1,\ \frac{\partial}{\partial p} = \frac{\partial}{\partial h}} + \alpha_H \frac{\delta\eta^2}{12}\left(\frac{\partial \phi_k}{\partial h}\right)_{i-1}$
$\Delta H''_{T_i} : 0$	$\Delta H''_{T_{i-1}} : 0$
$\Delta \tilde{K}_{kk_i} : \left[A_{11}\right]_i + B_{11}$	$\Delta \tilde{K}_{kk_{i-1}} : -\left[A_{11}\right]_{i-1} + C_{11}$
$\Delta \tilde{K}'_{kk_i} : \left[A_{12}\right]_i + B_{12}$	$\Delta \tilde{K}'_{kk_{i-1}} : -\left[A_{12}\right]_{i-1} + \alpha_H \frac{\delta\eta^2}{12}\left(\frac{\partial \phi_k}{\partial \tilde{K}_{kk}}\right)_{i-1}$
$\Delta \tilde{K}''_{kk_i} : B_{13}$	$\Delta \tilde{K}''_{kk_{i-1}} : C_{13}$
$\Delta \alpha_{H_i} : \left[A_{14}\right]_i + B_{14}$	$\Delta \alpha_{H_{i-1}} : -\left[A_{14}\right]_{i-1} + C_{14}$

TABLE III (continued)

$$A_7 = -\frac{u_e^2}{\alpha_H^2}\left(f'' D_6 + f' D_7\right)\frac{\partial}{\partial p} = \frac{\partial}{\partial h}$$

$$A_{11} = \left[D_7\right]_{\frac{\partial}{\partial p} = \frac{\partial}{\partial \tilde{K}_{kk}}} + \left[(1 + d_0) f + d_1 f_{\ell-1} + d_2 f_{\ell-2} - \frac{C}{\alpha_H \overline{Sc}}\mu_4'\right]_{k = kk \text{ only}}$$

$$A_{12} = \left[D_6\right]_{\frac{\partial}{\partial p} = \frac{\partial}{\partial \tilde{K}_{kk}}}$$

$$A_{14} = \frac{u_e^2}{\alpha_H^3} f'\left(2f'' D_6 + f' D_7\right)\frac{\partial}{\partial p} = \frac{\partial}{\partial h} - \frac{C}{\alpha_h \overline{Sc}}\frac{1}{\alpha_H}\left[\tilde{Z}_k' + (\tilde{Z}_k - \tilde{K}_k)\mu_4'\right]$$

$$B_7 = -\left[ZP_1 + (1 + 2d_0)\, XP_1\right]_{p_i = \tilde{K}_{k_i}}$$

$$- \alpha_H \frac{u_e^2}{\alpha_H^2}\frac{\delta\eta}{2}\left[\left(f_i' - \frac{\delta\eta}{6} f_i''\right)\left(\frac{\partial \phi_k}{\partial h}\right)_i - \frac{\delta\eta}{6} f_i' \left(D_8\right)_{i,\, \frac{\partial}{\partial p} = \frac{\partial}{\partial h}}\right]$$

$$B_8 = -\left[ZP_2 + (1 + 2d_0)\, XP_2\right]_{p_i = \tilde{K}_{k_i}} + \alpha_H \frac{u_e^2}{\alpha_H^2}\frac{\delta\eta^2}{12} f_i'\left(\frac{\partial \phi_k}{\partial h}\right)_i$$

$$B_9 = -\left[ZP_3 + (1 + 2d_0)\, XP_3\right]_{p_i = \tilde{K}_{k_i}}$$

$$B_{10} = \alpha_H \frac{\delta\eta}{2}\left[\left(\frac{\partial \phi_k}{\partial h}\right)_i - \frac{\delta\eta}{6}\left(D_8\right)_{i,\, \frac{\partial}{\partial p} = \frac{\partial}{\partial h}}\right]$$

TABLE III (continued)

$$B_{11} = -\left[ZP_1 + (1 + 2d_0)\ XP_1\right]_{p_i = f_i',\ k = kk \text{ only}}$$

$$+ \alpha_H \frac{\delta\eta}{2}\left[\left(\frac{\partial\phi_k}{\partial\tilde{K}_{kk}}\right)_i - \frac{\delta\eta}{6}(D_8)_i,\ \frac{\partial}{\partial p} = \frac{\partial}{\partial\tilde{K}_{kk}}\right]$$

$$B_{12} = -\left[ZP_2 + (1 + 2d_0)\ XP_2\right]_{p_i = f_i',\ k = kk \text{ only}} - \alpha_H \frac{\delta\eta^2}{12}\left(\frac{\partial\phi_k}{\partial\tilde{K}_{kk}}\right)_i$$

$$B_{13} = -\left[ZP_3 + (1 + 2d_0)\ XP_3\right]_{p_i = f_i',\ k = kk \text{ only}}$$

$$B_{14} = \frac{u_e^2}{\alpha_H^2}\frac{\delta\eta}{2} f_i'\left[\left(f_i' - \frac{\delta\eta}{3} f_i''\right)\left(\frac{\partial\phi_k}{\partial h}\right)_i - \frac{\delta\eta}{6} f_i'\,(D_8)_i,\ \frac{\partial}{\partial p} = \frac{\partial}{\partial h}\right]$$

$$+ \frac{\delta\eta}{2}\left[\phi_{k_i} + \phi_{k_{i-1}} - \left(\phi'_{k_i} - \phi'_{k_{i-1}}\right)\frac{\delta\eta}{6}\right]$$

$$C_7 = -\alpha_H \frac{u_e^2}{\alpha_H^2}\frac{\delta\eta}{2}\left[\left(f'_{i-1} + \frac{\delta\eta}{6} f''_{i-1}\right)\left(\frac{\partial\phi_k}{\partial h}\right)_{i-1} + \frac{\delta\eta}{6} f'_{i-1}\,(D_8)_{i-1},\ \frac{\partial}{\partial p} = \frac{\partial}{\partial h}\right]$$

$$C_8 = -\alpha_H \frac{u_e^2}{\alpha_H^2}\frac{\delta\eta^2}{12} f'_{i-1}\left(\frac{\partial\phi_k}{\partial h}\right)_{i-1}$$

$$C_9 = -\left[ZP_4 + (1 + 2d_0)\ XP_4\right]_{p_i = \tilde{K}_{k_i}}$$

$$C_{10} = \alpha_H \frac{\delta\eta}{2}\left[\left(\frac{\partial\phi_k}{\partial h}\right)_{i-1} + \frac{\delta\eta}{6}(D_8)_{i-1},\ \frac{\partial}{\partial p} = \frac{\partial}{\partial h}\right]$$

$$C_{11} = \alpha_H \frac{\delta\eta}{2}\left[\left(\frac{\partial\phi_k}{\partial\tilde{K}_{kk}}\right)_{i-1} + \frac{\delta\eta}{6}(D_8)_{i-1},\ \frac{\partial}{\partial p} = \frac{\partial}{\partial\tilde{K}_{kk}}\right]$$

TABLE III (concluded)

$$C_{13} = -\left[ZP_4 + (1 + 2d_0)\ XP_4\right]_{p_i = f'_i,\ k = kk\ only}$$

$$C_{14} = \frac{u_e^2}{\alpha_H^2}\frac{\delta\eta}{2} f'_{i-1}\left[\left(f'_{i-1} + \frac{\delta\eta}{3} f''_{i-1}\right)\left(\frac{\partial\phi_k}{\partial h}\right)_{i-1} + \frac{\delta\eta}{6} f'_{i-1}\ (D_8)_{i-1},\ \frac{\partial}{\partial p} = \frac{\partial}{\partial h}\right]$$

$$D_6 = \frac{C}{\alpha_H \overline{Sc}}\left[\frac{\partial \tilde{Z}_k}{\partial p} + (\tilde{Z}_k - \tilde{K}_k)\frac{\partial \mu_4}{\partial p}\right]$$

$$D_7 = \frac{C}{\alpha_H \overline{Sc}}\left\{\mu'_4 \frac{\partial \tilde{Z}_k}{\partial p} + \left[\tilde{Z}'_k + (\tilde{Z}_k - \tilde{K}_k)\mu'_4\right]\left(\frac{1}{C}\frac{\partial C}{\partial p} - \frac{1}{\overline{Sc}}\frac{\partial \overline{Sc}}{\partial p}\right)\right.$$

$$+ \left[\sum_{kkk} \tilde{K}'_{kkk}\left(\frac{\partial^2 \tilde{Z}_k}{\partial p \partial \tilde{K}_{kkk}}\right) + h'\left(\frac{\partial^2 \tilde{Z}_k}{\partial p \partial h}\right)\right]$$

$$\left. + (\tilde{Z}_k - \tilde{K}_k)\left[\sum_{kkk} \tilde{K}'_{kkk}\left(\frac{\partial^2 \mu_4}{\partial p \partial \tilde{K}_{kkk}}\right) + h'\left(\frac{\partial^2 \mu_4}{\partial p \partial h}\right)\right]\right\}$$

$$D_8 = \sum_{kkk} \tilde{K}'_{kkk}\left(\frac{\partial^2 \phi_k}{\partial p \partial \tilde{K}_{kkk}}\right) + h'\left(\frac{\partial^2 \phi_k}{\partial p \partial h}\right)$$

$$- \Delta f''_{edge} + \left[\frac{d\left[\frac{u}{u_e}(f,\xi)\right]}{df}\right]_{edge} (f'_{edge}\Delta\alpha_H + \alpha_H \Delta f'_{edge})$$

$$+ \alpha_H f'_{edge} \left[\frac{d^2\left[\frac{u}{u_e}(f,\xi)\right]}{df^2}\right]_{edge} \Delta f_{edge} = - \text{ERROR}$$

$$= - \left\{ - f''_{edge} + \alpha_H \left[f' \frac{d\left[\frac{u}{u_e}(f,\xi)\right]}{df} \right]_{edge} \right\}_m \tag{139}$$

In the absence of an entropy layer, Eqs. (71) yield the following recurrence formulas:

$$\Delta f'_e - \Delta\alpha_H = - \text{ERROR} = - (f'_e - \alpha_H)_m \tag{140}$$

$$\Delta f''_e = - \text{ERROR} = - f''_e \tag{141}$$

Although Eqs. (140) and (141) are linear, these boundary conditions are included in the nonlinear set because of the possibility of an entropy layer.

As pointed out in Section 3, the wall boundary conditions can assume a variety of forms. When the boundary layer is coupled to a transient charring ablation solution, there are a total of $K + 2$ nonlinear wall boundary conditions supplying, in effect, $\rho_w v_w$ (and thus f_w by means of Eq. (60)), H_{T_w} and $K\,\tilde{K}_{k_w}$. Therefore, although some of these boundary conditions become linear for simpler problems, they also must be considered as nonlinear for the general solution procedure. Solution for the wall boundary conditions for the fully coupled problem are discussed in Ref. 10. The wall conditions for two simpler problems are described herein.

In the case that the surface conditions are assigned a priori, these boundary conditions become particularly simple. For example, if $\rho_w v_w$, H_{T_w} and $\tilde{K}_{k_w}$ are assigned, the following recurrence formulas result:

$$\frac{\partial(\rho_w v_w)^*}{\partial f_w}\,\Delta f_w = -\text{ERROR} = -\left[(\rho_w v_w)^* - (\rho_w v_w)^*\Big|_{\text{actual}}\right]_m \tag{142}$$

$$\Delta H_{T_w} = -\text{ERROR} = -\left[H_{T_w} - H_{T_w}\Big|_{\text{actual}}\right]_m \tag{143}$$

$$\Delta \tilde{K}_{k_w} = -\text{ERROR} = -\left[\tilde{K}_{k_w} - \tilde{K}_{k_w}\Big|_{\text{actual}}\right]_m \tag{144}$$

where from Eqs. (59) and (87) it follows that

$$\frac{\partial(\rho_w v_w)^*}{\partial f_w} = -(1 + d_0) \tag{145}$$

To illustrate a more complicated situation, consider the case of steady-state ablation of carbon. The appropriate wall boundary conditions (given by Eqs. (64) through (66)) yield the following recurrence formulas:

$$(\rho_w v_w)^*\,\Delta H_{T_w} + H_{T_w}\frac{\partial(\rho_w v_w)^*}{\partial f_w}\Delta f_w + \Delta q^*_{a_w} + \frac{4\sigma\epsilon_w}{\alpha^*}T_w^3\,\Delta T_w = -\text{ERROR} \tag{146}$$

$$\left.\begin{aligned}(\rho_w v_w)^*\,\Delta \tilde{K}_{C_w} + (\tilde{K}_{C_w} - 1)\frac{\partial(\rho_w v_w)^*}{\partial f_w}\Delta f_w + \Delta j^*_{C_w} &= -\text{ERROR}\\ (\rho_w v_w)^*\,\Delta \tilde{K}_{N_w} + \tilde{K}_{N_w}\frac{\partial(\rho_w v_w)^*}{\partial f_w}\Delta f_w + \Delta j^*_{N_w} &= -\text{ERROR}\end{aligned}\right\} \tag{147}$$

$$\frac{1}{3}\,\Delta(\ell n\, P_{C_3{}_w}) - \frac{\partial K_{p_{eq}}(T_w)}{\partial T_w}\,\Delta T_w = -\text{ERROR} \tag{148}$$

where the ERRORS are given by the left-hand-sides of Eqs. (64) through (66), respectively, evaluated for the m^{th} iteration, the $\partial(\rho_w v_w)^*/\partial f_w$ is given by Eq. (145), the $\Delta q^*_{a_w}$ and $\Delta j^*_{K_w}$ are given by Eqs. (126) and (128), respectively, evaluated at the wall, and the ΔT_w and $\Delta(\ell n\, P_{C_3{}_w})$ are reduced to the primary variables by use of Eq. (129).

In many problems it has not been necessary to consider all of the terms in all of the coefficients in the recurrence formulas. The retention of the

major terms has been seen generally to improve convergence and thereby reduce the number of iterations. However, overall computational time and storage requirements can be improved by dropping the lesser important terms. At present, the terms involving second derivatives and some of the lesser important terms involving first derivatives are excluded. Of course, the dismissal of terms from the recurrence formulas does not affect the accuracy of the final result as long as the ERRORS are evaluated precisely; rather, the errors are driven to zero along different paths.

The coefficients for the recurrence formulas for the Taylor series expansions (Eqs. (116) through (118)), the linear boundary conditions (Eqs. (119) through (123)), the α_H constraint (Eq. (137)), the nonlinear edge boundary conditions (Eqs. (138) and (139)), and the boundary-layer equations (Eqs. (136)) evaluated for the m^{th} iteration form a non-square matrix $[A]$ with $I = (7 + 3K)(N - 1) + 6 + 2K$ rows (the number of equations, excluding the nonlinear surface boundary conditions) and $J = (7 + 3K)N + 1$ columns (the number of correction variables). This matrix equation is given by

$$\left[A \right]_{IxJ} \quad \left[\Delta V \right]_{J} = - \left[E \right]_{I} \tag{149}$$

where ΔV_j represents the correction on the j^{th} primary variable (Δf_1, $\Delta f_2, \ldots$, $\Delta f_1'$, etc.) and E_i represents the error associated with the i^{th} equation.

This matrix can be reduced such that all corrections are expressible in terms of Δf_w, ΔH_{T_w} and the $\Delta \tilde{K}_{k_w}$. This approach makes it convenient to treat varied and complex surface boundary conditions. Any consistent set of surface boundary conditions can be added as an option with a minimum of program modification. The primary reason for this approach, however, was to improve the numerical stability if the boundary layer were to be iteratively coupled to a transient charring ablation solution procedure, by relegating the highly nonlinear surface boundary conditions to a subsidiary iteration with the charring ablation solution. The influence of the boundary layer would be contained in the reduced coefficients of the Δf_w, ΔH_{T_w} and $\Delta \tilde{K}_{k_w}$ somewhat analogous to convective transfer coefficients.

The matrix $[A]$ is quite sparse (i.e., it contains many zeros) in an orderly way. Substantial savings in computation time and storage allocations can be realized if full advantage is taken of this ordered sparseness. This is extremely important since the solution of a boundary layer with several

elemental species would otherwise be very costly. For this reason, the matrix solution procedure will be discussed in some detail.

The first step in the matrix solution is to divide the equations into linear (symbol L) and nonlinear (symbol NL) sets, namely

$$\left[\begin{array}{c|c} AL & BL \\ \hline ANL & BNL \end{array}\right]_{I \times J} \left[\begin{array}{c} \Delta VL \\ \hline \Delta VNL \end{array}\right]_{J} = - \left[\begin{array}{c} EL \\ \hline ENL \end{array}\right]_{I} \tag{150}$$

where for convenience the variables are also classified as "linear" and "nonlinear". The distribution into linear and nonlinear variables is somewhat arbitrary, but care must be taken that the square matrix $[AL]$ not be singular. It has been found convenient to select the following linear corrections and to arrange them in the order as listed: $\Delta VL_F(\Delta f_2, \Delta f_3, .., \Delta f_n, \Delta f'_w \Delta f'_2, .., \Delta f'_n, \Delta f''_w, \Delta f''_2, ..., \Delta f''_{n-1})$; $\Delta VL_H(\Delta H''_{T_n}, \Delta H_{T_2}, \Delta H_{T_3}, ..., \Delta H_{T_n}, \Delta H'_{T_w}, \Delta H'_{T_2}, ... \Delta H'_{T_n})$; and K sets of $\Delta VL_K(\Delta \tilde{K}''_{k_n}, \Delta \tilde{K}_{k_2}, \Delta \tilde{K}_{k_3}, ..., \Delta \tilde{K}_{k_n}, \Delta \tilde{K}'_{k_w}, \Delta \tilde{K}'_{k_2}, ..., \Delta \tilde{K}'_{k_n})$. The nonlinear corrections are conveniently arranged as follows: ΔVNL_F $\Delta \alpha_H$, Δf_w, $\Delta f''_n$, $\Delta f'''_w$, $\Delta f'''_2$, ..., $\Delta f'''_n$); $\Delta VNL_H(\Delta H_{T_w}, \Delta H''_{T_w}, \Delta H''_{T_2}, .., \Delta H''_{T_{n-1}})$; and K sets of $\Delta VNL_K(\Delta \tilde{K}_{k_w}, \Delta \tilde{K}''_{k_w}, \Delta \tilde{K}''_{k_2}, ..., \Delta \tilde{K}''_{k_{n-1}}$. Here the nodal stations are sequenced from 1 at the wall (subscript w) to n at the outer edge of the boundary layer. The linear equations are conveniently sequenced as follows: L_F (linear boundary conditions and Taylor series expansions for f and its first and second derivatives); L_H (linear boundary conditions and Taylor series expansions for H_T and H'_T); and K sets of L_k (linear boundary conditions and Taylor series expansions for $\tilde{K}_k$ and $\tilde{K}'_k$). The nonlinear equations are sequenced as follows: NL_F (the momentum equation evaluated between each neighboring pair of nodal stations together with the two nonlinear boundary conditions and α_H constraint); NL_H (the energy equation evaluated between each neighboring pair of nodal stations); and K sets of NL_K (each of the elemental species equations evaluated between each neighboring pair of nodal stations). The form of the resulting matrix equation is shown in Figure 3. Here, for example, $[ANL_{FH}]$ and $[BNL_{FH}]$ are matrices representing the coefficients of the corrections $[\Delta VL_H]$ and $[\Delta VNL_H]$, respectively, arising from the nonlinear set of equations NL_F with the corresponding errors given by the single column matrix $[ENL_F]$.

The first step in the matrix solution procedure is to invert the submatrices $[AL_{pp}]$ and to form the matrix products $[AL_{pp}]^{-1}$ $[BL_{pp}]$ and $[AL_{pp}]^{-1}$ $[EL_p]$ for p = F, H and K. The former products have to be done only for p = F and H since the linear equations relating the k^{th} elemental species

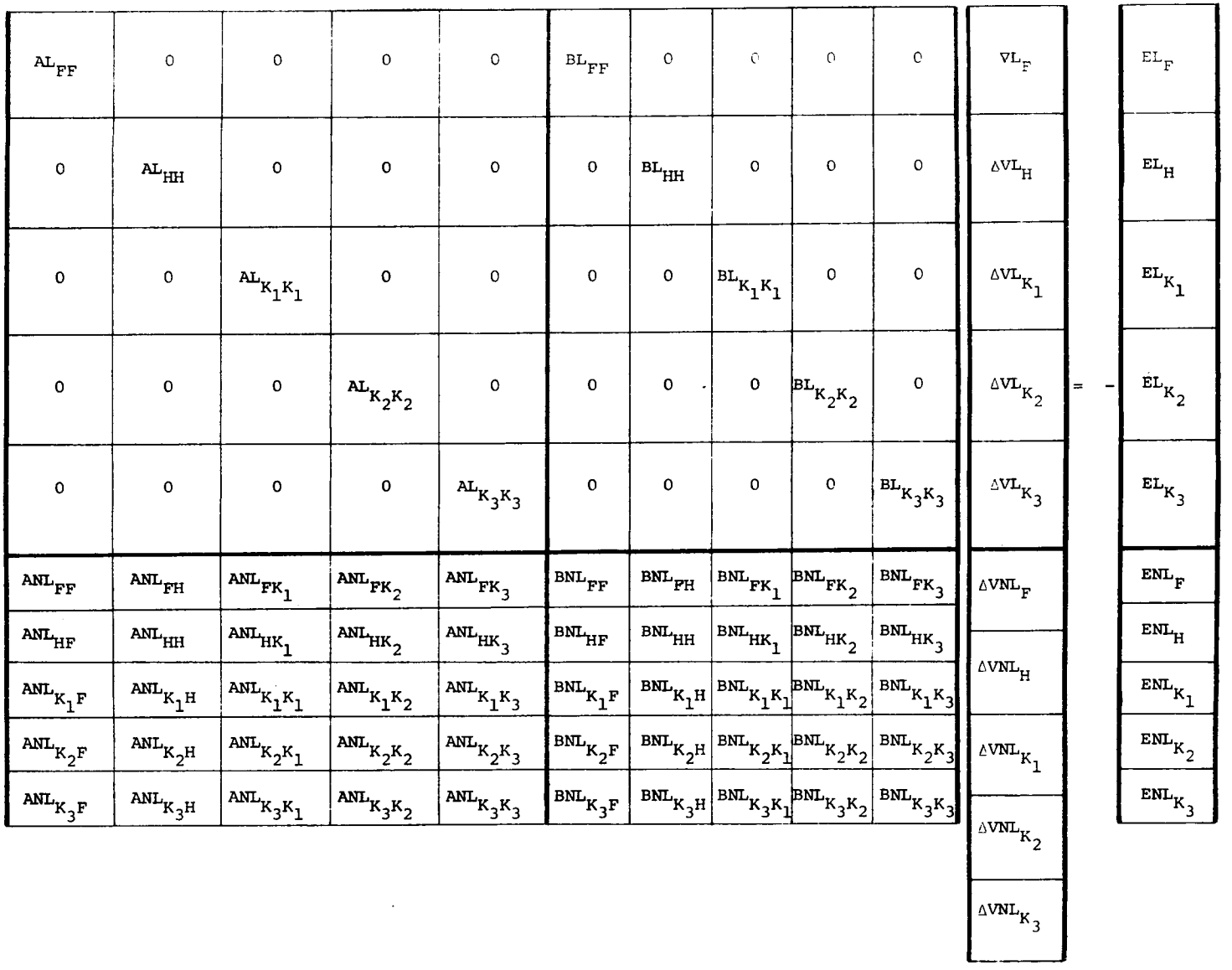

Figure 3. Schematic of Matrix Equation Relating the Newton-Raphson Corrections on the Primary Variables to the Errors for the m^{th} Iteration

to its derivatives (L_K) have the same form as the linear equations relating total enthalpy and its derivatives (L_H). Furthermore, this has to be done only once for a given problem as the matrices $[AL_{pp}]$ and $[BL_{pp}]$ depend only upon the boundary layer η-spacing which can remain fixed as a consequence of the stretching parameter α_H.

The linear corrections $[\Delta VL_p]$ can then be expressed in terms of the nonlinear corrections $[\Delta VNL_p]$ and the linear errors $[EL_p]$ as follows:

$$\left[\Delta VL_p\right]_I = -\left[AL_{pp}\right]^{-1}_{I\times I}\left[BL_{pp}\right]_{I\times J}\left[\Delta VNL_p\right]_J + \left[AL_{pp}\right]^{-1}_{I\times I}\left[-EL_p\right]_I \tag{151}$$

where $I = 3N - 2$ and $J = N + 3$ for $p = F$ and $I = 2N$ and $J = N$ for $p \neq H$ or K with N the number of nodal points in the boundary layer. These can be introduced into the nonlinear equations to yield the reduced problem:

$$\left[\overline{BNL}\right]_{I\times J}\left[\Delta VNL\right]_J = \left[\overline{ENL}\right]_I \tag{152}$$

where $I = (K + 2)(N - 1) + 3$, $J = (K + 2)N + 3$, and the coefficients in the matrix $\left[\overline{BNL}\right]$ are given by

$$\overline{BNL}_{ij} = BNL_{ij} - \sum_{\ell=1}^{m} ANL_{i,\ell+r}\left\{\left[AL_{pp}\right]^{-1}\left[BL_{pp}\right]\right\}_{\ell,j-s} \tag{153}$$

where $p = F$, $m = 3N - 2$ and $r = s = 0$ for $1 \leq j \leq (N + 3)$; $p = H$, $m = 2N$, $r = 3N - 2$ and $s = N + 3$ for $(N + 4) \leq j \leq (2N + 3)$; and $p = K$, $m = 2N$, $r = 3N - 2 + 2NK$ and $s = 3 + N(K + 1)$ for $[(K + 1)N + 4] \leq j \leq [(K + 2)N + 3]$ for the choice of linear and nonlinear corrections listed earlier. The coefficients in the $\left[\overline{ENL}\right]$ matrix are given by

$$\overline{ENL}_i = -ENL_i - \sum_{p}\sum_{\ell=1}^{m} ANL_{i,\ell+r}\left\{\left[AL_{pp}\right]^{-1}\left[-EL_{pp}\right]\right\}_{\ell} \tag{154}$$

for $p = F$, H and K with the m and r having the same values as in Eq. (153) for each p.

Each time a coefficient in one of the original nonlinear equations (i.e., an ANL_{ij} or a BNL_{ij}) is formed, its contribution to $[\overline{BNL}]$ and $[\overline{ENL}]$ can be computed. Thus, the rather large matrix $[ANL]$ never has to be stored. In fact, it is highly significant that the only major blocks of coefficients which must be stored for the representation of all of the linear and nonlinear equations and for their solution are $[BL_{FF}]$ which is $3N - 2$ by $N + 3$, $[BL_{HH}]$ which is $2N$ by N, and $[BNL]$ which is $[(K + 2)(N - 1) + 3]$ by $[(K + 2)N + 3]$ where N is the number of nodal points and K is one less than the number of elemental species. This should be contrasted with the size of the matrix of the complete set of linear and nonlinear equations which is $[(7 + 3K)N + 1]$ square.

The matrix Eq. (142) is substantially reduced further as follows. First, the columns are rearranged so that the nonlinear corrections can be divided into two sets: ΔVNL_a ($\Delta\alpha_H$, $\Delta f_n''$, $\Delta f_w'''$, $\Delta f_2'''$, ..., $\Delta f_n'''$, $\Delta H_{T_w}''$, $\Delta H_{T_2}''$, ..., $\Delta H_{T_{n-1}}''$, $\Delta\tilde{K}_{k_w}''$, $\Delta\tilde{K}_{k_2}''$, ..., $\Delta\tilde{K}_{k_{n-1}}''$) and ΔVNL_b ($\Delta f_w'$, ΔH_{T_w} and the $\Delta\tilde{K}_{k_w}$). Eq. (152) can then be expressed as

$$\left[\begin{array}{c|c} \overline{BNL}_a & \overline{BNL}_b \end{array}\right]_{I \times J} \left[\begin{array}{c} \Delta VNL_a \\ \hline \Delta VNL_b \end{array}\right] = \left[\overline{ENL}\right]_I \tag{155}$$

where $[\overline{BNL}_a]$ is a square matrix, being the coefficients of the I corrections $[\Delta VNL_a]$, with $I = (K + 2)(N - 1) + 3$ and $J = (K + 2)N + 3$. Utilizing the same matrix reduction procedure employed previously (in going from Eq. (150) to Eq. (152)), the $[\Delta VNL_a]$ can be expressed in terms of the reduced set of corrections $[\Delta VNL_b]$ as

$$\left[\Delta VNL_a\right]_I = -\left[\overline{BNL}_a\right]^{-1}_{I \times I} \left[\overline{BNL}_b\right]_{I \times J} \left[\Delta VNL_b\right]_J + \left[\overline{BNL}_a\right]^{-1}_{I \times I} \left[\overline{ENL}\right]_I \tag{156}$$

where $I = (K + 2)(N - 1) + 3$ and $J = K + 2$.

The reduced set of nonlinear corrections $[\Delta VNL_b]$ ($\Delta f_w'$, ΔH_{T_w} and the $\Delta\tilde{K}_{k_w}$) are obtained from a consideration of the nonlinear wall boundary conditions.

Once these are determined, the remaining nonlinear corrections $[\Delta VNL_a]$ are obtained directly by use of Eq. (156). The linear corrections $[\Delta VL_p]$ are then calculated using Eq. (151). These linear and nonlinear corrections are then added to the corresponding primary variables in accordance with Eq. (115), thus completing the m^{th} iteration. The magnitude of the errors are checked and the procedure advances into the $m+1^{th}$ iteration if the absolute errors exceed prescribed upper limits. If not, the iteration is completed for the current value of the streamwise position ξ and time t.

Recurrence formulas for nonlinear wall boundary conditions are given by Eqs. (142) through (144) for assigned $\rho_w v_w$, H_{T_w} and $\tilde{K}_{k_w}$, by Eqs. (146) through (148) for steady-state carbon ablation, or can be obtained from any other consistent wall boundary condition. It is apparent that these equations must be expressed in terms of the $[\Delta VNL_b]$. When $\rho_w v_w$ (or f_w), H_{T_w} (or T_w), and the $\tilde{K}_{k_w}$ are assigned, the $[\Delta VNL_b]$ are given directly (e.g., Eqs. (142) through(144)). However, when fluxes are assigned or mass and/or energy balances are required, the $\Delta j^*_{k_w}$ and/or $\Delta q^*_{a_w}$ (given by Eqs. (128) and (126), respectively, evaluated at the wall) are functions of $[\Delta VL]$ and $[\Delta VNL_a]$ as well as $[\Delta VNL_b]$. That is

$$\Delta FLUX_i = \sum_j \frac{\partial FLUX_i}{\partial VL_j} \Delta VL_j + \sum_j \frac{\partial FLUX_i}{\partial VNL_{a_j}} \Delta VNL_{a_j} + \sum_j \frac{\partial FLUX_i}{\partial VNL_{b_j}} \Delta VNL_{b_j} \qquad (157)$$

where $FLUX_i$ can be $j^*_{k_w}$ and/or $q^*_{a_w}$ and the summations are performed over linear and nonlinear variables with nonzero coefficients. The $[\Delta VL]$ and $[\Delta VNL_a]$ can be eliminated from these relations by making use of Eqs. (151) and (156). For this purpose it is convenient to look upon Eqs. (157) as additional nonlinear equations in the matrix Eq. (150):

$$\left[\Delta FLUX\right]_I = \left[\begin{array}{c|c} AF & BF \end{array}\right]_{I \times J} \left[\begin{array}{c} \Delta VL \\ \hline \Delta VNL \end{array}\right]_J \qquad (157a)$$

where I is the number of flux equations of concern, $J = (7 + 3K)N + 1$, $AF_{ij} = \partial FLUX_i/\partial VL_j$ and $BF_{ij} = \partial FLUX_i/\partial VNL_j$. First, Eq. (151) is utilized to eliminate the $[\Delta VL]$ from Eq. (157), yielding the result

$$\left[\Delta FLUX\right]_I = \left[\overline{BF}\right]_{I \times J} \left[\Delta VNL\right]_J - \left[\overline{EF}\right]_I \qquad (158)$$

where I is the number of flux equations, J = (K + 2)N + 3 (the number of nonlinear variables), and the coefficients are given by

$$\overline{BF}_{ij} = BF_{ij} - \sum_{\ell=1}^{m} AF_{i,\ell+r} \left\{ \left[AL_{pp} \right]^{-1} \left[BL_{pp} \right] \right\}_{\ell,j-s} \tag{159}$$

$$\overline{EF}_{i} = - \sum_{p} \sum_{\ell=1}^{m} AF_{i,\ell+r} \left\{ \left[AL_{pp} \right]^{-1} \left[-EL_{pp} \right] \right\}_{\ell} \tag{160}$$

where the subscripts are the same as those defined after Eqs. (153) and (154). Next, Eq. (158) is rearranged as

$$\left[\Delta FLUX \right]_{I} = \left[\overline{BF}_{a} \,\middle|\, \overline{BF}_{b} \right]_{I \times J} \left[\begin{array}{c} \Delta VNL_{a} \\ \hline \Delta VNL_{b} \end{array} \right]_{J} - \left[\overline{EF} \right]_{I} \tag{161}$$

Equation (156) is then used to eliminate the $\left[\Delta VNL_{a}\right]$ from Eq. (161), yielding

$$\left[\Delta FLUX \right]_{I} = \left[\overline{\overline{BF}}_{b} \right]_{I \times J} \left[\Delta VNL_{b} \right]_{J} - \left[\overline{\overline{EF}} \right]_{I} \tag{162}$$

where I is the number of flux equations, J = K + 2, and the coefficients are given by

$$\overline{\overline{BF}}_{b_{ij}} = \overline{BF}_{b_{ij}} - \sum_{\ell=1}^{m} \overline{BF}_{a_{i\ell}} \left\{ \left[\overline{BNL}_{a} \right]^{-1} \left[\overline{BNL}_{b} \right] \right\}_{\ell j} \tag{163}$$

$$\overline{\overline{EF}}_{i} = \overline{EF}_{i} - \sum_{\ell=1}^{m} \overline{BF}_{a_{i\ell}} \left\{ \left[\overline{BNL}_{a} \right]^{-1} \left[\overline{ENL} \right] \right\}_{\ell} \tag{164}$$

with m = (K + 2)(N - 1) + 3. For clarity, it can be seen that the matrix Eq. (162) is equivalent to

$$
\left.
\begin{aligned}
-\Delta j^{*}_{k_w} &= \sum_{kk=1}^{K} a_{k,kk}\Delta\tilde{K}_{kk_w} + b_k\Delta H_{T_w} + c_k\Delta f_w + d_k \\
-\Delta q^{*}_{w} &= \sum_{kk=1}^{K} a_{K+1,kk}\Delta\tilde{K}_{kk_w} + b_{K+1}\Delta H_{T_w} + c_{K+1}\Delta f_w + d_{K+1}
\end{aligned}
\right\} \qquad (162a)
$$

where the coefficients are constants during the m^{th} iteration. Thus, corrections in the wall fluxes have been reduced to linear functions of corrections in wall state and total mass flux into the boundary layer (utilizing Eq. (145) and noting that $H_{T_w} = h_w$).

Equations (162) can be substituted into the recurrence formulas for the energy and mass balances (e.g., Eqs. (146) and (147)) for steady-state carbon ablation. The resulting equations together with the additional recurrence formula(s) for the nonlinear wall boundary conditions yield the following matrix equation:

$$
\left[C \right]_{I \times I} \left[\Delta VNL_b \right]_I = \left[D \right]_I \qquad (165)
$$

where $I = K + 2$. The ΔVNL_b are then determined by matrix inversion

$$
\left[\Delta VNL_b \right]_I = \left[C \right]^{-1}_{I \times I} \left[D \right]_I \qquad (166)
$$

It should be noted that the time required to invert this matrix is trivial. The time-consuming inversion is that of $\left[\overline{BNL}_a\right]^{-1}$, required for Eqs. (156), (163) and (164), which has the dimension $(K + 2)(N - 1) + 3$.

In this section the Newton-Raphson recurrence formulas for the linear and nonlinear equations have been developed. An efficient method for solving these equations has been outlined. The analysis is completed for the case of a boundary layer coupled to steady-state mass and energy balances. The procedure utilized for coupling to a transient solution for internal conduction is described in Ref. 10.

SECTION 6

RESULTS FOR INCOMPRESSIBLE AND COMPRESSIBLE SINGLE-COMPONENT BOUNDARY LAYERS

The equations presented in Section 3 have been programmed in Fortran IV utilizing the numerical procedure described in Sections 4 and 5. Solutions have been compared to available results for several incompressible and compressible single-component boundary-layer problems as tests of the accuracy and convergence of the procedure. It has been seen that reasonably accurate results can be obtained with as few as five nodal points (the wall, three internal points, and the boundary-layer edge) and that three to four place accuracy can generally be obtained with seven points, although about 11 points have been required for some severe tests to obtain this level of accuracy. Convergence has been consistently satisfactory, four or five iterations being required for a starting solution and three iterations generally being adequate for subsequent (downstream) solutions. Some typical convergence and accuracy checks are presented in this section.

Typical convergence of a velocity profile in an incompressible similar boundary layer with adverse pressure gradient is shown in Fig. 4 in terms of the conventional* Levy-Lees transverse coordinate. Starting with an assumed linear profile, the first iteration established the basic shape of the profile, the second iteration brought the solution within two to three percent, and the third iteration yielded results which were converged to three significant figures and compared favorably with the tabulated results of Loitsianskii.[26]

Validity checks for the nonsimilar incompressible boundary-layer problems of uniform blowing and uniform suction on a flat plate are presented in Fig.5. The wall shear function, f''_w, for these two cases is shown in Fig. 5(a) in terms of the stream function at the wall, f_w.** The solution of Lew and Fanucci[27] is shown for comparison. Convergence required about three iterations at each streamwise station. Profiles of velocity ratio, f', and shear function, f'', are presented in Figs. 5(b) and 5(c). It is of interest that both blowing and

*The normalizing parameter α_H has been removed from η subsequent to the calculations in the accuracy checks presented in this section.

**It should be noted that f_w is zero at the leading edge of the plate, increasing with streamwise dimension for the case of suction and decreasing with streamwise dimension for the case of blowing.

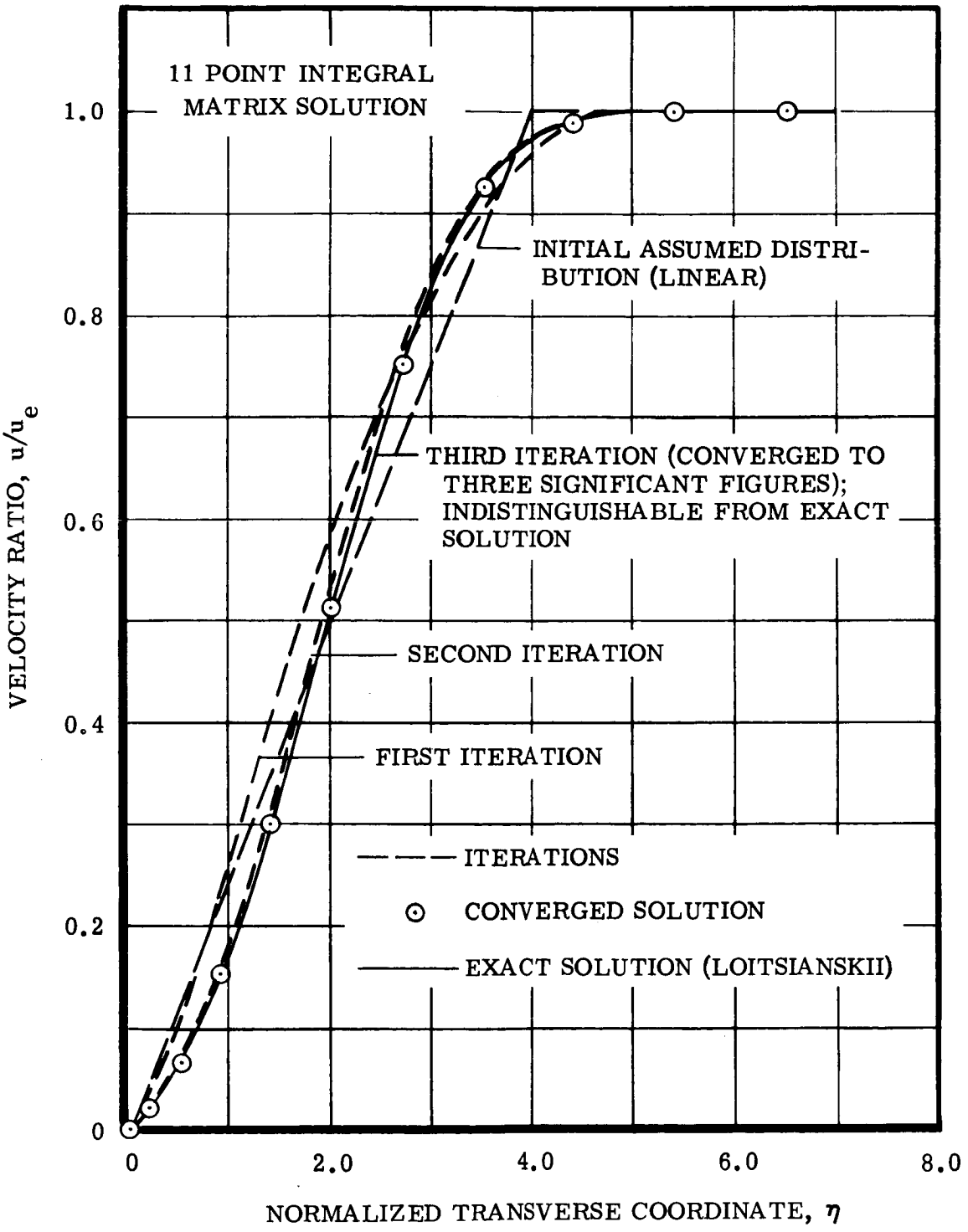

Figure 4. Iteration History for a Similar Incompressible Boundary-Layer Solution Near Separation (β = -0.19, Separation at -0.1988)

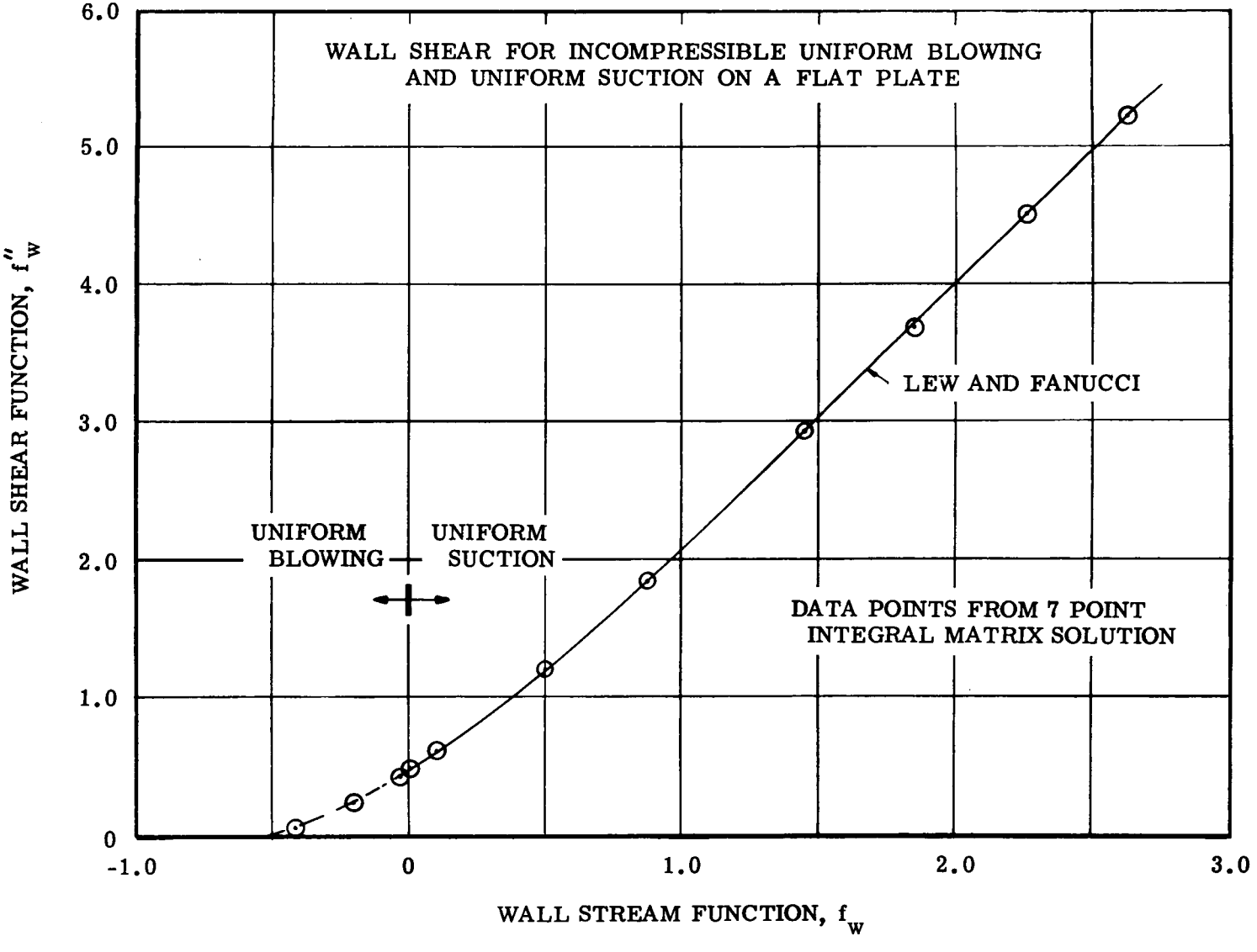

(a) Wall Shear

Figure 5. Solutions for Incompressible Uniform Blowing and Uniform Suction on a Flat Plate

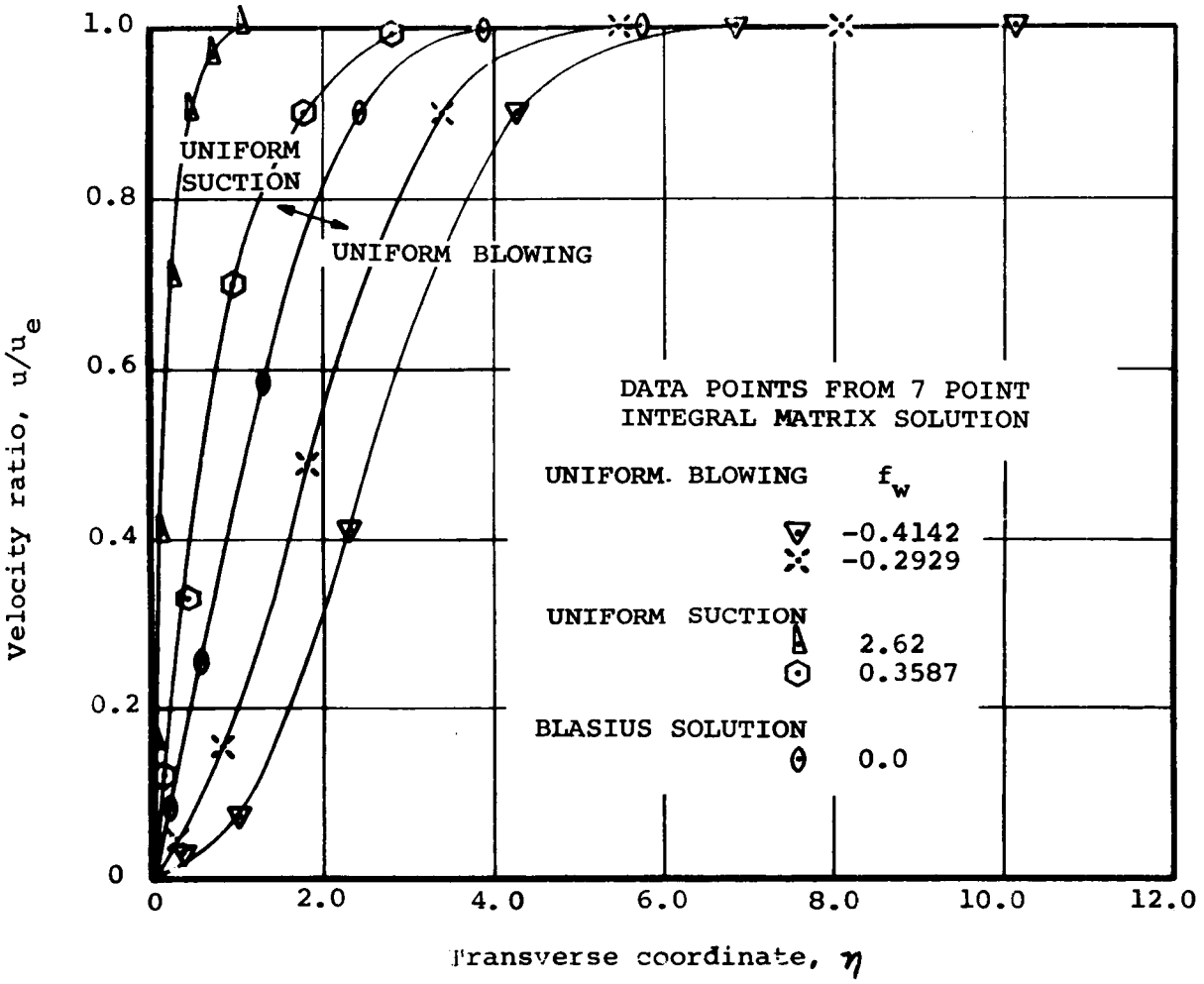

(b) Velocity Profiles

Figure 5. Continued

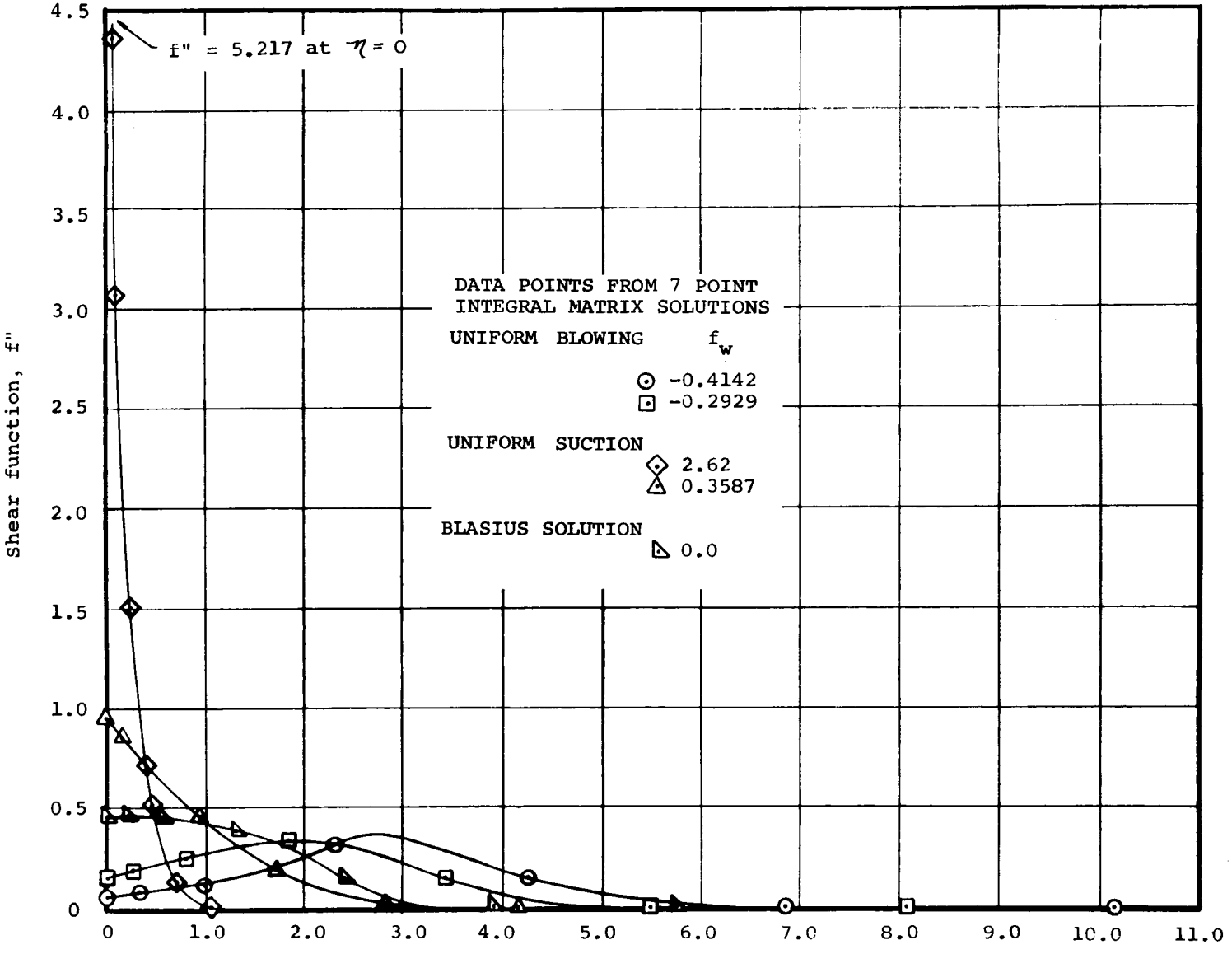

(c) Shear Function Profiles

Figure 5. Concluded

suction results were efficiently obtained with the same $\bar{\eta}$ spacing, in spite of a ten-fold variation in boundary-layer thickness, by the use of the coordinate stretching parameter, α_H, introduced in Section 3.

The wall shear function for uniform blowing into an incompressible boundary layer is presented in Fig. 6 as a function of streamwise distance for a pressure of 1 atmosphere, temperature of 2000°R, and mass injection rate of 0.005 lb/sec ft^2. Results are also shown for the case where blowing is terminated at a streamwise position of 2 feet. It may be of interest to note that the nonsimilar effect of upstream transpiration decays quite rapidly, but that some influence persists for an appreciable distance downstream.

Velocity profiles, shear function profiles, and maps of enthalpy ratio versus velocity ratio are presented in Fig. 7 for incompressible and compressible similar boundary layers with Prandtl number of unity and various positive and negative pressure gradients and wall-to-edge enthalpy ratios. The results compare favorably with those of Hartree[28] and Cohen and Reshotko.[29] These results were obtained with a 7-point nodal network. Two to five (generally three) iterations were required for each problem, where the previous result was in each case employed as a first guess.

Calculations were made for several single-component compressible boundary layers with variable properties corresponding to that of air at moderate temperatures ($\lambda \propto T^{0.85}$, $C_p \propto T^{0.19}$, $\mu \propto T^{0.70}$ and $Pr_w = 0.7$) for various values of β, H_{T_w}/H_{T_e}, and $u_e^2/2H_{T_e}$. As an example, profiles of velocity ratio, shear function, and temperature are presented in Fig. 8 for P = 1 atm, $T_w = 1200°R$, $H_{T_w}/H_{T_e} = 0.2$ and $\beta = 0$ for several values of $u_e^2/2H_{T_e}$. Convergence was similar to that obtained in the Cohen and Roshotko comparisons.

As an example of a nonsimilar compressible boundary-layer solution, results are compared in Fig. 9 to results obtained at the NASA Ames Research Laboratory with the Smith and Clutter finite-difference procedure[5] for the problem of Mach 10.4 flow over a 7½ degree cone with uniform injection downstream of the 0.1574 foot station. The wall shear is compared in Fig. 9(a) whereas representative velocity profiles are compared in Fig. 9(b). The results agree to nearly four significant figures for the similar no-blowing solution and the first few stations downstream of the point where mass injection is initiated. Further downstream, the results are still in reasonably good agreement, considering the ξ-derivatives and possibly the f_w and ξ are computed somewhat differently by the two methods. The present results were invariant with streamwise spacing. The effect of nodal distribution across the boundary layer was not investigated. The effect of streamwise step size on Smith and Clutter results was not available. The first solution required 4 iterations, whereas the downstream stations, including those near the

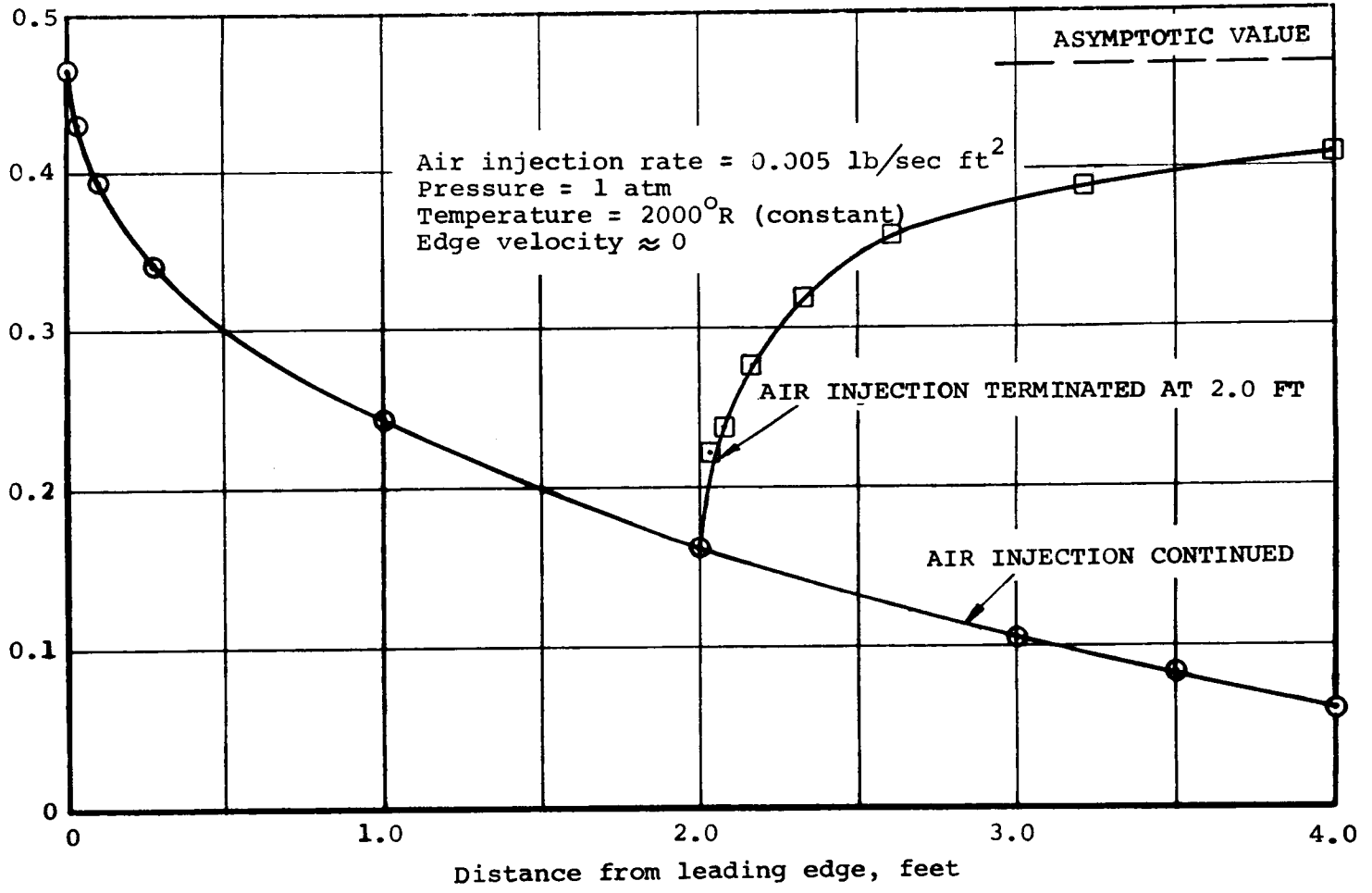

Figure 6. Effect on Wall Shear of Upstream Air-to-Air Injection on a Flat Plate

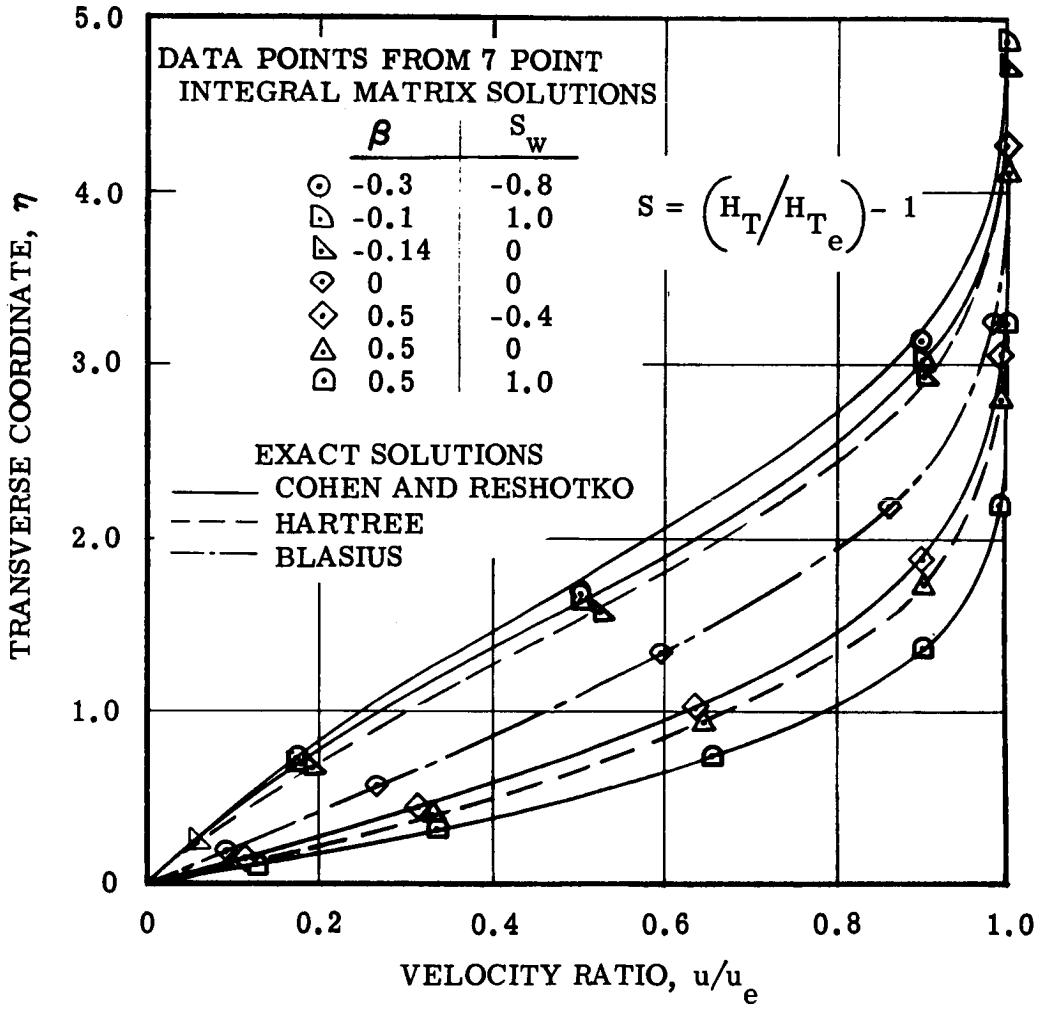

(a) Velocity Profiles

Figure 7. Solutions for Similar Compressible Boundary Layers with Prandtl Number of Unity for Several Values of β and Wall-to-Edge Enthalpy Ratios

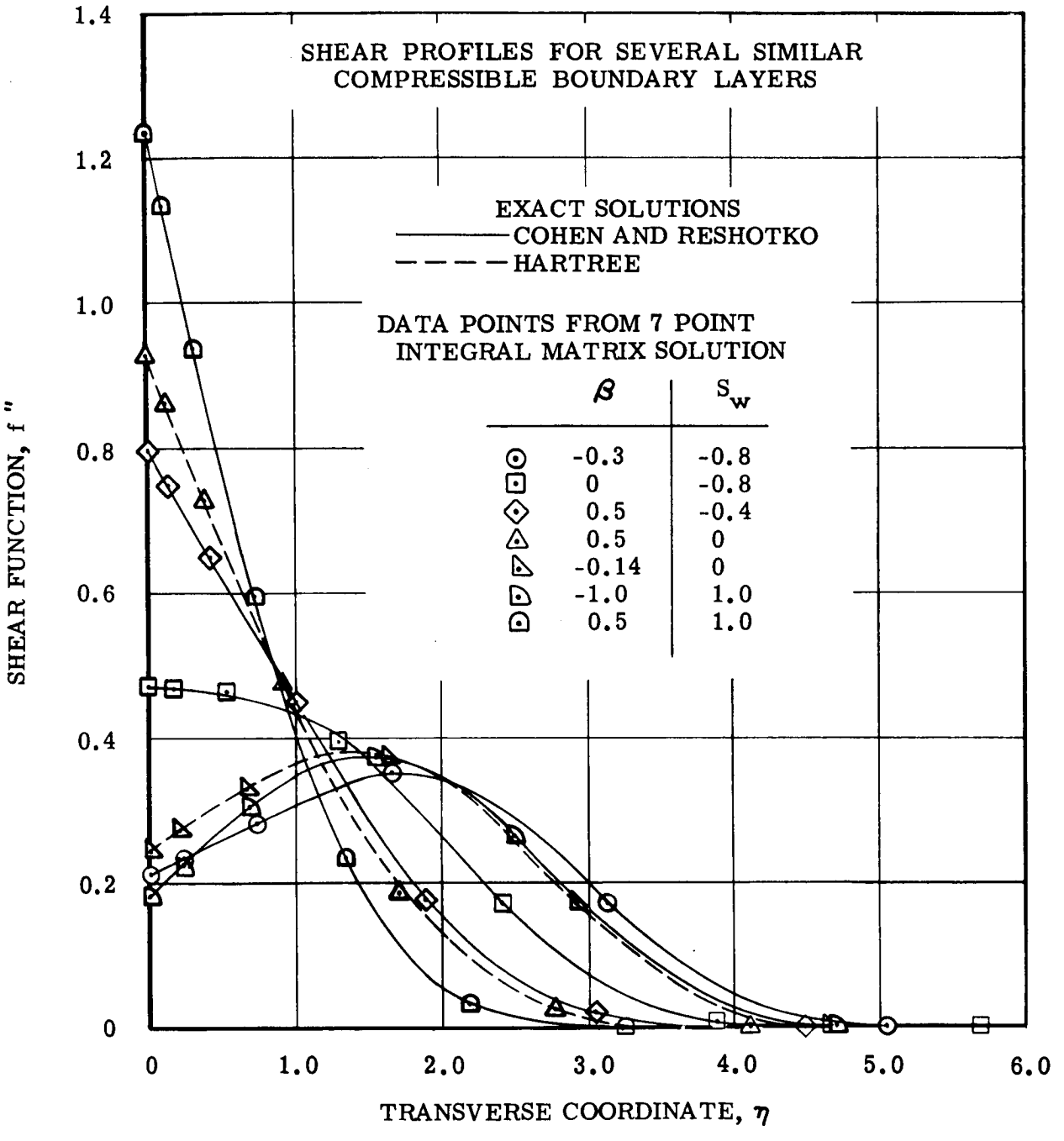

(b) Shear Function Profiles

Figure 7. Continued

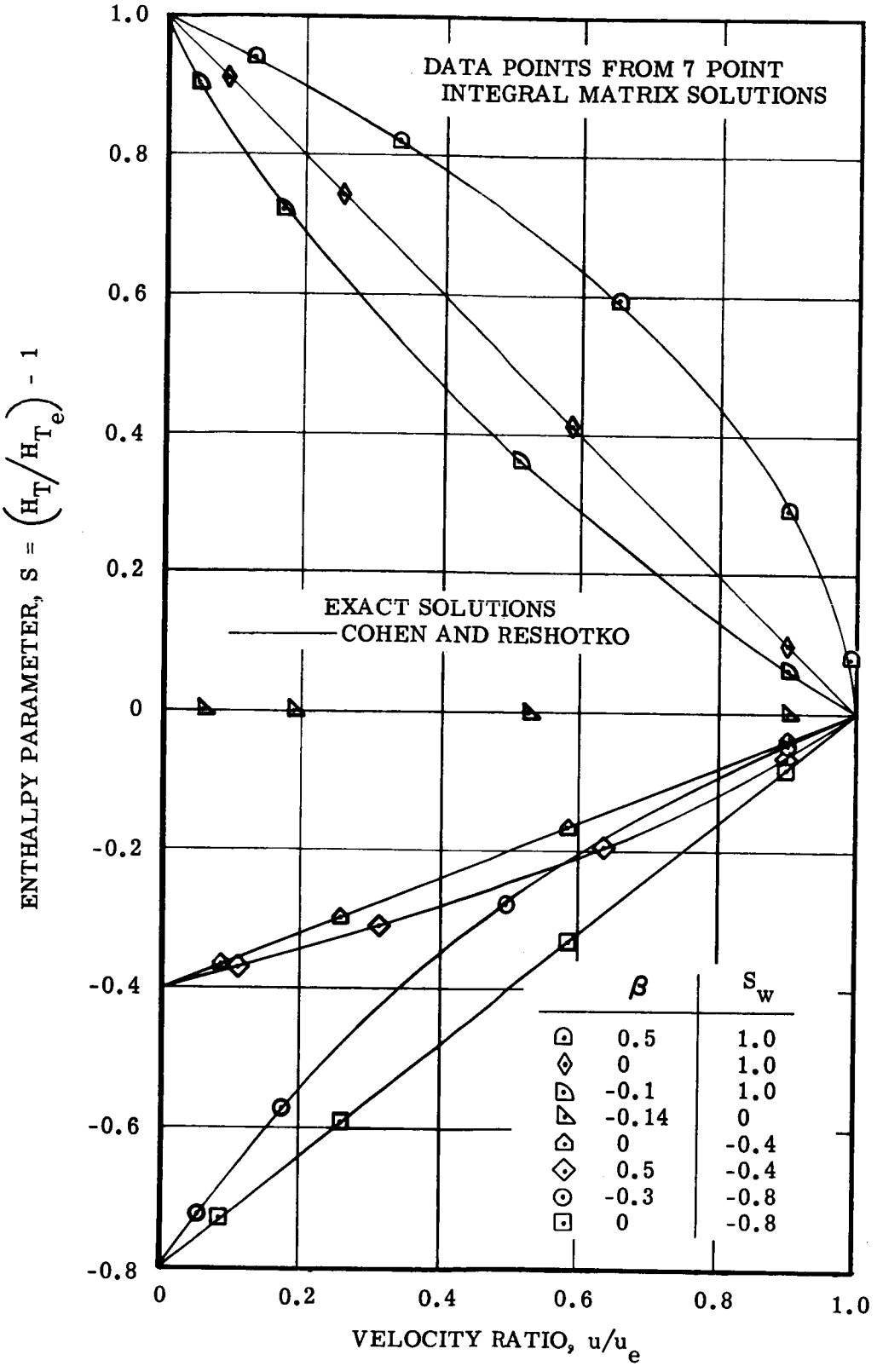

(c) Enthalpy Profiles

Figure 7. Concluded

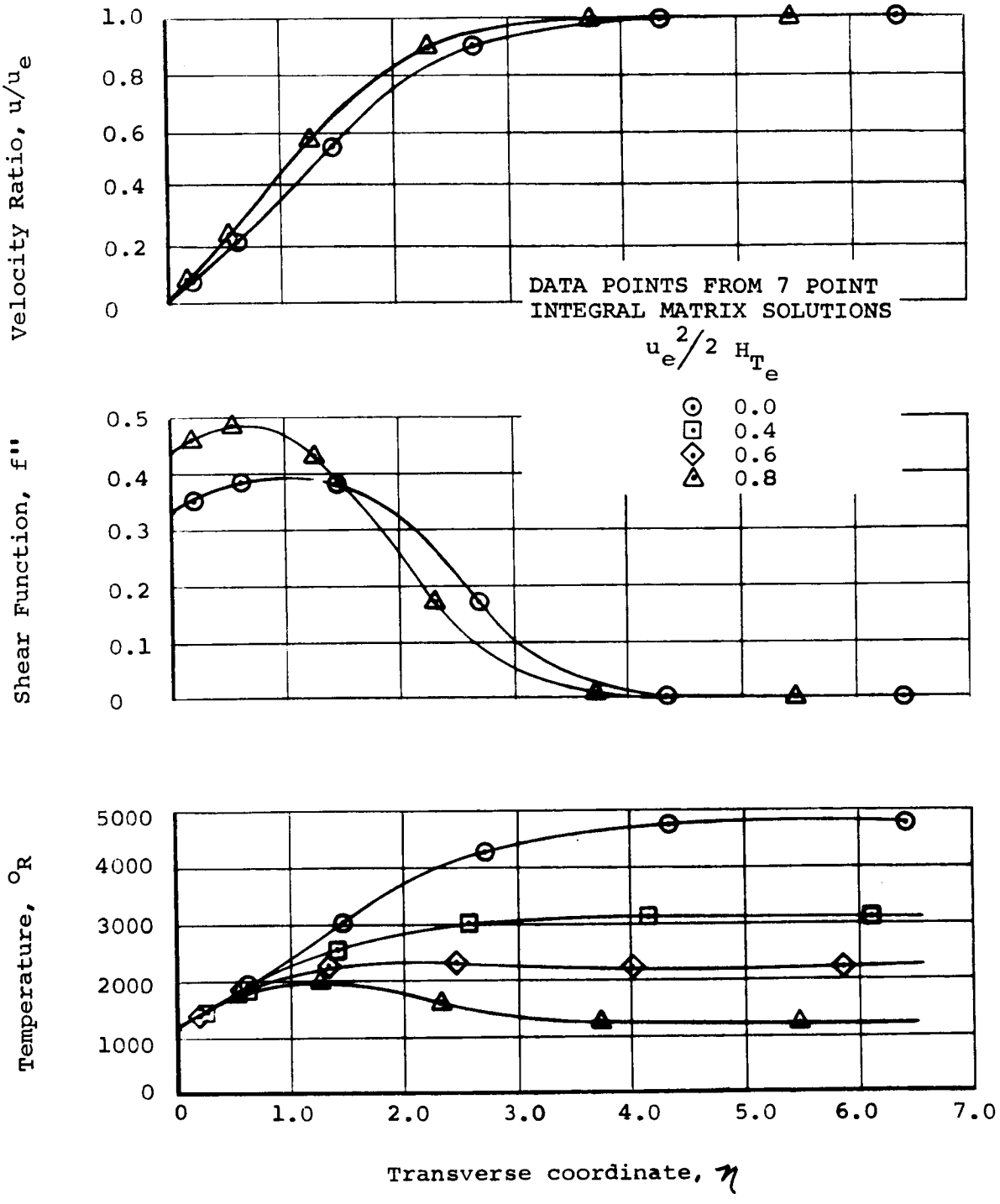

Figure 8. Profiles of Velocity Ratio, Shear Function and Temperature for Variable-Property Air Boundary Layers for Various Values of Edge Kinetic Energy

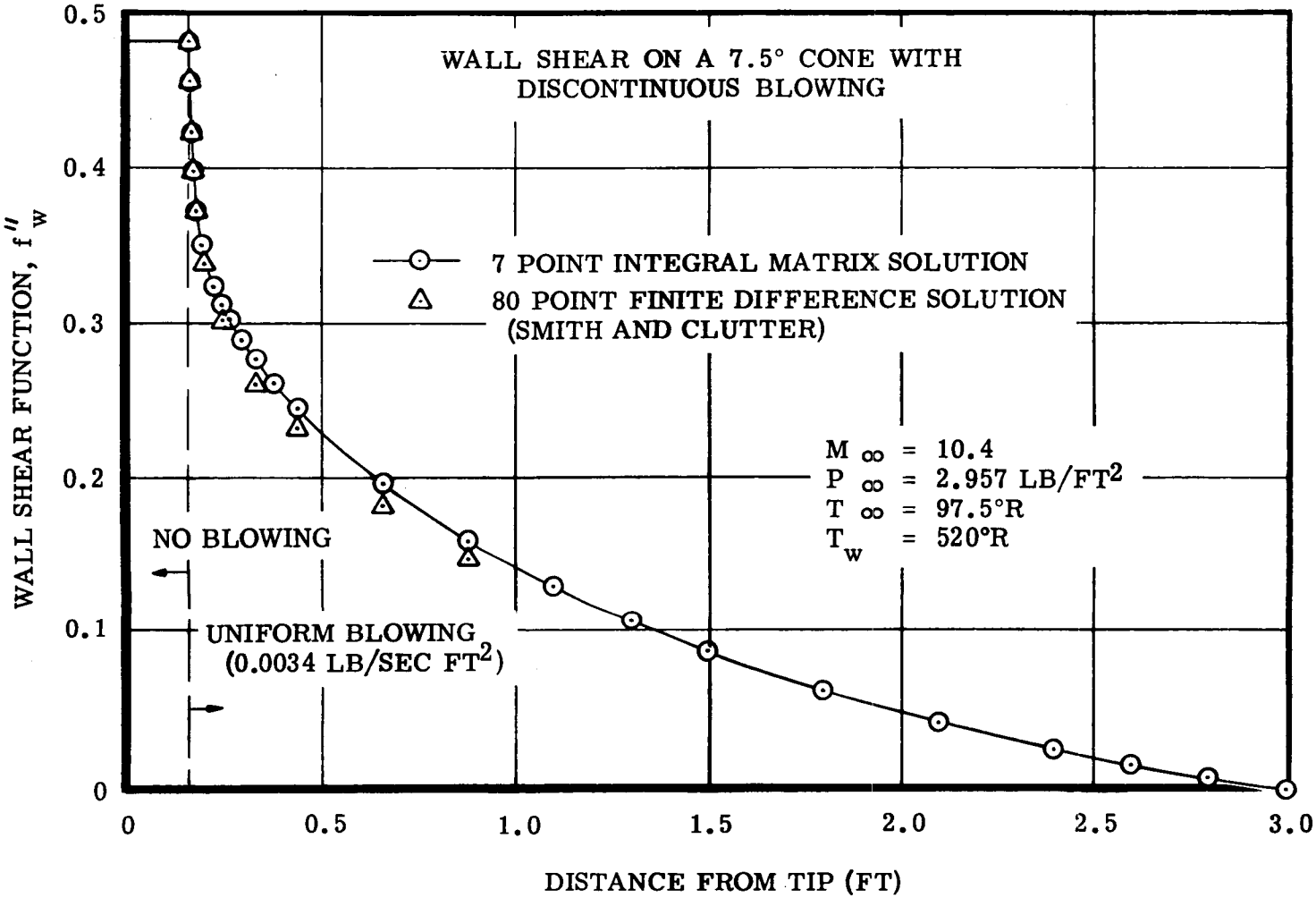

(a) Wall Shear Distribution

Figure 9. Air-to-Air Transpiration into a Compressible Boundary Layer over a 7.5° Cone with an Impermeable Sharp Nose Tip

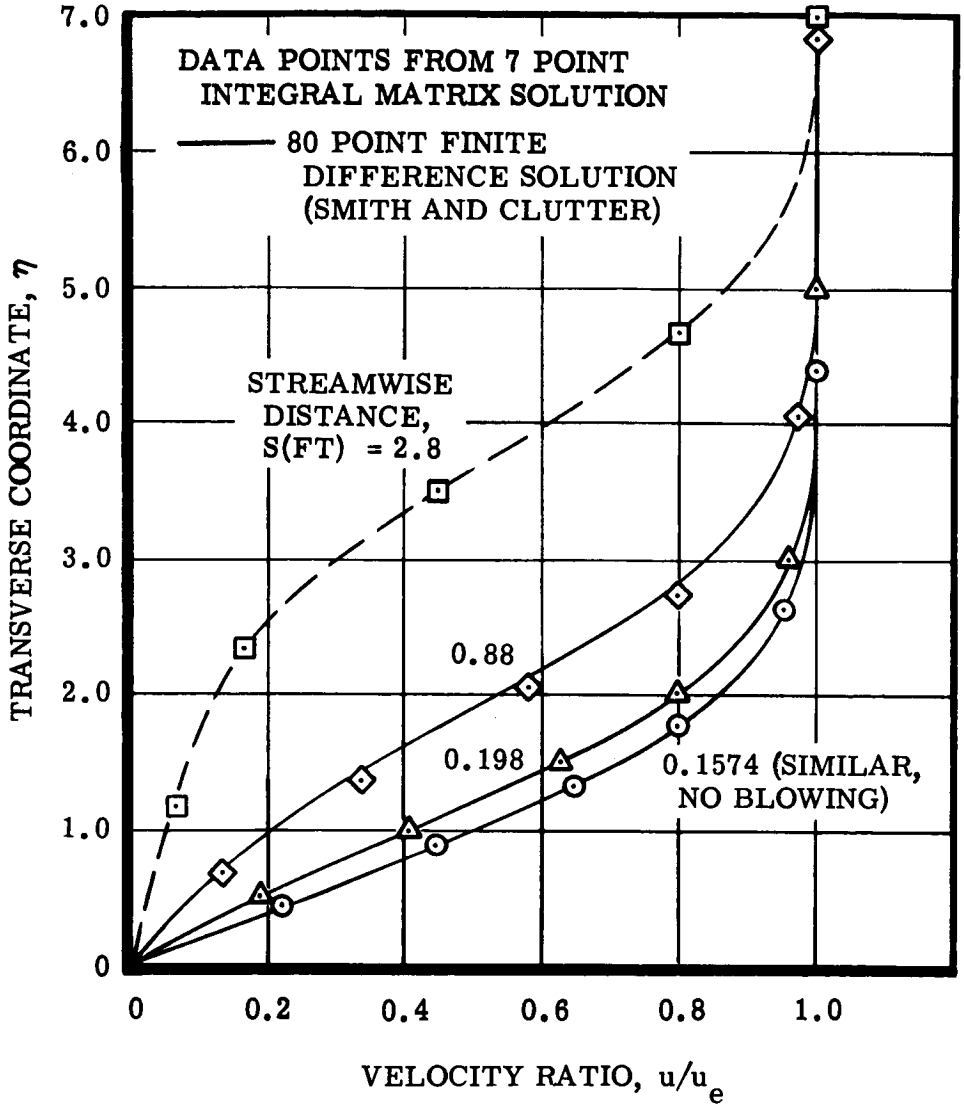

(b) Velocity Profiles

Figure 9. Concluded

zero wall-shear condition, required three iterations each. The entire solution was generated in 45 seconds on the IBM 7094 computer, an order of magnitude less than the results obtained with the Smith and Clutter procedure. The stability of the present procedure is indicated by the fact that no difficulty was incurred in obtaining solutions down to the zero-shear condition.

In order to gain some confidence in the ability of the solution procedure to compute physical boundary-layer thickness, results were correlated with experimental data reported by Watson et al[30] for laminar shock interaction over a flat surface. A velocity profile is presented in Fig. 10. The correlation is good with the exception of values near the wall where it is reasonable to expect some experimental error due to probe-shock interaction.

Results were obtained for a boundary layer in a ficticious gas with rapidly varying properties (e.g., Prandtl number variation from 0.6 to 10 across the boundary layer) in order to study convergence in an extreme situation. A converged solution was obtained in 7 iterations, starting with the usual, uninspired, built-in first guesses.

The problem shown in Fig. 8 (where Mach number effects were investigated) with moderately varying properties and the problem of rapidly varying properties were repeated with various partial derivatives which are used in the iteration process but do not appear in the boundary-layer equations (such as $\partial Pr/\partial h$ and $\partial C/\partial h$) set equal to zero. In the former case, the total number of iterations was increased by two for the entire set of five solutions. In the more severe case, 11 iterations were required (whereas 7 were required previously). The final results, of course, were unaffected.

SECTION 7
SOME RESULTS FOR MULTICOMPONENT BOUNDARY LAYERS

To date no accuracy studies have been performed for multicomponent chemically-reacting boundary-layer problems. However, convergence has consistently been satisfactory. To illustrate, an iteration history is given in Table IV for graphite ablation in air. In this problem, the ablation rate was assigned and surface temperature was determined by a coupled mass balance at the surface together with heterogeneous equilibrium. Considering that the initial guesses for velocity ratio, total enthalpy, and elemental mass fractions are built-in, linear profiles with respect to η, and that there are no constraints on the size of the corrections, convergence such as that shown in Table IV is highly encouraging. Furthermore, it is significant that

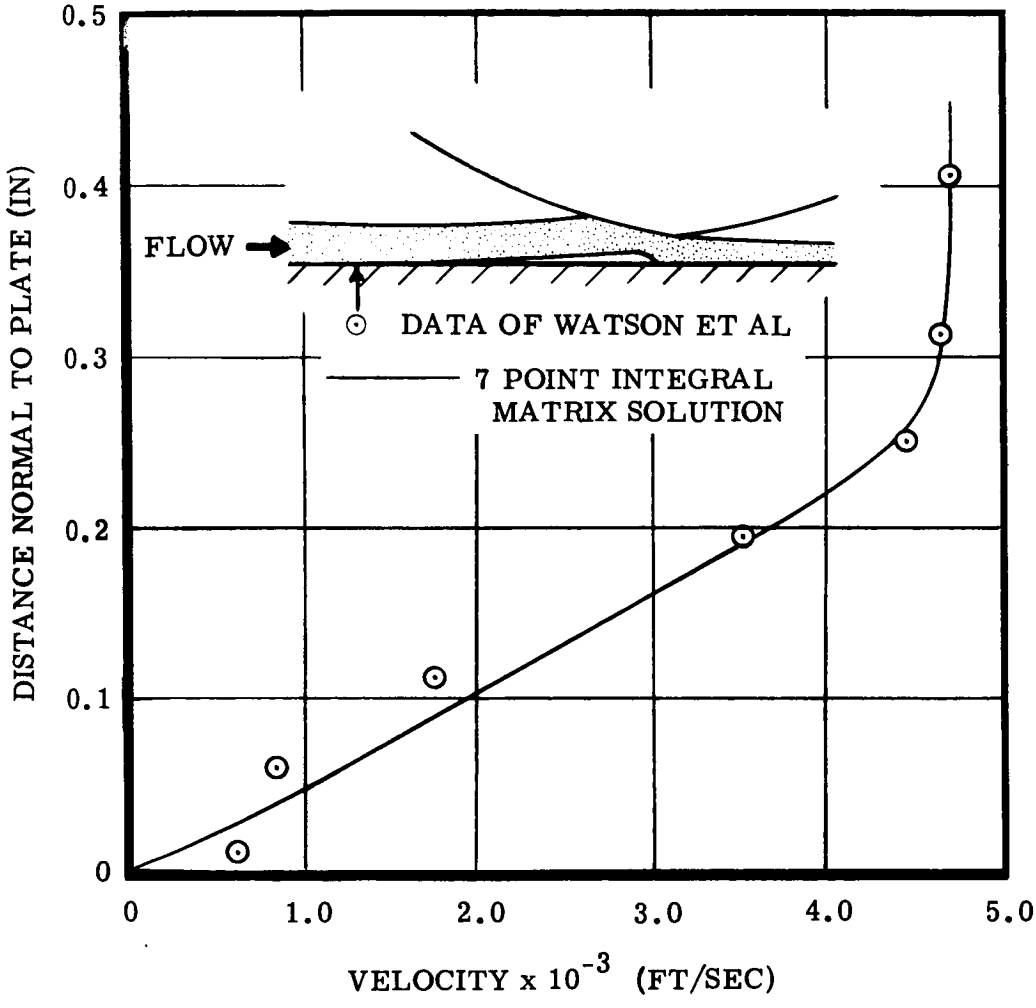

Figure 10. Laminar Interaction on a Flat Surface: $M_\infty = 10.5$ $T_w = 535^\circ R$

this convergence has been obtained while ignoring all second derivatives and some first derivatives in the iteration process.

TABLE IV

CONVERGENCE FOR A TYPICAL GRAPHITE-IN-AIR ABLATION PROBLEM
(Assigned Ablation Rate, Surface Conditions Determined by Coupled Mass Balance)

Iteration	Normalized Wall Shear	Wall Enthalpy, Btu/Lb	Wall Temperature, ^{o}R	Maximum Relative Errors* In Momentum Equation	Energy Equation	Elemental Species Equations
1	0.3135	-223.0	1992	1.0	3.7	0.31
2	0.1727	-804.0	1469	0.29	0.77	0.13
3	0.1628	-795.2	1478	0.10	0.53	0.025
4	0.1670	-794.2	1479	0.0064	0.0028	2.7×10^{-3}
5	0.1670	-794.3	1479	6.9×10^{-4}	1.9×10^{-3}	1.3×10^{-5}

*A relative error of 1×10^{-3} corresponds to nominal 4-place accuracy

Boundary-layer profiles of velocity ratio, temperature, and elemental mass fractions are presented in Table V for an air boundary layer over a flat plate with unequal diffusion coefficients for all species, with and without thermal diffusion. Mole fractions are presented graphically in Fig. 11. For assumed equal diffusion coefficients and in the absence of thermal diffusion, the elemental mass fractions remain constant across the boundary layer at the assigned edge values of 0.23 and 0.77 for oxygen and nitrogen, respectively. Consideration of unequal diffusion coefficients for all species is thus seen to have a substantial effect on elemental mass fractions. With unequal diffusion, the elemental mass fraction of oxygen first decreases slightly and then rises to a maximum value of 0.2723 at the wall. When thermal diffusion is also taken into consideration, the elemental mass fraction at the wall is decreased slightly to a wall value of 0.2709. These wall values of elemental mass fractions necessary to maintain zero mass flux at the wall are analogous to the adiabatic wall temperature for zero heat flux at the wall.

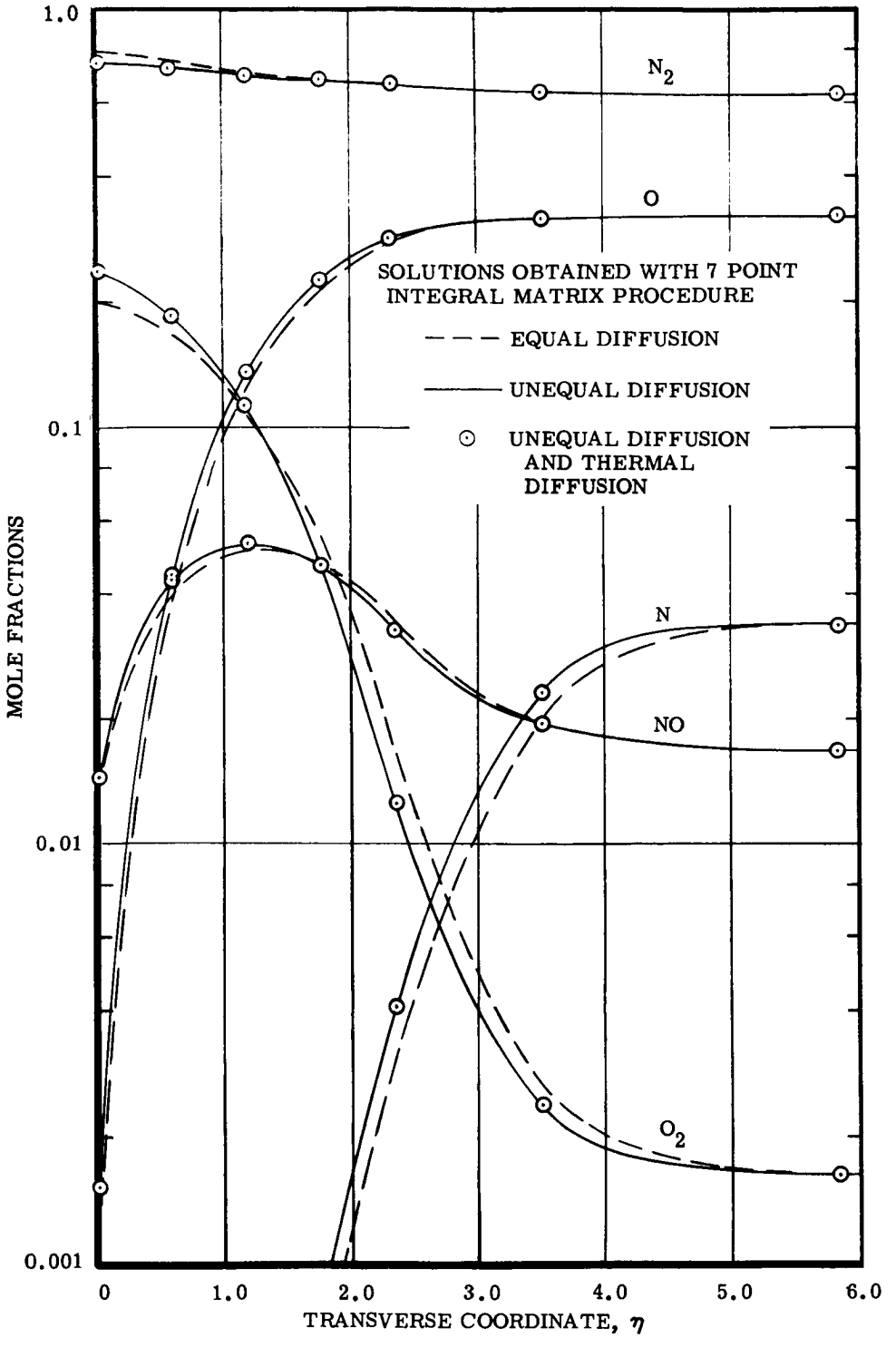

Figure 11. Multicomponent Air Boundary Layer Over a Flat Plate: P = 1 atm, H_{T_e} = 5000 Btu/lb, T_w = 5000°R, s = 1 foot

TABLE V

AIR BOUNDARY LAYER OVER A FLAT PLATE
WITH UNEQUAL DIFFUSION COEFFICIENTS:
(P = 1 atm, H_{T_e} = 5000 Btu/lb, T_w = 5000°R, s = 1 foot)

η	y, ft	u/u_e	$\tilde{K}_O$	$\tilde{K}_N$	T, °R
Thermal diffusion neglected					
0	0	0	0.2723	0.7277	4000
0.584	.00075	0.1889	0.2626	0.7374	5355
1.168	.00171	0.4044	0.2475	0.7525	6165
1.752	.00284	0.6148	0.2308	0.7692	6861
2.336	.00418	0.8000	0.2239	0.7761	7722
3.504	.00735	0.9699	0.2269	0.7731	8892
5.840	.01427	1.0000	0.2300	0.7700	9204
Thermal diffusion included					
0	0	0	0.2709	0.7291	4000
0.584	.00075	0.1887	0.2594	0.7406	5350
1.168	.00171	0.4040	0.2447	0.7553	6170
1.752	.00284	0.6145	0.2288	0.7712	6877
2.336	.00418	0.8000	0.2240	0.7760	7748
3.504	.00736	0.9700	0.2279	0.7721	8903
5.839	.01429	1.0000	0.2300	0.7700	9204

This effect could be significant in ablation problems since substantially more oxygen is available at the wall for reaction. Therefore, it is pertinent to investigate the cause of the observed behavior. As a consequence of the lower dissociation temperature of O_2 relative to N_2, the oxygen is almost completely dissociated into the relatively more mobile atomic oxygen at the edge of the boundary layer, whereas the nitrogen is only slightly dissociated (see Fig. 11). Moving from the boundary-layer edge toward the wall, the nitrogen recombines more readily than the oxygen. As a consequence, the gradient in the atomic nitrogen concentration, although small, is greater than that for atomic oxygen until an η of 2.5 or so is reached. Thus there is a small net flux of nitrogen inward from the boundary-layer edge with a consequential small decrease in oxygen elemental composition. Closer to the wall, substantial recombination of the oxygen occurs, producing a large gradient in atomic oxygen concentration and thus a flux of oxygen toward the wall.

Thermal diffusion produces a small effect in the present problem since temperature gradients are relatively small. Calculations performed at high edge enthalpies have shown large thermal diffusion effects, as a consequence of the larger temperature gradients, resulting in wall oxygen concentrations below edge values.

Profiles of velocity ratio, temperature, shear function, and mole fractions across a boundary layer into which a large quantity of Apollo heat-shield material is being injected are presented in Fig. 12. These results were obtained for an assigned surface temperature and assigned component fluxes ($\dot{m}_g$ and $\dot{m}_c$) and utilized a 30-component chemical model. A converged solution was obtained in 7 iterations, starting with an air boundary-layer solution with the same wall temperature and same edge conditions but with no mass injection. The convergence histories of the wall shear function and maximum relative errors are presented in Table VI. In this calculation, the corrections in the elemental species equations were not allowed to exceed 0.30.

TABLE VI

CONVERGENCE FOR ABLATION OF THE APOLLO HEAT-SHIELD MATERIAL INTO AIR
(Assigned Surface Temperature and Component Fluxes)

		Maximum Relative Errors* In		
Iteration	Normalized Wall Shear	Momentum Equation	Energy Equation	Elemental Species Equations
First Guess	.2007	--	--	--
1	.0883	0.26	0.16	0.30
2	.1343	0.19	0.42	0.30
3	.1016	0.095	0.38	0.23
4	.0995	0.069	0.21	0.11
5	.0987	1.4×10^{-3}	0.045	0.026
6	.0987	4.8×10^{-5}	6.5×10^{-3}	5.1×10^{-3}
7	.0987	2.6×10^{-6}	9.0×10^{-4}	7.5×10^{-4}

*A relative error of 1×10^{-3} corresponds to nominal 4-place accuracy

The nonsimilar boundary layer around a sphere-cone reentry body with water injection was studied to determine the injection rates required around the body to maintain a uniform wall temperature of 5000°R. A 16-component chemical model was employed in these calculations. The distribution of water

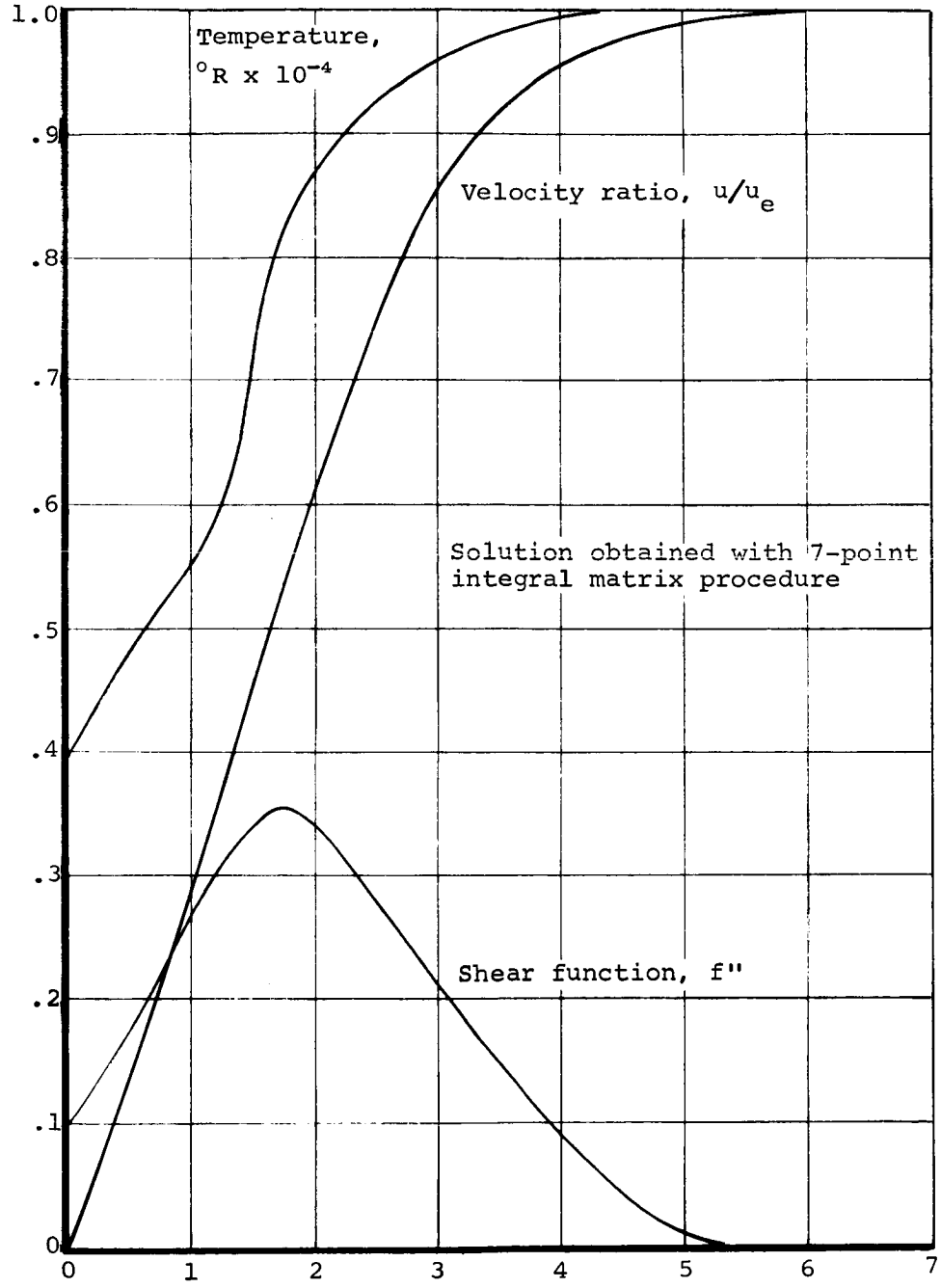

(a) Velocity Ratio, Temperature, and Shear Function

Figure 12. Boundary-Layer Profiles Over the Apollo Heat-Shield Material: Assigned Wall Temperature and Component Mass Fluxes ($\dot{m}_g$ and $\dot{m}_c$)

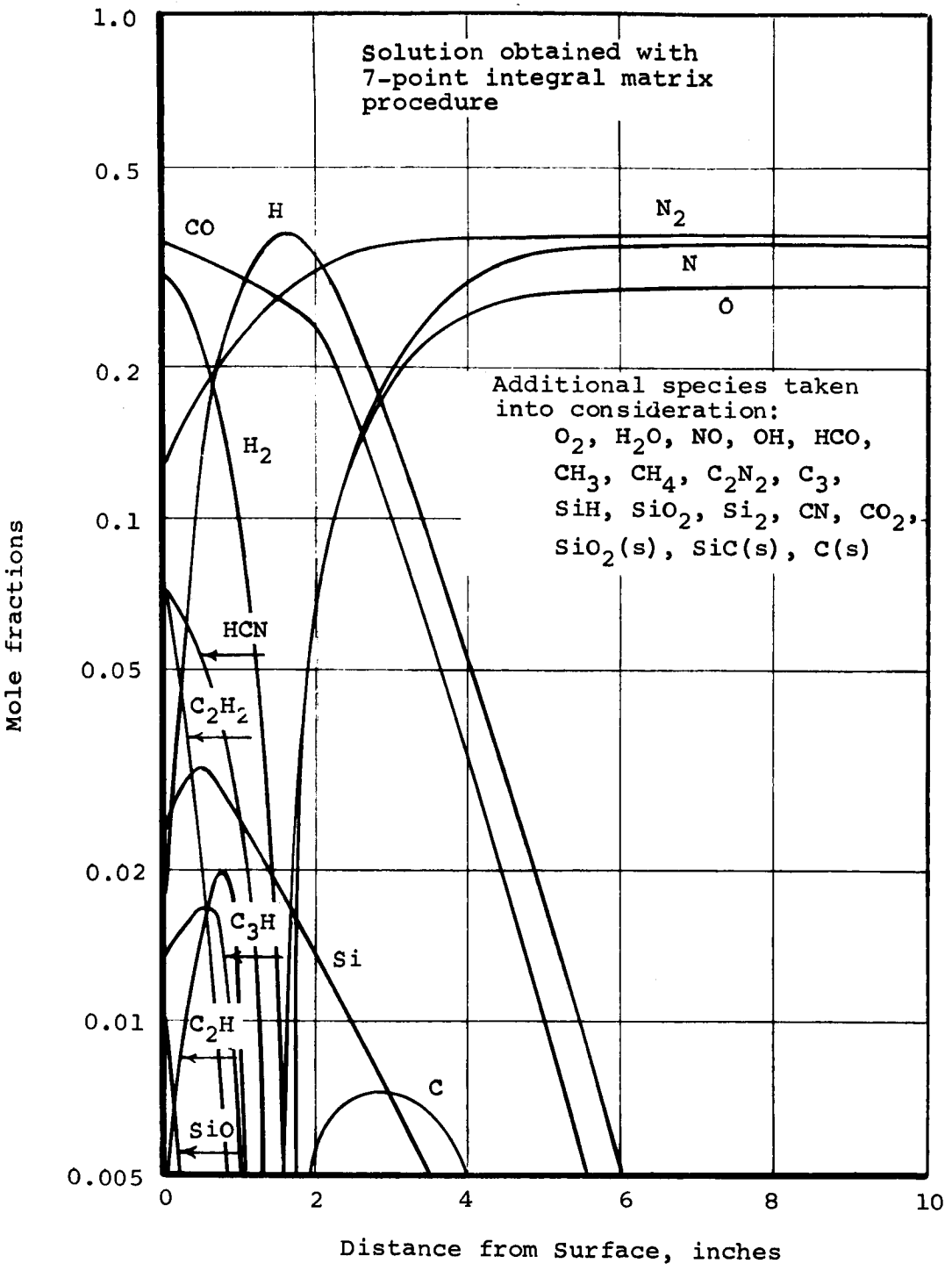

(b) Mole Fractions

Figure 12. Concluded

injection rates and the distribution of velocity profiles around the body are presented in Figs. 13(a) and (b), respectively. These solutions, which included evaluation of edge conditions, a similar solution at the stagnation point, and nonsimilar solutions at ten additional stations, were obtained in approximately 2.5 minutes on an IBM 7094 computer. Approximately 60 percent of this time was spent in the equilibrium chemistry subroutines. It is thus pertinent to mention that the total computational time could be substantially reduced by the use of a specialized chemical procedure for the particular system of interest. Also, substantial time was spent in tape operation introduced by the use of overlays.

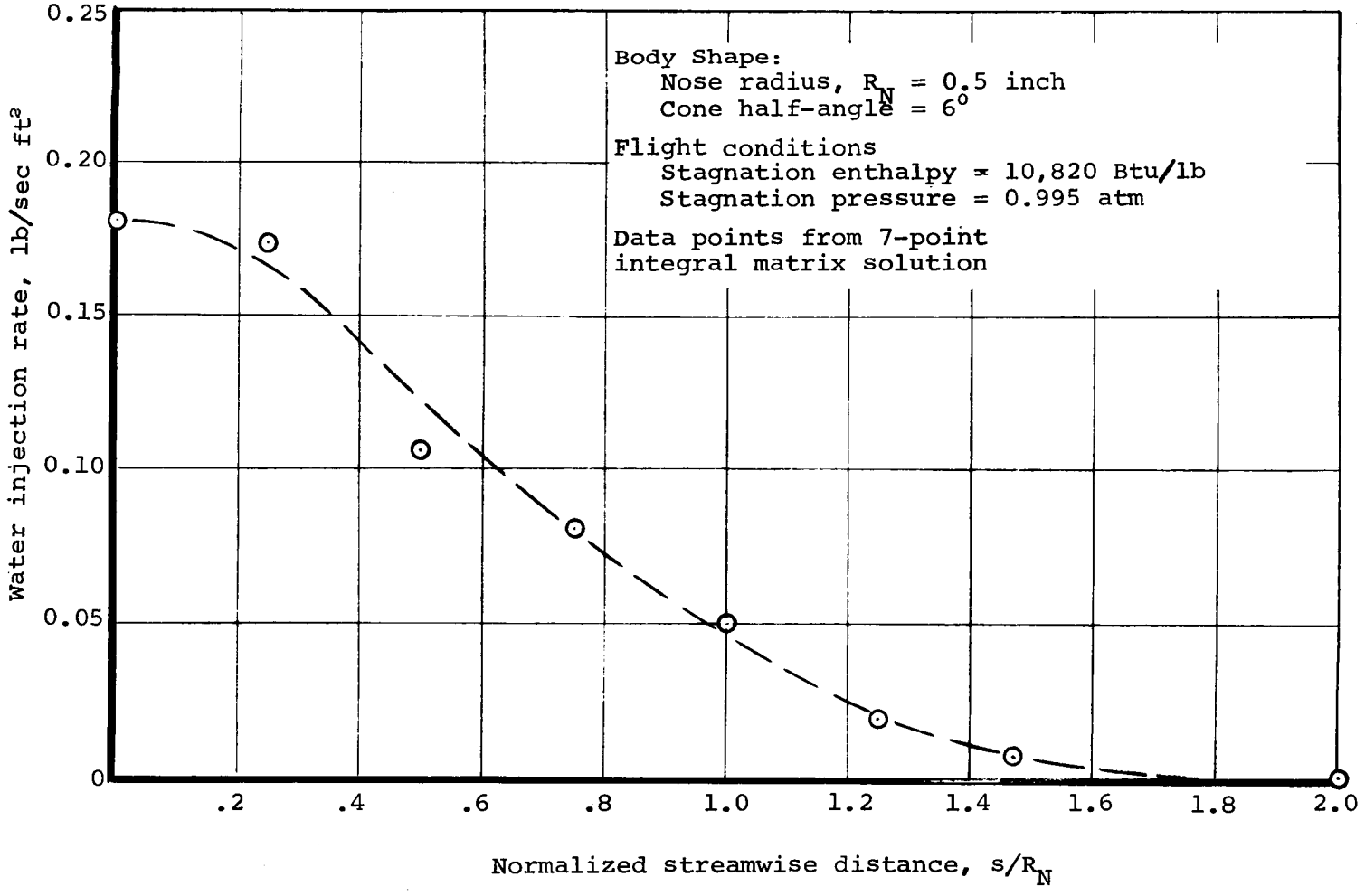

(a) Distribution of Water Injection Rates Around the Body

Figure 13. Nonsimilar Boundary Layer Around a Sphere-Cone Reentry Body With Water Injection to Maintain a Wall Temperature of 5000°R

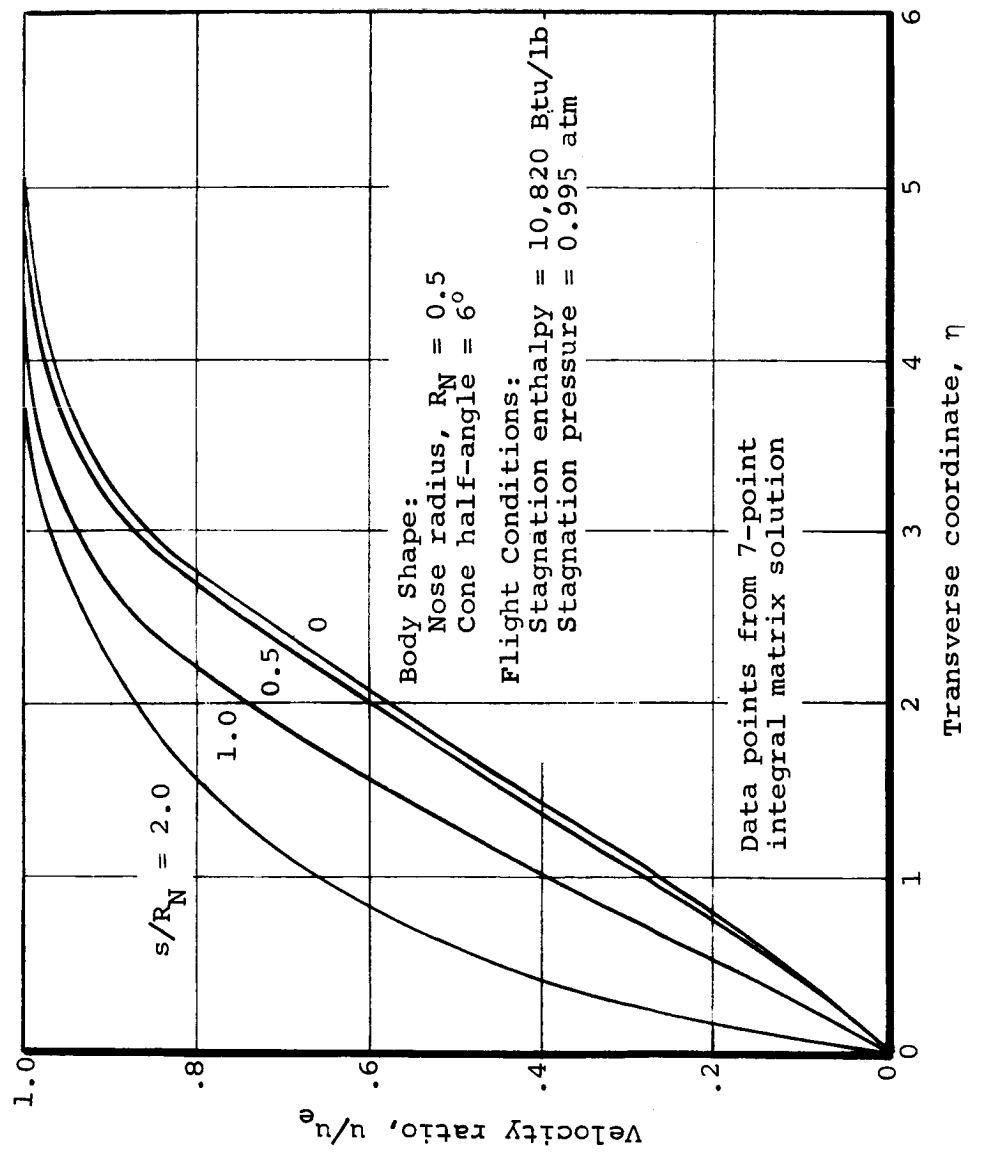

(b) Velocity Profiles

Figure 13. Concluded

REFERENCES

1. Aerotherm Corporation, Palo Alto, California, User's Manual, Boundary Layer Integral Matrix Program (BLIMP), in preparation.

2. Walsh, J. L., Ahlberg, J. H., and Nilson, E. N.: Best Approximation Properties of the Spline Fit. J. Math. and Mech., Vol. 11, 1962, pp. 225-234.

3. Pallone, A. J.:Nonsimilar Solutions of the Compressible-Laminar-Boundary-Layer Equations with Applications to the Upstream-Transpiration Cooling Problem. J. Aerospace Sci., Vol. 28, No. 6, June 1961, pp. 449-456, 492.

4. Dorodnitsyn, A. A.: General Method of Integral Relations and its Application to Boundary Layer Theory. Advances in Aeronautical Sciences, Vol. 3, MacMillan, New York, 1960, pp. 207-219.

5. Smith, A. M. O. and Clutter, D. W.: Machine Calculation of Compressible Laminar Boundary Layers. AIAA J., Vol. 3, No. 4, April 1965, pp. 639-647.

6. Leigh, D. C. F.: The Laminar Boundary Layer Equation: A Method of Solution by Means of an Automatic Computer. Cambridge Phil. Soc. Proc., Vol. 51, 1955, pp. 320-332.

7. Kendall, R. M.: A General Approach to the Thermochemical Solution of Mixed Equilibrium-Nonequilibrium, Homogeneous or Heterogeneous Systems. Aerotherm Corporation, Palo Alto, California, Aerotherm Report No. 66-7, Part V, March 14, 1967.

8. Cess, R. D.: Radiation Effects Upon Boundary-Layer Flow of an Absorbing Gas. J. Heat Transfer, Vol. 83, No. 4, Nov. 1964, pp. 469-475.

9. Bartlett, E. P., Kendall, R. M., and Rindal, R. A.: A Unified Approximation for Mixture Transport Properties for Multicomponent Boundary-Layer Applications. Aerotherm Corporation, Palo Alto, California, Aerotherm Report No. 66-7, Part IV, March 14, 1967.

10. Kendall, R. M., Bartlett, E. P., Rindal, R. A., and Moyer, C. B.: An Analysis of the Coupled Chemically Reacting Boundary Layer and Charring Ablator. Aerotherm Corporation, Palo Alto, California, Aerotherm Report No. 66-7, Part I, March 14, 1967.

11. Dorrance, W. H.: Viscous Hypersonic Flow. McGraw-Hill Book Co., New York, 1962, pp. 180-182.

12. Van Driest, E. R.: Turbulent Boundary Layer in Compressible Fluids. Jour. Aero. Sci., Vol. 18, No. 3, March 1951, pp. 145-161.

13. Hirschfelder, J. O., Curtiss, C. F., and Bird, R. B.: Molecular Theory of Gases and Liquids, Second printing, corrected, with notes added, John Wiley and Sons, Inc., New York, 1964.

14. Scala, S. M. and Gilbert, L. M.: Sublimation of Graphite at Hypersonic Speeds. AIAA J., Vol. 3, No. 9, Sept. 1965, pp. 1635-1644.

15. Libby, P. A. and Pierucci, M.: Laminar Boundary Layer with Hydrogen Injection Including Multicomponent Diffusion. AIAA J., Vol. 2, No. 12, Dec. 1964, pp. 2118-2126.

16. Pallone, A. J., Moore, J. A., and Erdos, J. I.: Nonequilibrium Nonsimilar Solutions of the Laminar Boundary-Layer Equations. AIAA J., Vol. 2, No. 10, Oct. 1964, pp. 1706-1713.

17. Bird, R. B.: Diffusion in Multicomponent Gas Mixtures. 25th Anniversary Congress Society of Chemical Engineers (Japan), Nov. 6-14, 1961. Published in abbreviated form in Kagaku Kogaku, Vol. 26, 1962, pp. 718-721.

18. Laranjeira, M. F.: Experimental and Theoretical Thermal Diffusion Factors in Binary and Ternary Mixtures. Klein Offsetdrukkerij, Poortpers N.V., 1959.

19. Lees, L.: Laminar Heat Transfer Over Blunt-Nosed Bodies at Hypersonic Flight Speeds. Jet Propulsion, Vol. 26, No. 4, April 1956, pp. 259-269, 274.

20. Moyer, C. B. and Rindal, R. A.: Finite Difference Solution for the In-depth Response of Charring Materials Considering Surface Chemical and Energy Balances. Aerotherm Corporation, Palo Alto, California, Aerotherm Report No. 66-7, Part II, March 14, 1967.

21. Zeleznik, F. J. and Gordon, S.: A General IBM 704 or 7090 Computer Program for Computation of Chemical Equilibrium Compositions, Rocket Performance, and Chapman-Jouguet Detonations. NASA TN D-1454, 1962.

22. Browne, H. N. and Williams, M. M.: The Theoretical Computation of Equilibrium Compositions, Thermodynamic Properties and Performance Characteristics of Propellant Systems. U.S. Naval Ordnance Test Station, NAVWEPS Report 7043, June 1960.

23. Buddenberg, J. W. and Wilke, C. R.: Calculation of Gas Mixture Viscosities. Ind. and Eng. Chem., Vol. 41, 1949, pp. 1345-1347.

24. Mason, E. A. and Saxena, S. C.: An Approximate Formula for the Thermal Conductivity of Multicomponent Gas Mixtures. Phys. Fluids, Vol. 1, 1958, pp. 361-369.

25. Hirschfelder, J. O.: Heat Conductivity in Polyatomic, Electronically Excited, or Chemically Reacting Mixtures. Sixth Symposium (International) on Combustion, Reinhold Publishing Corp., New York, 1957, pp. 351-366.

26. Loitsianskii, L. G.: Laminarnyi Pogranichnyi Sloi. Fitzmatgiz, Moscow, 1962.

27. Lew, H. G. and Fanucci, J. B.: On the Laminar Compressible Boundary Layer Over a Flat Plate With Suction or Injection. J. Aero. Sci., Vol. 22, 1955, pp. 589-597.

28. Hartree, D. R.: On an Equation Occurring in Falkner and Skan's Approximate Treatment of the Equations of the Boundary Layer. Proc. Cambridge Phil. Soc., Vol. 33, Pt. 2, April 1937.

29. Cohen, C. B. and Reshotko, E.: Similar Solutions for the Compressible Laminar Boundary Layer With Heat Transfer and Pressure Gradient. NACA Tech. Rep. 1293, 1955.

30. Watson, E. C., Gnos, A. V., Gallo, W. F., and Latham, E. A.: Boundary Layers and Hypersonic Inlet Flow Fields. AIAA Paper No. 66-606, June 1966.

APPENDIX A

INTRODUCTION OF THE APPROXIMATION FOR MULTICOMPONENT THERMAL DIFFUSION COEFFICIENTS INTO DIFFUSIVE FLUX RELATIONS

In this appendix the approximation for multicomponent thermal diffusion coefficients is introduced into the expression for diffusive mass flux of species i, diffusive mass flux of element k, and diffusive heat flux.

The diffusive flux of species i in a multicomponent gas incorporating the bifurcation approximation for binary diffusion coefficients can be expressed as Eq. (23):

$$j_i = -\left\{ \frac{\rho \bar{D} \mu_2}{\mu_1 \mathcal{M}} \left[\frac{\partial Z_i}{\partial y} + (Z_i - K_i) \frac{\partial \ell n \, \mu_2}{\partial y} \right] + D_i^T \frac{\partial \ell n \, T}{\partial y} \right\} \tag{A-1}$$

when the diffusion factors, F_i, are considered to be invariant with temperature. Introducing the approximation for multicomponent thermal diffusion coefficients (Eq. (26))

$$D_i^T \approx \frac{c_t \rho \bar{D} \mu_2}{\mu_1 \mathcal{M}} (Z_i - K_i) \tag{A-2}$$

into Eq. (A-1) yields

$$j_i = -\frac{\rho \bar{D} \mu_2}{\mu_1 \mathcal{M}} \left[\frac{\partial Z_i}{\partial y} + \left(Z_i - K_i \right) \left(\frac{\partial \ell n \, \mu_2}{\partial y} + c_t \frac{\partial \ell n \, T}{\partial y} \right) \right] \tag{A-3}$$

or, equivalently,

$$j_i = -\frac{\rho \bar{D} \mu_2}{\mu_1 \mathcal{M}} \left[\frac{\partial Z_i}{\partial y} + (Z_i - K_i) \frac{\partial \ell n \, (\mu_2 T^{c_t})}{\partial y} \right] \tag{A-4}$$

which is the desired form for the diffusive flux of species i including the approximation for unequal diffusion coefficients embodied in Eq. (26).

Likewise, the diffusive mass flux of element k is given by

$$j_k = -\left\{\frac{\rho\bar{D}\mu_2}{\mu_1 m}\left[\frac{\partial \tilde{Z}_k}{\partial y} + (\tilde{Z}_k - \tilde{K}_k)\frac{\partial \ell n\, \mu_2}{\partial y}\right] + \tilde{D}_k^{\,T}\frac{\partial \ell n\, T}{\partial y}\right\} \qquad \text{(A-5)}$$

where

$$\tilde{D}_k^{\,T} \equiv \sum_i \alpha_{ki} D_i^{\,T} \qquad \text{(A-6)}$$

Substituting Eq. (A-2) into Eq. (A-6) produces

$$\tilde{D}_k^{\,T} = \frac{c_t \rho\bar{D}\mu_2}{\mu_1 m}\sum_i \alpha_{ki}\,(Z_i - K_i) \qquad \text{(A-7)}$$

or by the definitions of Eqs. (16) and (25a)

$$\tilde{D}_k^{\,T} = \frac{c_t \rho\bar{D}\mu_2}{\mu_1 m}\,(\tilde{Z}_k - \tilde{K}_k) \qquad \text{(A-8)}$$

The elemental diffusive flux can thus be expressed as

$$j_k = -\frac{\rho\bar{D}\mu_2}{\mu_1 m}\left[\frac{\partial \tilde{Z}_k}{\partial y} + (\tilde{Z}_k - \tilde{K}_k)\frac{\partial \ell n\,(\mu_2 T^{c_t})}{\partial y}\right] \qquad \text{(A-9)}$$

The diffusive heat flux can be written as

$$q_a = -\left\{\rho(\epsilon_M + \nu)\frac{\partial(u^2/2)}{\partial y} + (\lambda + \rho\epsilon_H\bar{C}_p)\frac{\partial T}{\partial y} + \sum_i \left(\rho\epsilon_{D_i}\frac{\partial K_i}{\partial y} - j_i\right) h_i - S\right\} \quad \text{(A-10)}$$

where

$$S \equiv \frac{RT}{\rho}\sum_i\sum_j \frac{x_j D_i^T}{m_i \mathcal{D}_{ij}}\left(\frac{j_i}{K_i} - \frac{j_j}{K_j}\right) \quad \text{(A-11)}$$

Substituting for D_i^T and $\mathcal{D}_{ij}$, the term S becomes

$$S = \frac{c_t RT\mu_2}{\mu_1 m}\sum_i\sum_j \frac{F_i F_j x_j}{m_i}\left(Z_i - K_i\right)\left(\frac{j_i}{K_i} - \frac{j_j}{K_j}\right) \quad \text{(A-12)}$$

Replacing the mole fraction x_j by mK_j/m_j and utilizing the definition $Z_i \equiv mK_i/F_i\mu_2$, S becomes

$$S = \frac{c_t RT\mu_2}{\mu_1}\sum_i\sum_j \frac{K_j F_j}{m_j}\frac{F_i}{m_i}\left(\frac{m}{\mu_2 F_i} - 1\right)\left(j_i - \frac{K_i}{K_j} j_j\right) \quad \text{(A-13)}$$

Expanding

$$S = \frac{c_t RT\mu_2}{\mu_1}\left[\frac{m}{\mu_2}\sum_i\sum_j \frac{K_j F_j}{m_j}\frac{j_i}{m_i} - \sum_i\sum_j \frac{K_j F_j}{m_j}\frac{F_i j_i}{m_i} - \frac{m}{\mu_2}\sum_i\sum_j \frac{K_i}{m_i}\frac{F_j j_j}{m_j} + \sum_i\sum_j \frac{K_i F_i}{m_i}\frac{F_j j_j}{m_j}\right] \quad \text{(A-14)}$$

The second and fourth terms are identical upon interchange of subscripts but of opposite sign and hence cancel each other. Utilizing $1/\mathcal{M} = \sum K_j/\mathcal{M}_j$ and the definition of $\mu_1 \equiv \sum x_i F_i$, S becomes

$$S = \frac{c_t RT\mathcal{M}}{\mu_1}\left[\frac{\mu_1}{\mathcal{M}}\sum_i \frac{j_i}{\mathcal{M}_i} - \frac{1}{\mathcal{M}}\sum_i \frac{j_i F_i}{\mathcal{M}_i}\right] \tag{A-15}$$

Rearranging

$$S = c_t RT \sum_i \frac{j_i}{\mathcal{M}_i}\left(1 - \frac{F_i}{\mu_1}\right) \tag{A-16}$$

Substituting Eqs. (A-4) and (A-16) into Eq. (A-10), the expression for diffusive heat flux becomes

$$q_a = -\Bigg\{\rho(\varepsilon_M + \nu)\frac{\partial(u^2/2)}{\partial y} + (\lambda + \rho\varepsilon_H \bar{C}_p)\frac{\partial T}{\partial y} + \rho\varepsilon_D \sum_i h_i \frac{\partial K_i}{\partial y} + \frac{\rho\bar{D}\mu_2}{\mu_1 \mathcal{M}}\sum_i \left[\frac{\partial Z_i}{\partial y} + (Z_i - K_i)\frac{\partial \ell n\,(\mu_2 T^{c_t})}{\partial y}\right] x \left[h_i + \frac{c_t RT}{\mu_1 \mathcal{M}_i}(\mu_1 - F_i)\right]\Bigg\} \tag{A-17}$$

Now

$$\sum_i h_i \frac{\partial K_i}{\partial y} = \sum_i \frac{\partial(K_i h_i)}{\partial y} - \sum_i K_i \frac{\partial h_i}{\partial y}$$

$$= \frac{\partial}{\partial y}\left(\sum_i K_i h_i\right) - \frac{\partial T}{\partial y}\sum_i K_i C_{pi}$$

$$= \frac{\partial h}{\partial y} - \bar{C}_p \frac{\partial T}{\partial y} \tag{A-18}$$

Utilizing this and eliminating all summations in favor of defined system quantities yields the following result for q_a

$$q_a = -\left\{\rho(\epsilon_M + \nu)\frac{\partial(u^2/2)}{\partial y} + (\lambda + \rho\epsilon_H\bar{C}_p)\frac{\partial T}{\partial y}\right.$$

$$+ \rho\epsilon_D\left(\frac{\partial h}{\partial y} - \bar{C}_p\frac{\partial T}{\partial y}\right) + \frac{\rho\bar{D}\mu_2}{\mu_1 m}\left[\frac{\partial\tilde{h}}{\partial y} - \left(\tilde{C}_p + \frac{c_t^2 R}{\mu_1\mu_2}\right)\frac{\partial T}{\partial y} + c_t RT\frac{\partial\mu_3}{\partial y}\right.$$

$$\left.\left. + (\tilde{h} - h + c_t RT\mu_3)\frac{\partial\, \ell n\, (\mu_2 T^{c_t})}{\partial y}\right]\right\} \qquad \text{(A-19)}$$

where $\mu_2 \equiv \sum m_i x_i/F_i$, $\mu_3 \equiv \sum z_i/m_i$, $\tilde{h} \equiv \sum z_i h_i$, and $\tilde{C}_p \equiv \sum z_i C_{pi}$.

APPENDIX B

DERIVATION OF THE TRANSFORMED NONSIMILAR LAMINAR BOUNDARY-LAYER EQUATIONS

In this appendix, transformation relationships for the Levy-Lees transformation, modified by the use of a stretching parameter, are developed and applied to the expressions for diffusive fluxes and to the boundary-layer conservation equations.

The desired independent variables $\bar{\xi}$ and $\bar{\eta}$ are defined by Eq. (33)

$$\bar{\xi} = \xi \qquad \bar{\eta} = \frac{\eta}{\alpha_H} \tag{B-1}$$

where α_H is a function of $\bar{\xi}$ only, and

$$\xi = \int_o^s u_e \rho_e \mu_e r_o^{2\kappa}\, ds \tag{B-2}$$

$$\eta = \frac{r_o^{\kappa} u_e}{(2\xi)^{\frac{1}{2}}} \int_o^y \rho\, dy \tag{B-3}$$

In addition, f is defined as Eq. (35)

$$f - f_w \equiv \int_o^{\eta} \frac{u}{u_e}\, d\eta \tag{B-4}$$

from which it follows that $f' = u/u_e$ where the prime refers to partial differentiation with respect to η.

The old partial derivatives can be expressed in terms of the new partials by

$$\left.\frac{\partial}{\partial s}\right|_y = \left.\frac{\partial}{\partial \xi}\right|_\eta \left.\frac{\partial \xi}{\partial s}\right|_y + \left.\frac{\partial}{\partial \eta}\right|_\xi \left.\frac{\partial \eta}{\partial s}\right|_y \tag{B-5}$$

$$\left.\frac{\partial}{\partial y}\right|_s = \left.\frac{\partial}{\partial \xi}\right|_\eta \left.\frac{\partial \xi}{\partial y}\right|_s + \left.\frac{\partial}{\partial \eta}\right|_\xi \left.\frac{\partial \eta}{\partial y}\right|_s \tag{B-6}$$

where

$$\left.\frac{\partial \xi}{\partial y}\right|_s = 0 \tag{B-7}$$

$$\left.\frac{\partial \xi}{\partial s}\right|_y = \rho_e u_e \mu_e r_o^{2\kappa} \tag{B-8}$$

$$\left.\frac{\partial \eta}{\partial y}\right|_s = \frac{u_e r_o^{\kappa} \rho}{(2\xi)^{\frac{1}{2}}} \tag{B-9}$$

Furthermore

$$\left.\frac{\partial}{\partial \xi}\right|_{\eta} = \left.\frac{\partial}{\partial \bar{\xi}}\right|_{\bar{\eta}} \left.\frac{\partial \bar{\xi}}{\partial \xi}\right|_{\eta} + \left.\frac{\partial}{\partial \bar{\eta}}\right|_{\bar{\xi}} \left.\frac{\partial \bar{\eta}}{\partial \xi}\right|_{\eta} \tag{B-10}$$

$$\left.\frac{\partial}{\partial \eta}\right|_{\xi} = \left.\frac{\partial}{\partial \bar{\xi}}\right|_{\bar{\eta}} \left.\frac{\partial \bar{\xi}}{\partial \eta}\right|_{\xi} + \left.\frac{\partial}{\partial \bar{\eta}}\right|_{\bar{\xi}} \left.\frac{\partial \bar{\eta}}{\partial \eta}\right|_{\xi} \tag{B-11}$$

where

$$\left.\frac{\partial \bar{\xi}}{\partial \xi}\right|_{\eta} = 1 \tag{B-12}$$

$$\left.\frac{\partial \bar{\eta}}{\partial \xi}\right|_{\eta} = -\frac{\bar{\eta}}{\alpha_H}\frac{d\alpha_H}{d\bar{\xi}} \tag{B-13}$$

$$\left.\frac{\partial \bar{\xi}}{\partial \eta}\right|_{\xi} = 0 \tag{B-14}$$

$$\left.\frac{\partial \bar{\eta}}{\partial \eta}\right|_{\xi} = \frac{1}{\alpha_H} \tag{B-15}$$

such that

$$\left.\frac{\partial}{\partial \xi}\right|_{\eta} = \left.\frac{\partial}{\partial \bar{\xi}}\right|_{\bar{\eta}} - \left(\frac{\bar{\eta}}{\alpha_H}\frac{d\alpha_H}{d\bar{\xi}}\right)\left.\frac{\partial}{\partial \bar{\eta}}\right|_{\bar{\xi}} \tag{B-16}$$

$$\left.\frac{\partial}{\partial \eta}\right|_{\xi} = \frac{1}{\alpha_H}\left.\frac{\partial}{\partial \bar{\eta}}\right|_{\bar{\xi}} \tag{B-17}$$

It is necessary to evaluate the operator $D(\ )$ given by

$$D(\ ) = \rho u \frac{\partial(\ )}{\partial s} + \rho v \frac{\partial(\ )}{\partial y} \tag{B-18}$$

The global mass conservation equation (Eq. (3)) can be integrated to yield

$$\rho v - \rho_w v_w = -\frac{1}{r_o^{\kappa}} \frac{\partial}{\partial s} \left(r_o^{\kappa} \int_o^y \rho u \, dy \right) \tag{B-19}$$

Differentiating η for constant ξ, introducing f', solving for $(2\xi)^{\frac{1}{2}} f' \, d\eta$, and integrating yields the result:

$$(2\xi)^{\frac{1}{2}} \int_o^{\eta} f' \, d\eta = r_o^{\kappa} \int_o^y \rho u \, dy \tag{B-20}$$

Utilizing this and the definition of f, Equation (B-19) can be written as

$$\rho v = \rho_w v_w - \frac{1}{r_o^{\kappa}} \frac{\partial}{\partial s} \left[(2\xi)^{\frac{1}{2}} (f - f_w) \right] \tag{B-21}$$

With Eqs. (B-5) and (B-8), Eq. (21) becomes

$$\rho v = \rho_w v_w - \rho_e u_e \mu_e r_o^{\kappa} \frac{\partial}{\partial \xi} \left[(2\xi)^{\frac{1}{2}} (f - f_w) \right] - \frac{f'}{r_o^{\kappa}} (2\xi)^{\frac{1}{2}} \left. \frac{\partial \eta}{\partial s} \right|_y \tag{B-22}$$

Performing the differentiation

$$\rho v = \rho_w v_w - \rho_e u_e \mu_e r_o^{\kappa} \left[\frac{(f - f_w)}{(2\xi)^{\frac{1}{2}}} + (2\xi)^{\frac{1}{2}} \left(\frac{\partial f}{\partial \xi} - \frac{df_w}{d\xi} \right) \right] - \frac{f'}{r_o^{\kappa}} (2\xi)^{\frac{1}{2}} \left. \frac{\partial \eta}{\partial s} \right|_y \tag{B-23}$$

For convenience, define

$$\rho_w v_w = -\frac{\rho_e u_e \mu_e r_o^{\kappa}}{(2\xi)^{\frac{1}{2}}} \left(f_w + 2\xi \frac{df_w}{d\xi} \right) \tag{B-24}$$

Then

$$\rho v = -\frac{\rho_e u_e \mu_e r_o^{\kappa}}{(2\xi)^{\frac{1}{2}}} \left[f + (2\xi) \frac{\partial f}{\partial \xi} \right] - \frac{f'}{r_o^{\kappa}} (2\xi)^{\frac{1}{2}} \left. \frac{\partial \eta}{\partial s} \right|_y \tag{B-25}$$

Utilizing this, plus Equations (B-5) through (B-9)

$$\rho u \left.\frac{\partial}{\partial s}\right|_y + \rho v \left.\frac{\partial}{\partial y}\right|_s = \rho_e u_e^2 \mu_e r_o^{2\kappa} \left[f' \left.\frac{\partial}{\partial \xi}\right|_\eta - \left(\frac{f}{2\xi} + \frac{\partial f}{\partial \xi} \right) \left.\frac{\partial}{\partial \eta}\right|_\xi \right] \tag{B-26}$$

which is the desired form for the operator.

In accordance with Equation (B-24), the use of this operator requires that f_w be defined as

$$f_w = - (2\xi)^{-\frac{1}{2}} \int_0^\xi \frac{\rho_w v_w \, d\xi}{\rho_e u_e \mu_e r_o^\kappa} \tag{B-27}$$

The diffusive flux of species i is given by Eq. (27)

$$j_i = - \frac{\rho \bar{D} \mu_2}{\mu_1 \mathcal{M}} \left[\frac{\partial z_i}{\partial y} + (z_i - K_i) \frac{\partial \ell n \left(\mu_2 T^{c_t} \right)}{\partial y} \right] \tag{B-28}$$

Applying the transformation of Eq. (B-6) with the aid of Eqs. (B-7) and (B-9) yields

$$j_i = - \frac{\rho_e u_e \mu_e r_o^\kappa}{\sqrt{2\xi}} \frac{C}{\overline{Sc}} \left\{ z_i' + (z_i - K_i) \left[\ell n \left(\mu_2 T^{c_t} \right) \right]' \right\} \tag{B-29}$$

where $\overline{Sc}$ is defined as $\mu_1 \mu \mathcal{M} / \rho \bar{D} \mu_2$ and the prime refers to differentiation with respect to η. Utilizing Eq. (B-17):

$$j_i = - \frac{\rho_e u_e \mu_e r_o^\kappa}{\sqrt{2\xi}} \frac{C}{\alpha_H \overline{Sc}} \left\{ z_i' + (z_i - K_i) \left[\ell n \left(\mu_2 T^{c_t} \right) \right]' \right\} \tag{B-30}$$

where the prime now refers to differentiation with respect to $\bar{\eta}$.

The laminar form of the streamwise momentum equation is given by Eq. (5)

$$\rho u \frac{\partial u}{\partial s} + \rho v \frac{\partial u}{\partial y} = \frac{\partial}{\partial y} \left[\mu \frac{\partial u}{\partial y} \right] - \frac{\partial P}{\partial s} \tag{B-31}$$

Applying Eqs. (B-26), (B-5), and (B-6) yields by direct substitution:

$$\rho\rho_e u_e^2 \mu_e r_o^{2\kappa}\left[f'\frac{\partial u}{\partial \xi} - \left(\frac{f}{2\xi} + \frac{\partial f}{\partial \xi}\right)\frac{\partial u}{\partial \eta}\right] = \frac{u_e r_o^{\kappa}\rho}{(2\xi)^{\frac{1}{2}}}\frac{\partial}{\partial \eta}\left[\mu\frac{u_e r_o^{\kappa}\rho}{(2\xi)^{\frac{1}{2}}}\frac{\partial u}{\partial \eta}\right] - \rho_e u_e \mu_e r_o^{2\kappa}\frac{\partial P}{\partial \xi} - \left.\frac{\partial \eta}{\partial s}\right|_y \frac{\partial P}{\partial \eta} \tag{B-32}$$

Now $u = f'u_e$ where u_e is a function of ξ only *

$$\frac{\partial u}{\partial \eta} = u_e \frac{\partial f'}{\partial \eta} = u_e f'' \tag{B-33}$$

$$\frac{\partial u}{\partial \xi} = f'\frac{du_e}{d\xi} + u_e\frac{\partial f'}{\partial \xi} \tag{B-34}$$

So that

$$\rho\rho_e u_e^2 \mu_e r_o^{2\kappa}\left[f'\left(f'\frac{du_e}{d\xi} + u_e\frac{\partial f'}{\partial \xi}\right) - \left(\frac{f}{2\xi} + \frac{\partial f}{\partial \xi}\right)u_e f''\right] = \frac{u_e r_o^{\kappa}\rho}{(2\xi)^{\frac{1}{2}}}\left[\frac{\mu u_e r_o^{\kappa}\rho u_e f''}{(2\xi)^{\frac{1}{2}}}\right]' - \rho_e u_e \mu_e r_o^{2\kappa}\frac{\partial P}{\partial \xi} - \left.\frac{\partial \eta}{\partial s}\right|_y P' \tag{B-35}$$

where the prime denotes differentiation with respect to η. Multiplying by $(2\xi)/\rho\rho_e u_e^3 \mu_e r_o^{2\kappa}$ yields:

$$\frac{(2\xi)f'^2}{u_e}\frac{du_e}{d\xi} + (2\xi)f'\frac{\partial f'}{\partial \xi} - f f'' - (2\xi)f''\frac{\partial f}{\partial \xi} = \left(\frac{\rho\mu}{\rho_e\mu_e}f''\right)' - \frac{(2\xi)}{\rho u_e^2}\frac{\partial P}{\partial \xi} - \frac{(2\xi)\left.\frac{\partial \eta}{\partial s}\right|_y}{\rho\rho_e u_e^3 \mu_e r_o^{2\kappa}} P' \tag{B-36}$$

*Note that all properties evaluated at "e" are functions of ξ only.

Defining $C \equiv \rho\mu/\rho_e\mu_e$ and $\beta \equiv 2\frac{\xi}{u_e}\frac{du_e}{d\xi}$ yields

$$(Cf'')' + ff'' - \beta f'^2 - \frac{(2\xi)}{\rho u_e^2}\frac{\partial P}{\partial \xi} - \frac{(2\xi)\left.\frac{\partial \eta}{\partial s}\right|_y}{\rho\rho_e u_e^3 \mu_e r_o^{2\kappa}} P' = (2\xi)\left[f'\frac{\partial f'}{\partial \xi} - \frac{\partial f}{\partial \xi} f''\right] \tag{B-37}$$

The final term on the left-hand side of this equation involves $\left.\frac{\partial \eta}{\partial s}\right|_y$ which can be expressed with the aid of Eq. (B-8) as

$$\left.\frac{\partial \eta}{\partial s}\right|_y = \rho_e u_e \mu_e r_o^{2\kappa} \left.\frac{\partial \eta}{\partial \xi}\right|_y \tag{B-38}$$

Therefore

$$(Cf'')' + ff'' - \beta f'^2 - \frac{(2\xi)}{\rho u_e^2}\left[\frac{\partial P}{\partial \xi} + P'\left.\frac{\partial \eta}{\partial \xi}\right|_y\right]$$

$$= (2\xi)\left[f'\frac{\partial f'}{\partial \xi} - \frac{\partial f}{\partial \xi} f''\right] \tag{B-39}$$

Introducing the additional transformation of Eqs. (B-16) and (B-17)

$$\frac{1}{\alpha_H}\left[C\frac{1}{\alpha_H^2} f''\right]' + f\left(\frac{1}{\alpha_H^2} f''\right) - \beta\left(\frac{1}{\alpha_H^2} f'^2\right)$$

$$- \frac{2\bar{\xi}}{\rho u_e^2}\left\{\frac{\partial P}{\partial \bar{\xi}} - P'\frac{\bar{\eta}}{\alpha_H}\frac{d\alpha_H}{d\bar{\xi}} + P'\alpha_H\left[\frac{\partial}{\partial \bar{\xi}}\left(\frac{r_o^{\kappa} u_e}{\alpha_H (2\bar{\xi})^{\frac{1}{2}}}\int_o^y \rho\, dy\right)\right]_y\right\}$$

$$= 2\bar{\xi}\left\{\frac{1}{\alpha_H} f'\left[\frac{\partial}{\partial \bar{\xi}}\left(\frac{1}{\alpha_H} f'\right) - \left(\frac{\bar{\eta}}{\alpha_H}\frac{d\alpha_H}{d\bar{\xi}}\right)\left(\frac{1}{\alpha_H} f'\right)'\right]\right.$$

$$\left. - \left[\frac{\partial f}{\partial \bar{\xi}} - \left(\frac{\bar{\eta}}{\alpha_H}\frac{d\alpha_H}{d\bar{\xi}}\right) f'\right]\frac{1}{\alpha_H^2} f''\right\} \tag{B-40}$$

where the prime denotes differentiation with respect to $\bar{\eta}$ and use has been made of the relation

$$\left.\frac{\partial \eta}{\partial \bar{\xi}}\right|_y = \alpha_H \left.\frac{\partial \bar{\eta}}{\partial \bar{\xi}}\right|_y = \alpha_H \left[\frac{\partial}{\partial \bar{\xi}}\left(\frac{r_o^{\varkappa} u_e}{\alpha_H (2\bar{\xi})^{\frac{1}{2}}} \int_o^y \rho \, dy\right)\right]_y \tag{B-41}$$

Multiplying by α_H^2 and rearranging terms yields (noting that $\alpha_H = \alpha_H(\xi)$ only):

$$ff'' + \left[\frac{Cf''}{\alpha_H}\right]' - \frac{2\bar{\xi}\,\alpha_H^2}{\rho u_e^2}\left\{\frac{\partial P}{\partial \bar{\xi}} - P' \frac{\bar{\eta}}{\alpha_H}\frac{d\alpha_H}{d\bar{\xi}} + P'\alpha_H \left[\frac{\partial}{\partial \bar{\xi}}\left(\frac{r_o^{\varkappa} u_e}{\alpha_H (2\bar{\xi})^{\frac{1}{2}}} \int_o^y \rho \, dy\right)\right]_y\right\} - \beta f'^2$$

$$= 2\bar{\xi}\left[f' \frac{\partial f'}{\partial \bar{\xi}} - f'' \frac{\partial f}{\partial \bar{\xi}} - \frac{f'^2}{\alpha_H}\frac{d\alpha_H}{d\bar{\xi}}\right] \tag{B-42}$$

which is Eq. (52) of this report.

The normal momentum equation is given by Eq. (7)

$$\frac{\partial P}{\partial y} - \frac{\rho u^2}{r_c} = 0 \tag{B-43}$$

Applying Eq. (B-6) with the aid of Eqs. (B-7) and (B-9) yields directly

$$\frac{u_e r_o^{\varkappa} \rho}{(2\bar{\xi})^{\frac{1}{2}}} P' - \frac{\rho u^2}{r_c} = 0 \tag{B-44}$$

where the prime denotes differentiation with respect to η . Utilizing Eq. (17) and $f' = \alpha_H u/u_e$

$$P' - \frac{u_e f'^2 (2\bar{\xi})^{\frac{1}{2}}}{\alpha_H r_c r_o^{\varkappa}} = 0 \tag{B-45}$$

where the prime refers to differentiation with respect to $\bar{\eta}$. This is Eq. (54) of this report.

In the event that normal pressure gradient can be neglected, Eq. (B-45) is replaced by $P' = 0$ and the compressible Bernoulli equation yields

$$\frac{dP_e}{d\bar{\xi}} = -\rho_e u_e \frac{du_e}{d\bar{\xi}} \tag{B-46}$$

Applying this to Eq. (B-42), the streamwise momentum equation becomes

$$ff'' + \left[\frac{Cf''}{\alpha_H}\right]' + \beta\left(\alpha_H^2 \frac{\rho_e}{\rho} - f'^2\right)$$

$$= 2\bar{\xi}\left[f' \frac{\partial f'}{\partial \bar{\xi}} - f'' \frac{\partial f}{\partial \bar{\xi}} - \frac{f'^2}{\alpha_H} \frac{d\alpha_H}{d\bar{\xi}}\right] \qquad \text{(B-47)}$$

which is Eq. (55) of this report.

The laminar form of the energy equation is given by Eq. (30)

$$\rho u \frac{\partial H_T}{\partial s} + \rho v \frac{\partial H_T}{\partial y} = \frac{\partial}{\partial y}\left\{\mu \frac{\partial (u^2/2)}{\partial y} + \lambda \frac{\partial T}{\partial y}\right.$$

$$+ \frac{\rho \bar{D} u_2}{u_1 \mathcal{M}}\left[\frac{\partial \tilde{h}}{\partial y} - \left(\tilde{c}_p + \frac{c_t^2 R}{\mu_1 \mu_2}\right) \frac{\partial T}{\partial y} + c_t R T \frac{\partial \mu_3}{\partial y}\right.$$

$$\left.\left. + (\tilde{h} - h + c_t R T \mu_3) \frac{\partial \ell n \left(\mu_2 T^{c_t}\right)}{\partial y}\right] + q_r\right\} \qquad \text{(B-48)}$$

Applying Eqs. (B-6) and (B-26)

$$\rho \rho_e u_e^2 \mu_e r_o^{2\kappa}\left[f' \frac{\partial H_T}{\partial \xi} - \left(\frac{f}{2\xi} + \frac{\partial f}{\partial \xi}\right) H_T'\right]$$

$$= \frac{u_e r_o^{\kappa} \rho}{(2\xi)^{1/2}}\left\{\frac{u_e r_o^{\kappa} \rho}{(2\xi)^{1/2}}\left[\mu u_e^2 f'f'' + \lambda T'\right]\right.$$

$$+ \frac{\rho \bar{D} \mu_2}{\mu_1 \mathcal{M}}\left(\tilde{h}' - \left(\tilde{c}_p + \frac{c_t^2 R}{\mu_1 \mu_2}\right) T' + c_t R T u_3'\right.$$

$$\left.\left. + (\tilde{h} - h + c_t R T \mu_3)\left[\ell n \left(\mu_2 T^{c_t}\right)\right]'\right)\right] + q_r\Bigg\}' \qquad \text{(B-49)}$$

where the prime denotes differentiation with respect to η. Multiplying by $2\xi/\rho\rho_e u_e^2 \mu_e r_o^{2\kappa}$ and rearranging

$$fH_T' + \left\{ C\,u_e^2\,f'f'' + \frac{C\,\bar{C}_p\,T'}{Pr} + \frac{C}{\overline{Sc}}\left[\tilde{h}' - \left(\tilde{C}_p + \frac{c_t^2 R}{\mu_1\mu_2}\right)T' + c_t RT\mu_3' + (\tilde{h} - h + c_t RT\mu_3)\left[\ell n\left(\mu_2 T^{c_t}\right)\right]'\right] + \frac{q_r(2\xi)^{\frac{1}{2}}}{\rho_e u_e \mu_e r_o^{\kappa}}\right\}'$$

$$= 2\xi\left[f'\frac{\partial H_T}{\partial\xi} - H_T'\frac{\partial f}{\partial\xi}\right] \qquad \text{(B-50)}$$

where $Pr = \bar{C}_p\,\mu/\lambda$ and $\overline{Sc} = \mu_1\mu\,\mathcal{M}/\rho\bar{D}\,\mu_2$. Applying Eqs. (B-16) and (B-17) and multiplying by α_H yields

$$fH_T' + \left\{ \frac{C}{\alpha_H}\left[\frac{f'f''}{\alpha_H^2}\,u_e^2 + \frac{\bar{C}_p}{Pr}\,T' + \frac{1}{\overline{Sc}}\left(\tilde{h}' - \left(\tilde{C}_p + \frac{c_t^2 R}{\mu_1\mu_2}\right)T' + c_t RT\mu_3' + (\tilde{h} - h + c_t RT\mu_3)\left[\ell n\left(\mu_2 T^{c_t}\right)\right]'\right)\right] + \frac{q_r(2\bar{\xi})^{\frac{1}{2}}}{\rho_e u_e \mu_e r_o^{\kappa}}\right\}'$$

$$= 2\bar{\xi}\left[f'\frac{\partial H_T}{\partial\bar{\xi}} - f'\left(\frac{\bar{\eta}}{\alpha_H}\frac{d\alpha_H}{d\bar{\xi}}\right)H_T' - H_T'\frac{\partial f}{\partial\bar{\xi}} + H_T'\left(\frac{\bar{\eta}}{\alpha_H}\frac{d\alpha_H}{d\bar{\xi}}\right)f'\right]$$

$$= 2\bar{\xi}\left[f'\frac{\partial H_T}{\partial\bar{\xi}} - H_T'\frac{\partial f}{\partial\bar{\xi}}\right] \qquad \text{(B-51)}$$

where the prime denotes differentiation with respect to $\bar{\eta}$. This is Eq. (56) of this report.

The laminar form of the elemental species equation is given by Eq. (29)

$$\rho u\frac{\partial\tilde{K}_k}{\partial s} + \rho v\frac{\partial\tilde{K}_k}{\partial y} = \frac{\partial}{\partial y}\left\{\frac{\rho\bar{D}\mu_2}{\mu_1\mathcal{M}}\left[\frac{\partial\tilde{Z}_k}{\partial y} + (\tilde{Z}_k - \tilde{K}_k)\frac{\partial\,\ell n\left(\mu_2 T^{c_t}\right)}{\partial y}\right]\right\} + \phi_K \qquad \text{(B-52)}$$

Applying Eqs. (B-6) and (B-26)

$$\rho\rho_e u_e^2 \mu_e r_o^{2\varkappa} \left[f' \frac{\partial \tilde{K}_k}{\partial \xi} - \left(\frac{f}{2\xi} + \frac{\partial f}{\partial \xi} \right) \tilde{K}_k' \right]$$

$$= \frac{u_e r_o^{\varkappa} \rho}{(2\xi)^{\frac{1}{2}}} \left\{ \frac{u_e r_o^{\varkappa} \rho}{(2\xi)^{\frac{1}{2}}} \frac{\bar{\rho} \bar{D} \mu_2}{\mu_1 \overline{m}} \left[\tilde{Z}_k' + (\tilde{Z}_k - \tilde{K}_k) \left[\ell n \left(\mu_2 T^{c_t} \right) \right]' \right] \right\}' + \phi_k \qquad \text{(B-53)}$$

where the prime denotes differentiation with respect to η . Multiplying by $2\xi / \rho\rho_e u_e^2 \mu_e r_o^{2\varkappa}$ and rearranging yields

$$f\tilde{K}_k' + \left\{ \frac{C}{\overline{Sc}} \left[\tilde{Z}_k' + (\tilde{Z}_k - \tilde{K}_k) \left[\ell n \left(\mu_2 T^{c_t} \right) \right]' \right] \right\}' + \phi_k$$

$$= 2\xi \left[f' \frac{\partial \tilde{K}_k}{\partial \xi} - \tilde{K}_k' \frac{\partial f}{\partial \xi} \right] \qquad \text{(B-54)}$$

Applying Eqs. (B-16) and (B-17) and multiplying by α_H yields

$$f\tilde{K}_k' + \left\{ \frac{C}{\alpha_H \overline{Sc}} \left[\tilde{Z}_k' + (\tilde{Z}_k - \tilde{K}_k) \left[\ell n \left(\mu_2 T^{c_t} \right) \right]' \right] \right\}' + \alpha_H \phi_k$$

$$= 2\bar{\xi} \left[f' \frac{\partial \tilde{K}_k}{\partial \bar{\xi}} - f' \left(\frac{\bar{\eta}}{\alpha_H} \frac{d\alpha_H}{d\bar{\xi}} \right) \tilde{K}_k' - \tilde{K}_k' \frac{\partial f}{\partial \bar{\xi}} + \tilde{K}_k' \left(\frac{\bar{\eta}}{\alpha_H} \frac{d\alpha_H}{d\bar{\xi}} \right) f' \right]$$

$$= 2\bar{\xi} \left[f' \frac{\partial \tilde{K}_k}{\partial \bar{\xi}} - \tilde{K}_k' \frac{\partial f}{\partial \bar{\xi}} \right] \qquad \text{(B-55)}$$

where the prime denotes differentiation with respect to $\bar{\eta}$. This is Eq. (58) of this report.

APPENDIX C

SPECIAL STAGNATION POINT CONSIDERATIONS

In this appendix equations are developed which are applicable at the stagnation point of blunt bodies for the calculation of the flux normalizing parameter, α^*, the streamwise pressure-gradient parameter, β, and the wall stream function, f_w.

The flux normalizing parameter, α^*, is defined by Eq. (44) as

$$\alpha^* \equiv \frac{\rho_e \mu_e u_e r_o^{\kappa}}{(2\xi)^{\frac{1}{2}}} \tag{C-1}$$

In order to compute the value of α^* at the stagnation point, consider the streamwise pressure-gradient parameter, β, defined by Eq. (53)

$$\beta = 2 \frac{\xi}{u_e} \frac{du_e}{d\xi} \tag{C-2}$$

The transformed streamwise parameter, ξ, is defined by Eq. (31)

$$\xi = \int_0^s \rho_e u_e \mu_e r_o^{2\kappa} ds \tag{C-3}$$

Differentiating Eq. (C-3) and introducing the result into Eq. (C-2) yields

$$\beta = 2 \frac{\xi}{u_e} \frac{du_e}{ds} \frac{1}{\rho_e u_e \mu_e r_o^{2\kappa}} \tag{C-4}$$

Utilizing Eq. (C-1)

$$\beta = \frac{\rho_e \mu_e}{\alpha^{*2}} \frac{du_e}{ds} \tag{C-5}$$

Solving for α^* yields the result

$$\alpha^* = \left(\rho_e \mu_e \frac{du_e}{ds} \Big/ \beta \right)^{\frac{1}{2}} \tag{C-6}$$

The $du_e/ds|_o$ needed for evaluation of α^* if Eq. (C-6) is to be employed can be obtained as follows if Newtonian flow is assumed in the vicinity of the stagnation point. In the case of Newtonian flow,

$$P_e = P_{e_o} \cos^2 \theta \tag{C-7}$$

Near the stagnation point $\sin \theta = s/R_{eff}$ where R_{eff} is an effective nose radius of the body. Hence

$$P_e = P_o \left(1 - \frac{s^2}{R_{eff}^2} \right) \tag{C-8}$$

Utilizing the Bernoulli equation

$$P_o = P_e + \rho_e \frac{u_e^2}{2} \tag{C-9}$$

Equation (C-8) becomes

$$\frac{\rho_e u_e^2}{2} = P_o \frac{s^2}{R_{eff}^2} \tag{C-10}$$

or

$$u_e = \frac{s}{R_{eff}} \left(\frac{2P_o}{\rho_e} \right)^{\frac{1}{2}} \tag{C-11}$$

The density is nearly constant in the vicinity of the stagnation point. Hence

$$\left. \frac{du_e}{ds} \right|_o \approx \frac{1}{R_{eff}} \left(\frac{2P_o}{\rho_o} \right)^{\frac{1}{2}} \tag{C-12}$$

In order to compute the stagnation-point β, consider the definition of ξ (Eq. (C-3)) in the form

$$\xi = \int_0^s \rho_e \left(\frac{u_e}{s}\right) \mu_e \left(\frac{r_o}{s}\right)^{2\kappa} s^{2\kappa+1} ds$$

$$= \int_0^{s^{2\kappa+2}} \left[\frac{1}{2\kappa + 2} \rho_e \left(\frac{u_e}{s}\right) \mu_e \left(\frac{r_o}{s}\right)^{2\kappa}\right] d(s^{2\kappa+2}) \qquad \text{(C-13)}$$

For Newtonian flow, comparison of Eqs. (C-11) and (C-12) show that $u_e/s \rightarrow du_e/ds$ in the vicinity of the stagnation point. In addition, $r_o/s \rightarrow 1$ and $\rho_e\mu_e$ is a constant. Hence

$$\xi_{s\rightarrow o} = \frac{1}{2\kappa + 2} \rho_e\mu_e \frac{du_e}{ds} s^{2\kappa+2} \qquad \text{(C-14)}$$

Substituting into Eq. (C-4) yields

$$\beta_o = \frac{1}{\kappa + 1} \left(\frac{s}{u_e} \frac{du_e}{ds}\right)^2 \left(\frac{s}{r_o}\right)^{2\kappa} = \frac{1}{\kappa + 1} \qquad \text{(C-15)}$$

Hence, β_o is unity for planar blunt bodies and 1/2 for axisymmetric blunt bodies for assumed Newtonian flow.

The wall stream function, f_w, is defined by Eq. (60) as

$$f_w = - (2\xi)^{-\frac{1}{2}} \int_0^{\xi} \frac{\rho_w v_w d\xi}{\rho_e u_e \mu_e r_o^{\kappa}} \qquad \text{(C-16)}$$

Differentiating Eq. (C-3) and introducing the result into Eq. (C-16) yields

$$f_w = - (2\xi)^{-\frac{1}{2}} \int_0^s \rho_w v_w r_o^{\kappa} ds \qquad \text{(C-17)}$$

This can be written as

$$f_w = - (2\xi)^{-\frac{1}{2}} \int_0^s \rho_w v_w \left(\frac{r_o}{s}\right)^{\kappa} s^{\kappa} ds$$

$$= - (2\xi)^{-\frac{1}{2}} \int_0^{s^{\kappa+1}} \left[\frac{1}{\kappa + 1} \rho_w v_w \left(\frac{r_o}{s}\right)^{\kappa}\right] ds^{\kappa+1} \qquad \text{(C-18)}$$

where again $r_o/s \approx 1$ in the stagnation region. The integrand in Eq. (C-18) is well-behaved, starting with a finite value at $s = 0$. However, at the stagnation point, the value of the integral is zero and f_w is indeterminant since $\xi = 0$. Thus, it is necessary to develop a special relation for $f_w\Big|_o$. Applying l'Hospital's rule to Eq. (C-17),

$$f_w\Big|_o = - \frac{\rho_w v_w r_o^{\kappa} (2\xi)^{\frac{1}{2}}}{\left(\frac{d\xi}{ds}\right)} \tag{C-19}$$

Differentiating Eq. (C-3) and introducing the result into Eq. (C-19)

$$f_w\Big|_o = - \frac{(2\xi)^{\frac{1}{2}}}{\rho_e u_e \mu_e r_o^{\kappa}} \rho_w v_w$$

Introducing Eq. (C-1),

$$f_w\Big|_o = - (\rho_w v_w / \alpha^*)_o \tag{C-20}$$

In summary, Eqs. (C-6), (C-12), (C-13) and (C-20) can be used to calculate, respectively, the α^*, du_e/ds, β and f_w at the stagnation point of a blunt body, and Eqs. (C-13) and (C-18) are useful for evaluating the integrals ξ and f_w in the vicinity of the nose region.

APPENDIX D

ALTERATION OF THE BOUNDARY-LAYER EQUATIONS TO ENABLE CONSIDERATION OF GENERALIZED BOUNDARY-LAYER-EDGE CONDITIONS

In the conventional treatment of the hypersonic boundary layer, the boundary-layer-edge conditions are obtained from an inviscid solution as those conditions which exist on the "stagnation streamline" (i.e., that streamline which crosses the shock wave such as to become the stagnation point and wall streamline). This same procedure can still be utilized to include boundary-layer-displacement effects if a new body shape is considered according to the effective displacement of the flow due to the presence of the boundary layer. However, when entropy layer or nonadiabatic flowfield effects occur, this conventional approach is no longer adequate since the edge boundary conditions become functions of the local stream function as well as the streamwise coordinate. Hence, in these cases it is necessary to normalize the dependent parameters of the boundary layer in such a fashion that asymptotic solutions are achieved at the boundary-layer edge. A procedure for accomplishing this task is presented in this appendix.

The procedure used herein consists of normalizing the boundary-layer equations with respect to the $f = 0$ streamline when performing the Levy-Lees transformation described in Section 3 of this report. The equations then remain unchanged except that in all equations the subscript "e" is considered as this reference conditions, and "edge" as the actual edge condition. For example, the definition of f' becomes

$$f' = \alpha_H \frac{u}{u_e} = \alpha_H \frac{u}{u_{edge}} \left(\frac{u}{u_e}\right)_{edge} \tag{D-1}$$

where u_e is the reference condition and u_{edge} is now the boundary-layer-edge condition at some arbitrarily chosen $\overline{\eta}_{edge}$. Conversely, the new edge conditions are given by

$$u_{edge} = \left(\frac{u}{u_e}\right)_{edge} u_e \,, \qquad \rho_{edge} = \left(\frac{\rho}{\rho_e}\right)_{edge} \rho_e \tag{D-2}$$

and so on, where u_e , ρ_e , μ_e, etc., are supplied by the inviscid solution for the $f = 0$ streamline, and $(u/u_e)_{edge}$ and $(\rho/\rho_e)_{edge}$ are also supplied by the inviscid solution, but as functions of $\overline{\xi}$ and f. That is

$$u_e = u_e(\bar{\xi})\Big|_{f=0} \qquad \rho_e = \rho_e(\bar{\xi})\Big|_{f=0} \tag{D-3}$$

and

$$\left(\frac{u}{u_e}\right)_{edge} = \frac{u}{u_e}(\bar{\xi}, f)\Big|_{\bar{\eta}=\bar{\eta}_{edge}}, \quad \left(\frac{\rho}{\rho_e}\right)_{edge} = \frac{\rho}{\rho_e}(\bar{\xi}, f)\Big|_{\bar{\eta}=\bar{\eta}_{edge}} \tag{D-4}$$

In order to illustrate this procedure, consider the following sketches which represent typical profiles of $(u/u_e)_{edge}$, u/u_{edge} and f' at a given $\bar{\xi}$ for two selected values of $\bar{\eta}_{edge}$ in the presence of an entropy layer:

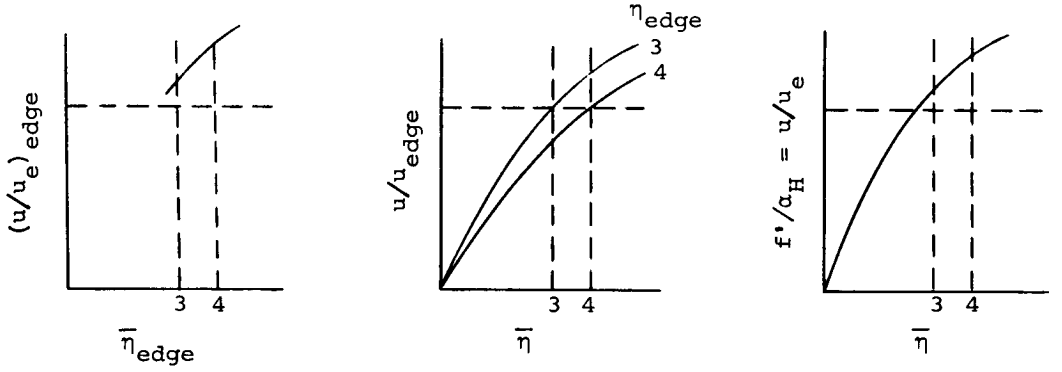

Sketch (a) Sketch (b) Sketch (c)

In this example, the viscous effects are considered to be confined to an $\bar{\eta}$ less than 3 so that both $\bar{\eta}_{edge}$ considered are out of the boundary layer but in the entropy layer. In Sketch (a), the $(u/u_e)_{edge}$ is shown to increase with distance from the surface, as would be expected. Since u_{edge} has different values depending on the choice of $\bar{\eta}_{edge}$, u/u_{edge} profiles would differ accordingly, as shown in Sketch (b). The u/u_e is, of course, independent of $\bar{\eta}_{edge}$ since u_e is a given value for a given ξ; however, as shown in Sketch (c), the f'/α_H does not approach unity at the edge of the boundary layer, and, in fact, depends on the value of $\bar{\eta}_{edge}$ chosen to represent the edge of the boundary layer.

In the absence of an entropy layer or other such effect, $u_{edge} = u_e$ and f'/α_H does approach unity at the edge of the boundary layer as in the conventional solutions. It is for this reason that the $f = 0$ streamline is a convenient choice for the reference condition.

APPENDIX E

ONE-DIMENSIONAL RADIANT HEAT FLUX IN AN ABSORBING BOUNDARY LAYER WITH ANGULAR-DEPENDENT INCIDENT RADIATION

In this Appendix an expression is derived for the net one-dimensional radiant heat flux in the boundary layer normal to the surface, q_r, which is needed in the energy equation (Eqs. (8), (30) or (56)). The wall value, q_{r_w}, which appears in the surface energy balance (Eq. (62)) is also presented. The multicomponent gas in the boundary layer is allowed to absorb diffusely as well as to emit, but scattering is neglected. The wall is assumed to emit spectrally and to reflect diffusely, but transmission of radiant energy is neglected. The incident radiation at the boundary layer edge is allowed to have an angular dependence to approximate intense radiation from the stagnation region of the inviscid flow field or from a nuclear explosion outside of the boundary layer. The derived relations are an extension of the basic relations of Goulard and Goulard (Eqs. (17) and (18) of Ref. E-1) to include the specific boundary conditions described above. The present result also reduces to that of Cess (Eq. (5) of Ref. E-2) if the radiation layer is considered to extend to infinity with no incident flux at this edge boundary condition.

The one-dimensional approximation implies that the flow field extends uniformly to infinity on planes which parallel the plane tangent to the surface at the streamwise position of interest, but that properties may vary from plane to plane. It also means that the net radiation transfer along a ray which lies in one of these planes and passes over the streamwise position of interest is constant but may differ from the value along a different ray in the same plane and passing over the same streamwise location. Although this approximation sounds crude at first exposure, it is probably satisfactory for most boundary-layer applications, since the contribution to q_r depends upon the cosine of the angle between the radiant source and the normal to the surface and decreases rapidly with distance. Use of the approximation affords great simplification in boundary-layer problems since q_r then depends only on the state of the boundary layer at the local streamwise station. On the basis of these considerations, the one-dimensional approximation has been used extensively in boundary-layer studies and seems appropriate for use in the present study.

Absorption has been shown to be important at high reentry velocities (above 45,000 feet per second) in an air boundary layer (e.g., Ref. E-3).

Furthermore, it can be significant at much lower velocities when foreign species are injected by ablation of the surface material. Hence, for generality, it is necessary to consider absorption as well as emission. The neglect of scattering, on the other hand, is a good assumption under reentry conditions as long as solid particles or droplets are not present in the flow field.[E-2]

For local thermodynamic equilibrium, the equation of radiative transfer can be expressed as[E-1]

$$-\frac{1}{\rho \kappa_\nu}\frac{dI_\nu}{d\ell} = I_\nu - B_\nu(T) \qquad \text{(E-1)}$$

where ρ is the density, κ_ν is the absorption coefficient for the multicomponent gas, I_ν is the specific intensity, and $B_\nu(T)$ is Planck's function defined by

$$B_\nu(T) \equiv \frac{2h}{c^2}\frac{\nu^3}{(e^{h\nu/kT} - 1)} \qquad \text{(E-2)}$$

where h is Planck's constant, c is the velocity of light, ν is the frequency, k is Boltzmann's constant, and T is temperature. The flux of radiative energy across the surface $d\sigma$ in the frequency interval $d\nu$ is obtained by integrating $I_\nu \cos\theta d\omega$ over all solid angles $d\omega = \sin\theta d\theta d\varphi$

$$q_{r_\nu} = \int_0^{\pi}\int_0^{2\pi} I_\nu(\theta,\varphi)\cos\theta\sin\theta d\varphi d\theta \qquad \text{(E-3)}$$

where θ is the angle between $\vec{n}$ (the normal to the surface $d\sigma$) and $\vec{\ell}$ (the direction of incident radiation) and φ is the angle between a reference line in the $d\sigma$ plane and the trace of $\vec{\ell}$ on the $d\sigma$ plane (see sketch).

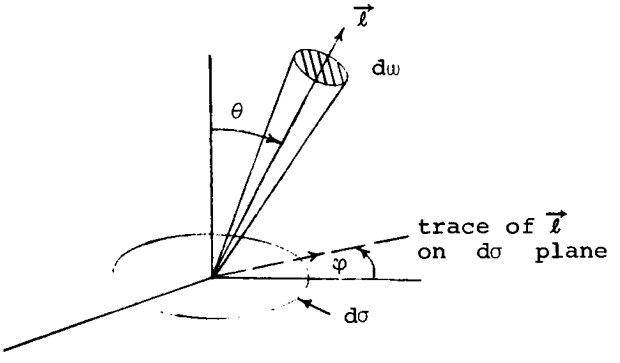

In order to allow the incident flux at the edge of the boundary layer to be a function of φ and θ it is expedient to consider the radiant flux in the angular interval $d\theta$, $q_{r_{\nu,\theta}}$, obtained by differentiating Eq. (E-3) with respect to θ.

It is also convenient for the purpose of evaluating boundary conditions to split the net flux $q_{r_{\nu,\theta}}$ into the contribution $q^{+}_{r_{\nu,\theta}}$ in the direction of the normal unit vector $\vec{n}$ and the contribution $q^{-}_{r_{\nu,\theta}}$ in the opposite direction. Then

$$q_{r_{\nu,\theta}} = q^{+}_{r_{\nu,\theta}} - q^{-}_{r_{\nu,\theta}} \tag{E-4}$$

where

$$\left.\begin{aligned} q^{+}_{r_{\nu,\theta}} &= \int_0^{2\pi} I_\nu(\theta,\varphi)\,\cos\theta\sin\theta\,d\varphi \qquad 0 < \theta < \pi/2 \\ q^{-}_{r_{\nu,\theta}} &= -\int_0^{2\pi} I_\nu(\theta,\varphi)\,\cos\theta\sin\theta\,d\varphi \qquad \pi/2 < \theta < \pi \end{aligned}\right\} \tag{E-5}$$

Substituting Eqs. (E-5) into Eq. (E-1) and multiplying by $2\pi\sin\theta$ yields

$$\left.\begin{aligned} -\frac{1}{\rho\kappa_\nu}\frac{dq^{+}_{r_{\nu,\theta}}}{d\ell}\frac{1}{\cos\theta} &= \frac{q^{+}_{r_{\nu,\theta}}}{\cos\theta} - 2\pi\sin\theta B_\nu(T) \qquad 0 < \theta < \pi/2 \\ \frac{1}{\rho\kappa_\nu}\frac{dq^{-}_{r_{\nu,\theta}}}{d\ell}\frac{1}{\cos\theta} &= -\frac{q^{-}_{r_{\nu,\theta}}}{\cos\theta} - 2\pi\sin\theta B_\nu(T) \qquad \pi/2 < \theta < \pi \end{aligned}\right\} \tag{E-6}$$

Considering the sign convention of the following sketch such that the heat

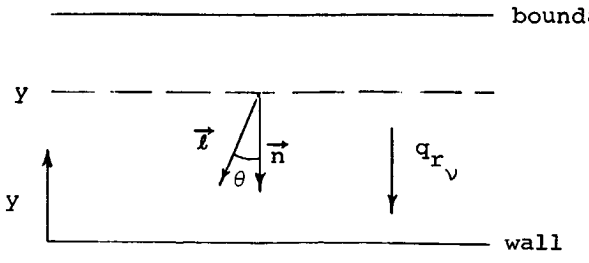

flux toward the surface is positive

$$dy = -\cos\theta d\ell \tag{E-7}$$

Equations (E-6) can then be written

$$\left.\begin{aligned} \frac{1}{\rho\kappa_\nu}\frac{dq^+_{r_{\nu,\theta}}}{dy} - \frac{q^+_{r_{\nu,\theta}}}{\cos\theta} &= -2\pi\sin\theta B_\nu(T) \qquad 0 < \theta < \pi/2 \\ \frac{1}{\rho\kappa_\nu}\frac{dq^-_{r_{\nu,\theta}}}{dy} - \frac{q^-_{r_{\nu,\theta}}}{\cos\theta} &= 2\pi\sin\theta B_\nu(T) \qquad \pi/2 < \theta < \pi \end{aligned}\right\} \tag{E-8}$$

Defining an optical thickness τ_ν

$$\tau_\nu \equiv \int_0^y \rho\kappa_\nu dy \tag{E-9}$$

Equations (E-8) become

$$\left.\begin{aligned} \frac{dq^+_{r_{\nu,\theta}}}{d\tau_\nu} - \frac{q^+_{r_{\nu,\theta}}}{\cos\theta} &= -2\pi\sin\theta B_\nu(T) \qquad 0 < \theta < \pi/2 \\ \frac{dq^-_{r_{\nu,\theta}}}{d\tau_\nu} - \frac{q^-_{r_{\nu,\theta}}}{\cos\theta} &= 2\pi\sin\theta B_\nu(T) \qquad \pi/2 < \theta < \pi \end{aligned}\right\} \tag{E-10}$$

Solution of Eqs. (E-10) yields

$$\left[q^+_{r_{\nu,\theta}} e^{-t/\cos\theta}\right]_0^{\tau_\nu} = -2\pi\int_0^{\tau_\nu} B_\nu(T)\sin\theta e^{-t/\cos\theta}dt \qquad 0 < \theta < \pi/2 \tag{E-11}$$

$$\left[q^-_{r_{\nu,\theta}} e^{-t/\cos\theta}\right]_{\tau_\nu}^{\tau_{\nu_e}} = 2\pi\int_{\tau_\nu}^{\tau_{\nu_e}} B_\nu(T)\sin\theta e^{-t/\cos\theta}dt \qquad \pi/2 < \theta < \pi \tag{E-12}$$

where the subscript e refers to the boundary-layer edge.

It is necessary to evaluate the boundary conditions on the left-hand-sides of Eqs. (E-11) and (E-12). First, consider the edge boundary condition for Eq. (E-12). The first step is to evaluate this equation at the wall.

$$q^-_{r_{\nu,\theta_e}} = \left[q^-_{r_{\nu,\theta_w}} + 2\pi \int_0^{\tau_{\nu_e}} B_\nu(T) \sin\theta e^{-t/\cos\theta} dt \right] e^{\tau_{\nu_e}/\cos\theta} \qquad \pi/2 < \theta < \pi \tag{E-13}$$

where the subscript w refers to the wall. Assuming diffuse reflection and spectral emission from the wall with a transmissivity of zero, the heat flux away from the wall is given by[E-4]

$$q^-_{r_{\nu,\theta_w}} = -2\sin\theta\cos\theta \left[q^+_{r_{\nu_w}} (1 - a_{\nu_w}) + \pi e_{\nu_w} B_\nu(T_w) \right] \qquad \pi/2 < \theta < \pi \tag{E-14}$$

where a_{ν_w} is the hemispheric surface absorptivity and e_{ν_w} is the hemispheric surface emissivity and the minus sign arises because of the definition of θ. If it is further assumed that the coefficients a_{ν_w} and e_{ν_w} for a given frequency ν depend only upon the nature of the surface and the surface temperature but not on the radiation field to which the surface is exposed[E-4]

$$e_{\nu_w} = a_{\nu_w} \tag{E-15}$$

and Eq. (E-14) reduces to

$$q^-_{r_{\nu,\theta_w}} = -2\sin\theta\cos\theta \left[q^+_{r_{\nu_w}} (1 - e_{\nu_w}) + \pi e_{\nu_w} B_\nu(T_w) \right] \qquad \pi/2 < \theta < \pi \tag{E-16}$$

The $q^+_{r_{\nu_w}}$ which appears in Eq. (E-16) can be expressed in terms of known quantities by evaluating Eq. (E-11) at the edge. That is

$$q^{+}_{r_{\nu,\theta_w}} = q^{+}_{r_{\nu,\theta_e}} e^{-\tau_{\nu_e}/\cos\theta} + 2\pi \int_0^{\tau_{\nu_e}} B_\nu(T) \sin\theta e^{-t/\cos\theta} dt \qquad 0 < \theta < \pi/2 \tag{E-17}$$

which upon integration yields

$$q^{+}_{r_{\nu_w}} = \int_0^{\pi/2} q^{+}_{r_{\nu,\theta_e}} e^{-\tau_{\nu_e}/\cos\theta} d\theta + 2\pi \int_0^{\pi/2} \int_0^{\tau_{\nu_e}} B_\nu(T) \sin\theta e^{-t/\cos\theta} dt d\theta \tag{E-18}$$

Exchanging the order of integration in the second term in Eq. (E-18) and utilizing the exponential integral, defined by

$$E_n(t) \equiv \int_0^1 \mu^{n-2} e^{-t/\mu} d\mu \tag{E-19}$$

yields the following expression for $q^{+}_{r_{\nu_w}}$

$$q^{+}_{r_{\nu_w}} = \int_0^{\pi/2} q^{+}_{r_{\nu,\theta_e}} e^{-\tau_{\nu_e}/\cos\theta} d\theta + 2\pi \int_0^{\tau_{\nu_e}} B_\nu(T) E_2(t) dt \tag{E-20}$$

Introducing Eq. (E-20) into Eq. (E-16) yields the following expression for the one-sided heat flux away from the wall evaluated at the wall

$$q^{-}_{r_{\nu,\theta_w}} = -2\sin\theta\cos\theta \left\{ (1 - e_{\nu_w}) \left[\int_0^{\pi/2} q^{+}_{r_{\nu,\theta_e}} e^{-\tau_{\nu_e}/\cos\theta} d\theta + 2\pi \int_0^{\tau_{\nu_e}} B_\nu(T) E_2(t) dt \right] + \pi e_{\nu_w} B_\nu(T_w) \right\} \qquad \pi/2 < \theta < \pi \tag{E-21}$$

Substituting Eq. (E-21) into Eq. (E-13) yields the following expression for the one-sided heat flux away from the wall evaluated at the boundary-layer edge

$$q^-_{r_{\nu,\theta_e}} = 2\pi e^{\tau_{\nu_e}/\cos\theta} \int_0^{\tau_{\nu_e}} B_\nu(T) \sin\theta e^{-t/\cos\theta} dt$$

$$- 2\sin\theta\cos\theta(1 - e_{\nu_w}) e^{\tau_{\nu_e}/\cos\theta} \int_0^{\pi/2} q^+_{r_{\nu,\theta'_e}} e^{-\tau_{\nu_e}/\cos\theta'} d\theta'$$

$$- 4\pi\sin\theta\cos\theta(1 - e_{\nu_w}) e^{\tau_{\nu_e}/\cos\theta} \int_0^{\tau_{\nu_e}} B_\nu(T) E_2(t) dt$$

$$- 2\pi\sin\theta\cos\theta e_{\nu_w} B_\nu(T_w) e^{\tau_{\nu_e}/\cos\theta} \qquad \pi/2 < \theta < \pi \qquad \text{(E-22)}$$

The first through fourth terms in Eq. (E-22) are, respectively, the contributions from the radiation emitted in the boundary layer at all angles θ away from the surface, the radiation incident at the boundary-layer edge reflected from the wall, the radiation emitted in the boundary layer at all angles θ toward the surface, and the radiation emitted from the surface. The common multiplier $e^{\tau_{\nu_e}/\cos\theta}$ represents the attenuation* of these types of radiation as they pass outward through the boundary layer whereas $E_2(t)$ represents the attenuation of the incident flux as it passes through the boundary layer from the edge to the wall.

The one-sided heat fluxes can now be evaluated. Integration of Eq. E-12) yields

*In that the valid range of θ is from $\pi/2$ to π, the $\cos\theta$ is always negative.

$$q^-_{r_\nu} = \int_{\pi/2}^{\pi} q^-_{r_{\nu,\theta_e}} e^{-(\tau_{\nu_e}-\tau_\nu)/\cos\theta} d\theta$$

$$- 2\pi \int_{\pi/2}^{\pi} \int_{\tau_\nu}^{\tau_{\nu_e}} B_\nu(T) \sin\theta e^{-(t-\tau_\nu)/\cos\theta} dt d\theta \qquad \text{(E-23)}$$

Substituting for $q^-_{r_{\nu,\theta_e}}$ from Eq. (E-22) and inverting the order of integration yields

$$q^-_{r_\nu} = 2\pi \int_0^{\tau_{\nu_e}} B_\nu(T) \int_{\pi/2}^{\pi} \sin\theta e^{(\tau_\nu - t)/\cos\theta} d\theta dt$$

$$- 2(1 - e_{\nu_w}) \left[\int_0^{\pi/2} q^+_{r_{\nu,\theta'_e}} e^{-\tau_{\nu_e}/\cos\theta'} d\theta' \right] \int_{\pi/2}^{\pi} \sin\theta\cos\theta e^{\tau_\nu/\cos\theta} d\theta$$

$$- 4\pi(1 - e_{\nu_w}) \left[\int_0^{\tau_{\nu_e}} B_\nu(T) E_2(t) dt \right] \int_{\pi/2}^{\pi} \sin\theta\cos\theta e^{\tau_\nu/\cos\theta} d\theta$$

$$- 2\pi e_{\nu_w} B_\nu(T_w) \int_{\pi/2}^{\pi} \sin\theta\cos\theta e^{\tau_\nu/\cos\theta} d\theta$$

$$- 2\pi \int_{\tau_\nu}^{\tau_{\nu_e}} B_\nu(T) \int_{\pi/2}^{\pi} \sin\theta e^{-(t-\tau_\nu)/\cos\theta} d\theta dt \qquad \text{(E-24)}$$

Utilizing the definition of the exponential integrals (Eq. (E-19)), Eq. (E-24) becomes

$$q^-_{r_\nu} = 2\pi \int_0^{\tau_{\nu_e}} B_\nu(T) E_2(\tau_\nu - t)\, dt$$

$$+ 2(1 - e_{\nu_w}) E_3(\tau_\nu) \int_0^{\pi/2} q^+_{r_{\nu,\theta_e}} e^{-\tau_{\nu_e}/\cos\theta} d\theta$$

$$+ 4\pi(1 - e_{\nu_w}) E_3(\tau_\nu) \int_0^{\tau_{\nu_e}} B_\nu(T) E_2(t)\, dt$$

$$+ 2\pi e_{\nu_w} B_\nu(T_w) E_3(\tau_\nu) - 2\pi \int_{\tau_\nu}^{\tau_{\nu_e}} B_\nu(T) E_2(\tau_\nu - t)\, dt \qquad \text{(E-25)}$$

Integration of Eq. (E-11) yields for the positive one-sided heat flux

$$q^+_{r_\nu} = \int_0^{\pi/2} q^+_{r_{\nu,\theta_w}} e^{\tau_\nu/\cos\theta} - 2\pi \int_0^{\pi/2} \int_0^{\tau_\nu} B_\nu(T) \sin\theta e^{-(t-\tau_\nu)/\cos\theta} dt d\theta \qquad \text{(E-26)}$$

Substituting for $q^+_{r_{\nu,\theta_w}}$ from Eq. (E-17)

$$q^+_{r_\nu} = \int_0^{\pi/2} q^+_{r_{\nu,\theta e}} e^{-(\tau_{\nu_e} - \tau_\nu)/\cos\theta} d\theta + 2\pi \int_0^{\tau_{\nu_e}} \int_0^{\pi/2} B_\nu(T) \sin\theta e^{-(t-\tau_\nu)/\cos\theta} d\theta dt$$

$$- 2\pi \int_0^{\tau_\nu} \int_0^{\pi/2} B_\nu(T) \sin\theta e^{-(t-\tau_\nu)/\cos\theta} d\theta dt \qquad \text{(E-27)}$$

Again, in terms of exponential integrals

$$q^{+}_{r_\nu} = \int_0^{\pi/2} q^{+}_{r_{\nu,\theta_e}} e^{-(\tau_{\nu_e} - \tau_\nu)/\cos\theta} d\theta$$

$$+ 2\pi \int_0^{\tau_{\nu_e}} B_\nu(T) E_2(t - \tau_\nu) dt - 2\pi \int_0^{\tau_\nu} B_\nu(T) E_2(t - \tau_\nu) dt \qquad \text{(E-28)}$$

In accordance with the definition of Eq. (E-4) the net radiant heat flux in the frequency interval $d\nu$ is given by the difference of Eq. (E-28) and Eq. (E-25). Upon combining terms

$$q_{r_\nu} = 2\pi \int_{\tau_\nu}^{\tau_{\nu_e}} B_\nu(T) E_2(t - \tau_\nu) dt - 2\pi \int_0^{\tau_\nu} B_\nu(T) E_2(\tau_\nu - t) dt$$

$$- 2\pi e_{\nu_w} B_\nu(T_w) E_3(\tau_\nu) - 4\pi(1 - e_{\nu_w}) E_3(\tau_\nu) \int_0^{\tau_{\nu_e}} B_\nu(T) E_2(t) dt$$

$$+ \int_0^{\pi/2} q^{+}_{r_{\nu,\theta_e}} e^{-(\tau_{\nu_e} - \tau_\nu)/\cos\theta} d\theta$$

$$- 2(1 - e_{\nu_w}) E_3(\tau_\nu) \int_0^{\pi/2} q^{+}_{r_{\nu,\theta_e}} e^{-\tau_{\nu_e}/\cos\theta} d\theta \qquad \text{(E-29)}$$

The net radiation heat flux, q_r, is obtained by integrating Eq. (E-29) over all frequencies

$$q_r = \int_0^{\infty} q_{r_\nu} d\nu \qquad \text{(E-30)}$$

This integration can be approximated by considering the entire range of ν to be subdivided into M spectral bands of width $\delta\nu_m$. The κ_ν and e_{ν_w} are assumed to be frequency independent within a single band but to vary from band to band and are thus designated as κ_m and e_{m_w}, respectively. The choice of the number of bands, M, and the frequency interval of each band, $\delta\nu_m$, can be made such as to approximate the actual κ_ν to a given degree of accuracy. The q_r for this smeared-band model is given by

$$q_r = \sum_{m=1}^{M} \int_{\nu_m}^{\nu_m+\delta\nu_m} q_{r_\nu} \, d\nu \tag{E-31}$$

It is convenient to define

$$B_m(T) = \frac{\int_{\nu_m}^{\nu_m+\delta\nu_m} B_\nu(T)\, d\nu}{\int_0^\infty B_\nu(T)\, d\nu} \tag{E-32}$$

where

$$\int_0^\infty B_\nu(T)\, d\nu = \frac{\sigma}{\pi} T^4 \tag{E-33}$$

The net radiant heat flux toward the surface at the nodal point i is then given by

$$\begin{aligned} q_{r_i} = \sum_{m=1}^{M} \Bigg\{ & 2\sigma \int_{\tau_{m_i}}^{\tau_{m_e}} T^4 B_m(T) E_2(t - \tau_{m_i})\, dt - 2\sigma \int_0^{\tau_{m_i}} T^4 B_m(T) E_2(\tau_{m_i} - t)\, dt \\ & - 2\sigma e_{m_w} T_w^4 B_m(T_w) E_3(\tau_{m_i}) - 4\sigma (1 - e_{m_w}) E_3(\tau_{m_i}) \int_0^{\tau_{m_e}} T^4 B_m(T) E_2(t)\, dt \\ & + \int_0^{\pi/2} \left[\int_{\nu_m}^{\nu_m+\delta\nu_m} q^+_{r_{\nu,\theta_e}} \, d\nu \right] \left[e^{-(\tau_{m_e} - \tau_{m_i})/\cos\theta} - 2(1 - e_{m_w}) E_3(\tau_{m_i}) e^{-\tau_{m_e}/\cos\theta} \right] d\theta \Bigg\} \end{aligned} \tag{E-34}$$

where from Eq. (E-9) τ_{m_i} is given by

$$\tau_{m_i} = \int_0^{y_i} \rho \kappa_m dy \tag{E-35}$$

At the wall Eq. (E-34) simplifies to

$$q_{r_w} = \sum_{m=1}^{M} \left\{ 2\sigma e_{m_w} \int_0^{\tau_{m_e}} T^4 B_m(T) E_2(t)\, dt - \sigma e_{m_w} T_w^4 B_m(T_w) \right.$$
$$\left. + \int_0^{\pi/2} \left[\int_{\nu_m}^{\nu_m+\delta\nu_m} q^+_{r_{\nu,\theta_e}} d\nu \right] e_{m_w} e^{-\tau_{m_e}/\cos\theta} d\theta \right\} \tag{E-36}$$

since $\tau_{m_w} = 0$ and $E_3(\tau_{m_w}) = 1/2$.

The incident flux at the boundary-layer edge can be a function of frequency and the angles θ and φ. Differentiating Eq. (E-3) with respect to θ while considering $\theta < \pi/2$ and integrating over the frequency range $\delta\nu_m$ yields

$$\int_{\nu_m}^{\nu_m+\delta\nu_m} q^+_{r_{\nu,\theta_e}} d\nu = \cos\theta \sin\theta \int_0^{2\pi} \int_{\nu_m}^{\nu_m+\delta\nu_m} I_{\nu_e}(\theta,\varphi)\, d\nu d\varphi \qquad 0 < \theta < \pi/2 \tag{E-37}$$

The integrations in this term with respect to ν and φ can be performed a priori for each spectral band. The result is then substituted into Eq. (E-34) and (E-35) where the integration with respect to θ is performed.

The calculation of q_{r_i} proceeds as follows. Given the temperature and particle densities across the boundary layer, the τ_{m_i} and $B_m(T_i)$ matrices are computed for each spectral band m and for a finite number of points across the boundary-layer i (nodal points in the numerical solution procedure). The integrations in Eqs. (E-34) and (E-35) are then performed for each spectral band, and the contribution from each spectral band is added to yield the q_{r_i}.

REFERENCES FOR APPENDIX E

E-1. Goulard, R. and Goulard, M.: One-Dimensional Energy Transfer in Radiant Media. Int. J. Heat and Mass Transfer, Vol. 1, No. 1, June 1960, pp.81-91.

E-2. Cess, R. D.: Radiation Effects Upon Boundary-Layer Flow of an Absorbing Gas. J. Heat Transfer, Vol. 83, No. 4, Nov. 1964, pp. 469-475.

E-3. Hoshizaki, H. and Wilson, K. H.: Viscous, Radiating Shock Layer About a Blunt Body. AIAA J., Vol. 3, No. 9, Sept. 1965, pp. 1614-1622.

E-4. Vincenti, W. G. and Kruger, C. H., Jr.: Introduction to Physical Gas Dynamics. John Wiley and Sons, Inc., New York, 1965.

APPENDIX F

A STUDY OF DIFFERENTIAL VERSUS INTEGRAL PROCEDURES EMPLOYING IDENTICAL SPLINE-FIT APPROXIMATIONS

There are three basic aspects to the integral matrix solution procedure described in this report: connected cubics (spline functions) are employed to relate the primary dependent variables to the transverse coordinate η ; the differential equations are solved in integral form with a weighting function which is unity between neighboring nodal points and zero elsewhere; and Newton-Raphson iteration is utilized to solve the resulting set of linear and nonlinear equations. The spline-fit approximation of the dependent variables was a natural choice since smooth functions were desired to minimize the number of nodal points and recent studies have shown spline functions to be superior to single higher-order polynomials. Newton-Raphson iteration was chosen in order to effect linearized coupling throughout the boundary layer. However, the decision of whether or not to integrate and the choice of a weighting factor necessitated some study. The results of these studies are reported in this appendix.

As pointed out by Dorodnitsyn[F-1], solution of the boundary-layer equations in differential form is equivalent to an integral solution using the Dirac delta function as the weighting function. The question at hand then resolves down to the choice of weighting functions. There are three approaches here: the Dirac delta function (differential approach), a step weighting function such as that used by Pallone[F-2], or a smooth weighting function across the entire boundary layer such as that employed by Dorodnitsyn.[F-1] The primary distinction between these three approaches is that the first takes an infinitesimally small sample (restricted to the nodal points themselves), the second samples over a portion of the boundary layer, and the third samples over the entire boundary layer.

Parallel developments were made for the first two approaches for non-similar incompressible boundary layers, the only distinction being the choice of weighting function. The results of this study were inconclusive with regard to accuracy, convergence stability, and the number of iterations required to achieve convergence. In particular, it was found that the accuracy depends more upon the distribution of the nodal points than upon the size of the sample. Therefore the choice of weighting function was made on the basis of algebraic simplicity which favored step weighting functions over Dirac delta functions or smoothly varying functions such as those used by Dorodnitsyn.

In the remainder of this appendix, Newton-Raphson recurrence formulas are presented for the nonsimilar incompressible momentum equation for the integral and the differential approaches. Results are then compared for the case of an incompressible boundary layer on a flat plate and for a nonsimilar boundary layer with an adverse pressure gradient. Finally, the algebraic complexity of the two approaches is discussed.

In the case of an incompressible boundary layer, the energy and species conservation equations are not needed, and the transformed momentum equation (Eq. (55)) reduces to

$$ff'' + \frac{f'''}{\alpha_H} + \beta(\alpha_H^2 - f'^2) - 2\left(f' \frac{\partial f'}{\partial \ell n\, \xi} - f'' \frac{\partial f}{\partial \ell n\, \xi} - f'^2 \frac{d\, \ell n\, \alpha_H}{d\, \ell n\, \xi}\right) = 0 \tag{F-1}$$

The boundary layer at a given streamwise station is divided into N nodal points, η_i, where $i = 1$ at the wall and N at the boundary-layer edge. In the integral approach, Eq. (F-1) is integrated at constant ξ between neighboring nodes, η_{i-1} and η_i:

$$\int_{i-1}^{i} ff''\, d\eta + \frac{1}{\alpha_H}\left[f''\right]_{i-1}^{i} + \beta\alpha_H^2\delta\eta - \beta\int_{i-1}^{i} f'^2 d\eta - 2\int_{i-1}^{i}\left(f' \frac{\partial f'}{\partial \ell n\, \xi} - f''\frac{\partial f}{\partial \ell n\, \xi}\right)d\eta$$

$$+ 2\,\frac{d\, \ell n\, \alpha_H}{d\, \ell n\, \xi}\int_{i-1}^{i} f'^2 d\eta = 0 \tag{F-2}$$

As discussed in the present report, the f_i, f_i', f_i'', and f_i''' are expanded about point i in terms of their η-derivatives by the use of Taylor series. These series are truncated by considering the f_i'''' to be constant between η_i and η_{i+1}. Thus, between each i and $i+1$ the f is represented as a quartic, the f' as a cubic, and the f'' as a quadratic, whereas the f''' is considered to vary linearly between each pair of η-stations, all of these functions joining continuously at the nodal points. Utilizing the same procedure described in the present report for representing the streamwise derivatives and evaluating the integrals which appear in Eq. (F-2), differentiation yields the following Newton-Raphson recurrence formulas:

$$\left[\frac{f''}{\alpha_H}\left(\frac{\Delta f''}{f''} - \frac{\Delta\alpha_H}{\alpha_H}\right) + \left[(1 + d_0)f + d_1 f_{\ell-1} + d_2 f_{\ell-2}\right]\Delta f' + f'(1 + d_0)\Delta f\right]_{n-1}^{n}$$

$$+ 2\beta\alpha_H \delta\eta\Delta\alpha_H - 2\left[1 + \beta + d_0 - \frac{d_1\alpha_{H_{\ell-1}} + d_2\alpha_{H_{\ell-2}}}{\alpha_H}\right]\left[X_1\Delta f'_n\right.$$

$$\left. + X_2\Delta f''_n + X_3\Delta f'''_n + X_4\Delta f''''_{n-1}\right] - \left(\frac{d_1\alpha_{H_{\ell-1}} + d_2\alpha_{H_{\ell-2}}}{\alpha_H^2}\right)\left[f'_n X_1 + f''_n X_2\right.$$

$$\left. + f'''_n X_3 + f'''_{n-1} X_4\right]\Delta\alpha_H - 2\left[Z_1\Delta f'_n + Z_2\Delta f''_n + Z_3\Delta f'''_n + Z_4\Delta f'''_{n-1}\right]$$

$$= - \text{ERROR} \qquad \text{(F-3)}$$

where the ERROR is given by the left-hand side of Eq. (F-2) evaluated in the previous iteration and the XP_1, XP_2, XP_3 and XP_4 are defined by Eqs. (86), the d_0, d_1 and d_2 by Eqs. (88) or (89), and the ZP_1, ZP_2, ZP_3 and ZP_4 by Eq. (94).

In the differential approach, Eq. (F-1) is solved at each nodal point i without integration. Utilizing the same procedure for representing the streamwise derivatives, differentiation yields the following Newton-Raphson recurrence formulas:

$$f''(1 + d_0)\,\Delta f - \left[2\beta\, f' + d_1\, f'_{\ell-1} + d_2\, f'_{\ell-2} - 2f'\left(\frac{d_1\alpha_{H_{\ell-1}} + d_2\alpha_{H_{\ell-2}}}{\alpha_H}\right)\right]\Delta f'$$

$$+ \left[f(1 + d_0) + d_1\, f_{\ell-1} + d_2\, f_{\ell-2}\right]\Delta f'' + \frac{1}{\alpha_H}\,\Delta f'''$$

$$+ \left[2\beta\alpha_H - \frac{1}{\alpha_H^2}\left(f''' + f'^2\left(d_1\,\alpha_{H_{\ell-1}} + d_2\,\alpha_{H_{\ell-2}}\right)\right)\right]\Delta\alpha_H = - \text{ERROR}$$

(F-4)

where the ERROR is given by the left-hand side of Eq. (F-1) evaluated in the previous iteration.

Velocity profiles for incompressible flow over a flat plate as reported by Howarth[F-3] and as obtained with the above-described integral and matrix procedures are presented in Table F-1 in terms of the η defined by Howarth (which is $\sqrt{2}$ times the η defined in the present report for this problem).

TABLE F-1

VELOCITY PROFILES FOR INCOMPRESSIBLE FLOW OVER A FLAT PLATE AFTER HOWARTH COMPARED TO 11-POINT INTEGRAL-MATRIX AND DIFFERENTIAL-MATRIX SOLUTIONS

	Velocity ratio		
η of Howarth	Howarth[F-3]	Integral-matrix	Differential-matrix
0	0	0	0
.4	0.13277	0.1328	0.1322
.8	0.26471	0.2646	0.2636
1.2	0.39378	0.3937	0.3916
1.6	0.51676	0.5166	0.5139
2.0	0.62977	0.6297	0.6263
3.0	0.84605	0.8462	0.8431
4.0	0.95552	0.9553	0.9564
5.0	0.99155	0.9913	0.9938
6.0	0.99898	0.9990	0.9999
7.0	0.99992	0.9999	1.0000
8.0	1.00000	1.0000	1.0000

Identical 11-point nodal distributions were employed in the present calculations, namely, η = 0, 0.2, 0.5, 0.9, 1.4, 2.0, 2.7, 3.5, 4.4, 5.4 and 6.5. The values of u/u_e reported in Table F-1 were then computed from the f_i' and their derivatives by use of the Taylor series expansions (Eqs. (78)). It can be seen that the integral-matrix solution agrees with Howarth's results to four significant places and that the differential-matrix solution agrees within a few tenths of a percent. Corresponding, the wall shear function, f_w'', was 0.3320 and 0.3308 for the integral and differential procedures, respectively, compared to 0.33206 reported by Howarth.

The problem of linearly retarded flow ($u_e/u_{e_o} = 1 - ax$ with $a = 1/8$), first studied by Howarth[F-3] and later investigated by Smith and Clutter[F-4], among others, was also considered. Wall shear function, f_w'', as obtained with 6-point and 10-point integral and differential solutions are compared in Table F-2 to results reported by Smith and Clutter. The latter results can be considered as precise since they agree closely with those of other investigators. They obtained this degree of accuracy by the use of small streamwise spacing. The present results, on the other hand, were obtained with relatively large streamwise spacing. (All stations considered in the present calculations are shown whereas only a sampling of the Smith and Clutter results are presented. The fact that streamwise spacing is affecting the present results

TABLE F-2

WALL SHEAR FUNCTION ALONG A FLAT PLATE WITH LINEARLY RETARDED FLOW, $u_e = 1 - x/8$, AFTER SMITH AND CLUTTER COMPARED TO 10-POINT AND 6-POINT INTEGRAL-MATRIX AND DIFFERENTIAL-MATRIX SOLUTIONS

Type	Ref. F-4**	Differ-ential	Integral	Integral	Differ-ential	Integral	Integral
No. of η-points*		10	10	10	6	6	6
Normalized distance, x	Shear function evaluated at the wall, f''_w						
0	.4696	.4678	.4695	.4695			
.01		.4645	.4663	.4663	.4656	.4660	.4660
.02				.4635	.4629	.4633	.4633
.04		.4555	.4573		.4579	.4582	
.08		.4451	.4469	.4471	.4472	.4473	.4468
.12		.4343	.4361		.4362	.4362	
.16		.4230	.4249	.4242	.4249	.4248	.4237
.20	.4114	.4114	.4133		.4133	.4130	
.28		.3866	.3886	.3872	.3887	.3879	.3862
.36		.3601	.3622		.3623	.3610	
.44		.3315	.3338	.3309	.3340	.3320	.3289
.52		.3006	.3030	.3002	.3034	.3002	.2972
.60		.2667	.2692	.2667	.2698	.2651	.2623
.68		.2288	.2316	.2291	.2323	.2251	.2225
.76		.1852	.1882	.1857	.1892	.1778	.1752
.80	.1653	.1605	.1638	.1612	.1649	.1504	.1478
.84		.1329	.1365	.1337	.1378	.1186	.1160
.88	.1100	.1000	.1042	.1010	.1059	.0809	.0784
.92	.0736	.0506	.0582	.0519	.0615	.0350	.0330
.94		non***		non	.0162	non	.0092
.96	0 (extrap.)		non		non		-.0132
.98							-.0351
1.00							-.0549
1.02							-.0754
1.04							-.0929
1.06							-.1135

*10-point (η = 0, 0.2, 0.5, 0.9, 1.4, 2.0, 2.7, 3.5, 4.4, 5.4),
6-point (η = 0, 0.8, 1.8, 3.0, 4.4, 6.0).

**Smith and Clutter results shown for representative streamwise stations only.

***nonconvergent

can be seen by comparing the two 10-point integral solutions and the two 6-point integral solutions.) Looking first at the 10-point solutions, the integral solution is slightly better except in the vicinity of $x = .20$ where the differential approach agrees with that of Smith and Clutter. In the 6-point solutions, the integral and differential methods yield comparable results until an x of 0.60 or so, after which the differential approach yields better accuracy.

Since the comparison between the integral and differential approaches was inconclusive with regard to accuracy and convergence considerations, it was appropriate to consider algebraic complexity. Comparison of Eqs. (F-3) and (F-4) indicates that the differential approach is algebraically simpler for the incompressible nonsimilar boundary layer. However, in the multicomponent boundary layer the situation is strikingly reversed. All of the complexities introduced by multicomponent thermodynamic and transport properties in the energy equation and elemental species equations appear in flux divergence terms (see Eqs. (56) and (58)). Integration by a unity weighting factor thus eliminates a derivative with respect to η so that it is not necessary to evaluate flux derivatives in the evaluation of the ERRORS. The fluxes, in turn, contain derivatives with respect to η (see, e.g., the q_a^* given by Eq. (50)). Thus, complete Newton-Raphson iteration requires evaluation of second derivatives of state functions with respect to h and $\tilde{K}_k$ as well as first derivatives (see Eqs. (129) and (132)). The differential approach, on the other hand, would require the evaluation of second and third derivatives of state functions with respect to h and $\tilde{K}_k$ for full Newton-Raphson iteration. Thus, integration between i and $i-1$ is by far the most desirable approach from the standpoint of algebraic simplicity.

REFERENCES

F-1 Dorodnitsyn, A. A.: General Method of Integral Relations and its Application to Boundary Layer Theory. Advances in Aeronautical Sciences, Vol. 3, Mac-Millan, New York, 1960, pp. 207-219.

F-2 Pallone, A. J.: Nonsimilar Solutions of the Compressible-Laminar-Boundary-Layer Equations with Applications to the Upstream-Transpiration Cooling Problem, J. Aerospace Sci., Vol. 28, No. 6, June 1961, pp. 449-456, 492.

F-3 Howarth, L.: On the Solution of the Laminar Boundary Layer Equations. Proc. Roy. Soc. (London), Series A, Vol. 164, 1938, pp. 547-558.

F-4 Smith, A. M. O. and Clutter, D. W.: Solution of the Incompressible Laminar Boundary-Layer Equations. AIAA J., Vol. 1, No. 9, Sept. 1963, pp. 2062-2071.